QUALITATIVE AND QUANTITATIVE MORPHOLOGICAL CHANGES IN THE BRAIN OF ADULT MICE USED AS AN ANIMAL MODEL OF FETAL ALCOHOL SYNDROME

Oladiran Ibukunolu Olateju

A Thesis submitted to the Faculty of Health Sciences, University of the Witwatersrand, Johannesburg, in fulfilment of the requirements for the degree of

Doctor of Philosophy

Johannesburg, 2017

DECLARATION

I, Oladiran Ibukunolu Olateju declare that this thesis is my own work. It is being submitted for the Degree of Doctor of Philosophy at the University of The Witwatersrand, Johannesburg. It has not been submitted before for any degree or examination at any other University.

Oladiran Ibukunolu Olateju 13th July, 2017

DEDICATION

To Jehovah

(For His love, guidance, strength, comfort and peace)

And to

My family,

'The OLATEJUs'

PRESENTATIONS ARISING FROM THIS THESIS

1. Alcohol abuse during pregnancy: Somatosensory defects in adult mice exposed to pre-natal alcohol – **Olateju O.I.**, Ihunwo O.A. and Manger P.R.

   Oral presentation at the 4th Africa & Middle East Congress on Addiction (AMECA), Tunisia (2016)

2. Neuronal generation in the hippocampus of adult mice is affected by chronic alcohol exposure during the fetal period – **Olateju O.I.**, Patzke N., Muhammed S., Ihunwo O.A., and Manger P.R.

   Oral presentation at the International Brain Research organization (IBRO) School on Neurotoxicity and brain disorders, Morocco (2015)

3. Hippocampal neurogenesis in adult mice is not affected by chronic alcohol exposure during the fetal period – **Olateju O.I.**, Patzke N., Muhammed S., Ihunwo O.A., and Manger P.R.

   Oral presentation at the Workshop on Behavioral Bioassay in Neuroscience: Brain and Behaviour from Invertebrates to Small Mammals, Kenya (2014), and

   Oral presentation at the Anatomical Society of Southern Africa (ASSA), (2014)

PUBLICATIONS ARISING FROM THIS THESIS

1. **Olateju O.I.**, Muhammed S., Patzke N., Ihunwo O.A., and Manger P.R.: Neurogenesis in the hippocampus of C57BL/6J mice at early adulthood (56 days post-natal) following chronic prenatal alcohol exposure. *Submitted, under review; Alcohol*

2. **Olateju O.I.**, Bhagwandin A., Ihunwo O.A., and Manger P.R.: Changes in the cholinergic, catecholaminergic, orexinergic and serotonergic sleep related neurons in adult mice exposed to intrauterine alcohol. *Manuscript submitted; Frontiers in Neuroscience*

3. **Olateju O.I.**, Bhagwandin A., Ihunwo O.A., and Manger P.R.: Lack of detectable changes to the cerebellar cortex of C57BL/6J mice at early adulthood (56 days post-natal) following chronic prenatal alcohol exposure. *Manuscript submitted; Metabolic Brain Disease*

4. **Olateju O.I.**, Ihunwo O.A., and Manger P.R.: Changes to the somatosensory barrel cortex in C57BL/6J mice at early adulthood (56 days post-natal) following chronic prenatal alcohol exposure. *In preparation*

ABSTRACT

We examined the effect of chronic prenatal alcohol exposure on the qualitative and quantitative changes in the brain of C57BL/6J mice once they had reached early adulthood (56 days post-natal). Pregnant mice, and their *in utero* litters, were exposed to alcohol, through oral gavage, on gestational days 7 – 16, with recorded blood alcohol concentrations averaging 1.84 mg/ml (chronic alcohol, or CA, group). Two control groups, an oral gavage sucrose control group (chronic alcohol control, or CAc, group) and a non-treated control group (NTc group), were also examined. Using appropriate antibodies specific for the neurons or nuclei of interest, the present study compared morphologically and quantified (I) the neuronal cell proliferation and the appearance of immature neurons in the hippocampal adult neurogenesis, (II) the changes in the PMBSF barrel sizes in the somatosensory cortex, (III) the cortical organization, cell number and cell sizes of cerebellar interneurons in the vermal cerebellum, and (IV) the nuclear organization, cell number and cell sizes of four specific clusters of nuclei for the control and regulation of sleep-wake cycle in the brains of all the experimental groups. The stained neurons and nuclei of interest were consistent in all the three experimental groups. The quantitative analyses showed that alcohol, in comparison with the two controls, had (I) no strong effect on the proliferative process but significantly reduced the numbers of immature neurons in the hippocampus, (II) no effect on the barrel sizes from the different measured parameters, despite a reduced barrel size in the alcohol group, but there was significant size reductions in barrel rows D and E, (III) no effect on the cell densities of Nissl and PV+ stained neurons in the molecular layer and the cell sizes of Purkinje cells immunolabelled with CB antibody, and (IV) no effect on the numbers of ChAT+ neurons, TH+ neurons, OxA+ neurons, however there were significantly larger OxA+ neurons and significantly smaller ChAT+ neurons while the TH+ neuron size was not significantly different. Some of these results are consistent with other studies that utilized FAS rodent

models thus suggesting the suitability of this mouse model for FAS studies. The significant findings could help explain the reasons for the neurodevelopmental and behavioural problems that are common to FAS subjects. The neuroanatomical evidence presented in this study could open avenues for interventions to improve the quality of life of FAS and FASD children.

ACKNOWLEDGEMENTS

I give utmost thanks to Jehovah Almighty for guiding me through the challenges and the successful completion of my PhD study. I thank Him for the comfort, peace, strength and love He bestowed on me. I extend my sincerest gratitude and appreciations to my supervisor, Prof Paul Manger, for his guidance, encouragement, expertize, advice, technical and moral support throughout my study. I have learnt a lot from him and I am extremely fortunate to have a supervisor like him, who cared about my career development and happiness. I also thank my co-supervisor, Prof Amadi Ihunwo, for ensuring that my teaching responsibilities did not interfere with my study. I thank him for his advice, support and encouragement and for providing a listening ear. Special thanks to Drs. Bhagwandin, Spocter, Patzke and Esan for assisting with immunohistochemistry, stereology and statistical analyses. Your skills and wealth of knowledge are significant for the completion of this study. I also like to thank the members of staff, especially Drs. Augustine, Olaleye, Ms. Gomes, Mrs. Ali, Mr. Du Plessis and Meadows, at the School of Anatomical Sciences, University of the Witwatersrand for their technical supports and friendship. I must express my heartfelt gratitude to my lovely wife, Dr. Margaret Olateju, for her relentless support throughout the duration of my study. And to my lovely son, Olushola Olateju, who provided a much needed form of escape from the lab- Daddy is always proud of you! Thanks to my mum and siblings for their moral support and encouragement. All your contributions will forever remain close to my heart. Finally, utmost appreciation to the International Brain Research Organization (IBRO) for their travel awards to attend neuroscience workshops and conferences and also to the NRF and Health Science Research Committee, University of The Witwatersrand, for their research grants awards.

TABLE OF CONTENTS

LIST OF FIGURES

LIST OF TABLES

CHAPTER ONE: Introduction and Literature Review, Aims, and Main Findings

1.1. Introduction:

Research has revealed an increased number of still-born, infant death, growth and developmental malformations in children born to alcoholic mothers (Ulleland, 1972; Niccols, 2007); however, it was not until the early 1970's that attention was focused on the severe effects of alcohol on the developing fetus (Ulleland, 1972; Niccols, 2007). The spectrum of abnormalities associated with alcohol teratogenicity in children born to mothers who consumed alcohol during pregnancy include neurodevelopmental abnormalities, neurobehavioral problems, learning impairments, cognitive problems, mental retardation and sleep disorders (Niccols, 2007; Incerti et al., 2010). These abnormalities are collectively called Fetal Alcohol Spectrum Disorders (Moore et al., 2002; Niccols, 2007; Incerti et al., 2010). The severe end of the FASD spectrum in children exposed to teratogenic effects of alcohol is called Fetal Alcohol Syndrome (FAS) (Sulik, 2005; Incerti et al., 2010; Gil-Mohapel et al., 2011).

FAS is characterized by specific mental retardation, growth hindrance, craniofacial dysmorphologies and neurodevelopmental anomalies (Sulik, 2005; Incerti et al., 2010; Gil-Mohapel et al., 2011). Craniofacial anomalies associated with FAS include small head size, small and widely placed eyes, flat mid-face, short and up-turned nose, smooth and wide philtrum and a thin upper lip (Sulik et al., 1981; Moore et al., 2002; Sulik, 2005). The FAS-related neurobehavioral and neurodevelopmental anomalies are severe psychiatric problems associated with

emotional processing, general intelligence, cognitive and memory impairments, social deficits, loss of motor skills, sleep disorders, stress, anxiety and depression (Famy et al., 1998; May et al., 2007; Oladehin et al., 2007; Gil-Mohapel et al., 2010; Hellemans et al., 2010; Crede et al., 2011; Chen et al., 2012; Ipsiroglu et al., 2013; May et al., 2015, 2016; Woods et al., 2015).

1.2. Prevalence of Fetal Alcohol Syndrome:

It has been difficult to accurately estimate the prevalence of FAS births globally (May et al., 2009). Data obtained from reports in the literature over a 10-year period estimated the prevalence of FAS as 0.2 to 8.2 per 1000 births (Landgraf et al., 2013). In the United States (US), the prevalence of FAS was estimated to be 0.2 to 1.5 per 1000 births (Riley et al., 2011). In clinic-based estimations, the prevalence is estimated as 0.33 to 2.2 per 1000 (in the United States of America, USA) (Abel and Sokol, 1991; Stratton et al., 1996; May and Gossage, 2001), 2.3 per 1000 (amongst African Americans in the US) (Abel, 1995; Abel, 1998) and an average of 0.97 per 1000 is estimated for developed countries (Abel and Sokol, 1987; Abel, 1998). In a comparison of FAS prevalence in schools in Italy, USA and South Africa, the prevalence was highest in South Africa (72.3 per 1000). This estimate quadruples the estimate in the USA (16.5 per 1000) and doubles the prevalence in Italian schools (35.7 per 1000) (Crede et al., 2011).

The Western Cape Province in South Africa is known to have one of the highest prevalences of FAS in the world, with an average of 43.5 FAS cases per 1000 births (May et al., 2000; Viljoen et al., 2005; May et al., 2007). Subsequent studies in the same province showed progressive increases in the average FAS prevalence rates:

69.7 and 78.6 per 1000 reported by Viljoen et al. (2005) and May et al. (2007) respectively. Excessive and dangerous alcohol drinking patterns amongst the inhabitants of the Western Cape Province is similar to the reckless drinking pattern observed in the pregnant mothers (May et al., 2007). The habits of excessive drinking could be traced to the abolished dop system (partial payment of labour with wines), cultural and economic status of the wine-producing Western Cape Province where many manual labourers (men and women) work on the vineyards (London et al., 1998; London, 1999; Watt et al., 2014). In addition, past trauma (Ethen et al., 2009; Watt et al., 2014), addiction to alcohol, stress, depression and stigma associated with divorce and unwanted pregnancy (Crankshaw et al., 2014; Watt et al., 2014) are often stated as reasons by mothers who consume alcohol during pregnancy; however, these difficulties and problems could be tackled through other social or health interventions such as counselling, therapies and community engagements. It must be noted that the neurodevelopmental abnormalities arising from alcohol consumption during pregnancy could simply be prevented or avoided if pregnant mothers do not consume alcohol during pregnancy, as the damage to the developing brain is very severe (Landgraf et al., 2013) making FAS children unable to perform certain tasks (Zimmerberg et al., 1991; Famy et al., 1998).

1.3. Neural Changes Associated with Fetal Alcohol Syndrome:

Damage to the hippocampus, which is the part of the brain involved in the formation and recall of memories, spatial navigation, and by extension learning and cognition, is implicated in the inability of FAS children to recall as many objects as normal children (Zimmerberg et al., 1991). Neuro-imaging has also shown a

reduction in hippocampal volume as well as the size of other brain areas in FAS subjects (Archibald et al., 2001; Autti-Rämö et al., 2002; Parnell et al., 2009). The functionality of the hippocampus depends, in part, on its ability to generate new neurons, termed adult hippocampal neurogenesis (addressed in Chapter 2), and to establish neuronal connections within the existing networks and with other brain regions. Although the true effect of alcohol on the hippocampal neurons and circuitry remains controversial, it has been found that alcohol impacts negatively on general neurogenesis and more specifically, generation of new neurons in the dentate gyrus of the hippocampus during brain development (Archibald et al., 2001; Autti-Rämö et al., 2002; Klintsova et al., 2007; Gil-Mohapel et al., 2010).

Apart from FAS-related memory and learning impairments, the auditory, olfactory, visual and somatosensory systems are impaired after consuming alcohol (Lewis et al., 1969; Roebuck et al., 1998a; Archibald et al., 2001; Autti-Rämö et al., 2002; Burd et al., 2003; Powrozek and Zhou, 2005; Klintsova et al., 2007; Oladehin et al., 2007; Gil-Mohapel et al., 2010). The somatosensory cortex, located in the anterior parietal region of the neocortex, is where tactile inputs from the body surface are processed, providing an individual with information about the external environment (Powrozek and Zhou, 2005). Alcohol administered during pregnancy in a rodent model has been found to negatively affect the development and the size of the barrel fields and individual barrels, in the somatosensory cortices of rodents (addressed in Chapter 3) (Powrozek and Zhou, 2005; Margret et al., 2006; Oladehin et al., 2007).

Another region of the brain that is directly affected by alcohol exposure during fetal development is the cerebellum. The cerebellum communicates with many parts of the brain including the vestibular system, spinal cord and the cerebral cortex, for

the control of eye movement, balance, muscle tone, motor skills, motor learning and cognition (Swenson, 2006; Oladehin et al., 2007). Slow reaction time to stimuli, slow foot tapping, postural instability and eye-blinking have also been observed in adult subjects after alcohol consumption (Streissguth et al., 1984; Oladehin et al., 2007). Slowed response times to stimuli are similarly found in FAS children with an associated reduction in volume of cerebellar white matter (Hamre and West, 1993; Roebuck et al., 1998a; Autti-Rämö et al., 2002; Powrozek and Zhou, 2005; Servais et al., 2007; Mattson et al., 2011; Riley et al., 2011; Spottiswoode et al., 2011). This is as a result of death of Purkinje cells, Golgi, granule and glia cells in the cerebellar cortex (addressed in Chapter 4) (Anderson and Sides, 1979; Hamre and West, 1993; Pantazis et al., 1993; Green et al., 2004; Dikranian et al., 2005; Joshi et al., 2006; Kane et al., 2011; Oliveira et al., 2014).

FAS is also associated with sleep disorders, and sleep disorders are becoming a common complaint by parents or caregivers of children with FAS. Problems encountered include multiple waking, unwillingness to go to bed and reduced total sleep time in children with FAS, which also indirectly affects the physical activities and mental alertness of their parents or caregivers on a daily basis (Meltzer and Mindell, 2004; Wengel et al., 2011). Sleep is a process that is directly controlled by the brain. A well-structured sleep-wake cycle is essential for the development of the brain and directly affects the manner in which the brain performs its activities (Chen et al., 2012; Ipsiroglu et al., 2013). Extensive sleep deprivation can cause psychotic, cognitive and social problems, as well as lead to death in very extreme cases (Jan et al., 2010a,b). It has been shown in FAS children that the rate at which sensory information is processed is also directly dependent on the sleep-wake cycle (Wengel et al., 2011). Therefore, sleep disruptions are a major problem in FAS, and may

exacerbate the problems associated with FAS. However, there appears to be no report correlating morphological changes of the sleep centres of the brain with the learning, cognitive and behavioural problems associated with sleep disruptions and FAS subjects. It is envisaged that the observed problems associated with sleep disruptions and FAS will impact the populations of neurons that are involved in sleep-wake cycle control (addressed in Chapter 5). These neurons are the cholinergic, catecholaminergic, histaminergic, serotonergic and orexinergic neurons located in the hypothalamus, midbrain and pons (Lai and Siegel, 1990; Bjarkam et al., 1997; Peyron et al., 1998; Kiyashchenko et al., 2002; Manger et al., 2003; Gerashchenko and Shiromani, 2004; Maseko et al., 2007; Lyamin et al., 2008).

1.4. Animal Models of Fetal Alcohol Syndrome:

Non-mammalian animals such as fish (Stockard, 1910; Blader and Strähle, 1998) and chickens (Cartwright and Smith, 1995) have been used as models to investigate the effect of fetal alcohol exposure. Fish embryos, after a 3-hour alcohol exposure during the gastrula stage, presented with severe brain defects, with an underdeveloped forebrain (Blader and Strähle, 1998), microphthalmia (abnormal small eye) and cyclopia (undivided eye orbits) (Stockard, 1910) and facial defects (Blader and Strähle, 1998). Similarly, chick embryos are particularly effective in investigating the development of the face (facial dysmorphology) in response to prenatal alcohol exposure (Cartwright and Smith, 1995). Non-human primates such as macaque monkeys (Clarrens et al., 1992; Bonthius et al., 1996; Astley et al., 1999) and non-primate mammals such as sheep (Richardson et al., 1985; Patrick et al., 1985; Cudd, 2005) have similarly been used as models to investigate the morphological and

physiological changes in the brain following prenatal alcohol exposure. The population of Purkinje cells in the macaque cerebellum was significantly reduced by prenatal alcohol exposure (Bonthius et al., 1996) and cerebral blood flow and brain activity seemed compromised by prenatal alcohol exposure in sheep models (Richardson et al., 1985; Patrick et al., 1985; Gleason and Hotchkiss, 1992).

Despite these studies, mouse or rat models of FAS are the most commonly used to study the effects of alcohol teratogenicity (Zafar et al., 2000; Livy et al., 2003; Cudd, 2005; Gil-Mohapel et al., 2010; Incerti et al., 2010; Balaszczuk et al., 2011) and these models have exhibited learning difficulties and memory problems similar to the patterns found in FAS children (Gil-Mohapel et al., 2010).

The similarity in the behavioural and morphological abnormalities resulting from alcohol exposure during early embryonic development in fish, chick, macaque monkey, sheep, mouse or rat models (Astley et al., 1999; Cudd, 2005; Sulik, 2005) is an indication of interspecies similarities in the patterns of developmental disorders (Sulik, 2005); however, Perrin (2014) commented that the physiological states of experimental animal models are not similar to what are observed in humans with FAS. Indeed, the effects of drugs in an animal model do not always mimic the effects that are observed in humans (Perrin, 2014). These observations then question the suitability of experimental model animals in investigating the effect of drugs or agents which are intended to be used in or known to have effects in humans (Perrin, 2014). Reports have shown that experimental animal models have presented with some FAS defects that mimic FAS in humans (Goodlett and Horn, 2001; Gil-Mohapel et al., 2010). Unfortunately, there is no single animal model that completely simulates all the characteristic features of FAS in humans (Cudd, 2005; Gil-Mohapel et al., 2010).

Therefore, new approaches and variations in designs of FAS model animals are continually being developed to simulate the FAS-related abnormalities seen in human subjects (Sulik, 2005). The variations in FAS model design include changing the gestational stage of alcohol exposure, the duration of exposure, and the mode of alcohol administration.

According to Sulik et al. (1981), a two-dose alcohol administration at day 7 of gestation in C57BL/6J mice produced severe embryonic facial deformities such as exencephaly, maxillary hypoplasia, cleft lips and palate (Sulik et al., 1981). A later study by Webster et al. (1983) on the same species of mouse but with a two-day alcohol administered at gestation days 7 and 8 reported similar facial defects as well as underdeveloped olfactory bulbs, cerebral hemispheres and enlarged ventricles. This is in agreement with other reports that alcohol administered at gestational day 7 (Godin et al., 2011) and day 8 (Parnell et al., 2009) resulted in facial and forebrain anomalies. However, other studies on alcohol teratogenicity utilized prolonged time frames of alcohol exposure that targeted different trimester equivalents (first and second trimesters). In these studies, alcohol was administered to pregnant rodents during gestational days 1 to 23 (Choi et al., 2005; Redila et al., 2006), while some studies focused on the third trimester equivalent, which corresponds to the postnatal days 4 to 10 in rodents (Klintsova et al., 2007; Oladehin et al., 2007; Helfer et al., 2009).

Different modes of alcohol administration such as intra-peritoneal (injection within the peritoneum) (Wozniak et al., 2004; Ieraci and Herrera, 2007), dietary intake (Choi et al., 2005; Redila et al., 2006) and oral-gavage (gastric intubation) (Klintsova et al., 2007; Helfer et al., 2009) are also utilized in FAS studies; however,

there seems to be no report that suggests the effectiveness or adequacy of one mode of alcohol administration over the other. Sulik et al. (1983) have surmised that the extent of the FAS defects is dependent on the gestational day the alcohol insult is introduced, but not on the mode of alcohol administration (orally or intra-peritoneally) (Sulik et al., 1981; Webster et al., 1983; Cudd, 2005).

These disparities in the designs of FAS models make direct comparisons on the effect of alcohol on brain morphology controversial (Gil-Mohapel et al., 2010). An example is the contradictory reports on the effect of alcohol on cell proliferation in the dentate gyrus of the hippocampus (addressed in Chapter 2). Some authors reported a deleterious effect of alcohol, others reported the opposite effect (the promotion of proliferation), while some studies found no effect (Miller et al., 1995; Nixon and Crews, 2002; Pawlak et al., 2002; Zharkovsky et al., 2003; Wozniak et al., 2004; Åberg et al., 2005; Klintsova et al., 2007; Helfer et al., 2009). As of yet, there seems to be no generally accepted FAS animal model, and the models are continually modified in accordance with the specific research objectives.

To re-emphasize, studies on FAS have revealed that alcohol impacts on the population of neurons, decreases release of neurotransmitters, delays somatosensory processing, causes sleep disruptions and impairs motor coordination (Zimmerberg et al., 1991; Famy et al., 1998; Sulik, 2005; Gil-Mohapel et al., 2010; Incerti et al., 2010). Some of these studies on sleep disorders, somatosensory processing and motor coordination focused on the behavioural presentations in FAS children. However, there seems to be no report in the literature to correlate the presentations in FAS children and the possible morphological differences that could be occurring in the brain, especially at adulthood, because reports have shown that the effect of alcohol

on the brain is irreversible and the FAS-associated problems persist into adulthood (Zimmerberg et al., 1991; Uecker and Nadel, 1996). Understanding the link between behavioural and morphological platforms will help in improving the health and educational needs of subjects with FAS, especially in South Africa where there is a high prevalence of FAS.

1.5 The Present Study:

In the present study, a chronic alcohol administration paradigm was used to develop an adult mouse model of FAS. Comparisons of the architecture of the adult mouse brain were performed using the Nissl staining method. Different antibodies, specific to different cell types, were used to immunostain different types of cells or neurons within the brain of an adult mouse model of FAS. The populations of these cells were estimated and compared with the controls. The selected areas of interest in the brain for this study are those areas associated with sleep (sleep centres such as hypothalamus and pons), memory and cognition (dentate gyrus of hippocampus), somatosensory processing (barrel fields of cerebral cortex) and motor coordination (cerebellum).

1.5.1. Main objective:

This study aims to test whether a specific mouse model of FAS presents with a range of select neurological deficits that mimic those seen in FAS humans – is this mouse model of FAS valid?

1.5.2. Specific objectives:

(A) To investigate adult hippocampal neurogenesis by quantifying the populations of actively proliferating cells and immature neurons in the hippocampal dentate gyrus in the brains of adult controls and mice FAS models (addressed in Chapter 2).

(B) To compare the size and pattern of distribution of the barrel fields located within the primary somatosensory cortex in the brains of adult controls and mice FAS models (addressed in Chapter 3).

(C) To compare and quantify the populations of different cell types (Purkinje, Golgi, granule and Basket cells) in the cerebellar cortex of adult controls and mice FAS models (addressed in Chapter 4).

(D) To compare and quantify the populations of different cell types (cholinergic, catecholaminergic, serotonergic and orexinergic cells) in the sleep centres (hypothalamus, midbrain and pons) of adult control and mice FAS model (addressed in Chapter 5).

1.6. Summary of Main Findings:

1.6.1. Neurogenesis in the hippocampus of C57BL/6J mice at early adulthood (56 days post-natal) following chronic prenatal alcohol exposure:

We examined the effect of chronic prenatal alcohol exposure on the process of adult neurogenesis in C57BL/6J mice once they had reached early adulthood, this

being 56 days post-natal. Pregnant mice, and their *in utero* litters, were exposed to alcohol, through oral gavage, on gestational days 7 – 16, with recorded blood alcohol concentrations averaging 1.84 mg/ml (chronic alcohol, or CA, group). Two control groups, an oral gavage sucrose control group (chronic alcohol control, or CAc, group) and a non-treated control group (NTc group), were also examined. At 56 days post-natal, the pups from each group, now in their early adulthood, were sacrificed and the left hemisphere of the brain sectioned in a sagittal plane, and stained for Nissl substance with cresyl violet, and immunostained for the endogeneous markers of adult neurogenesis, Ki-67 which labels proliferative cells, and doublecortin (DCX) which labels immature neurons. The overall pattern of adult neurogenesis throughout the brain was identical in all three groups studied, and resembles that generally reported for mammals, and specifically laboratory rodents. Quantification of the number of Ki-67 cells in the hippocampus indicated that no statistically significant difference between the three experimental groups was evident. Thus, the prenatal exposure to alcohol administered in this study does not appear to have a strong effect on the proliferative process in the adult hippocampus. In contrast, the numbers of immature neurons, labelled with DCX, was statistically significantly lower in the group of mice exposed to prenatal alcohol compared with the two control groups. Thus, the prenatal alcohol exposure appears to lower either the rate of conversion of proliferative cells to immature neurons or the survival of immature neurons in the hippocampus. This lowered number of immature neurons, and their associated function, appears to mirror the memory dysfunctions observed in FASD children.

1.6.2. Changes to the somatosensory barrel cortex in C57BL/6J mice at early adulthood (56 days post-natal) following chronic prenatal alcohol exposure:

Children with fetal alcohol spectrum disorder (FASD) have impaired sensory processing skills as a result of neurodevelopmental anomalies. The somatosensory barrel field in the neocortex of rodents is a readily accessible model for studying the effects of pre- and peri-natal alcohol exposure. Each barrel processes sensory input from 1 – 3 facial vibrissae, and within the barrel field, the posterior medial barrel subfield (PMBSF) receives inputs from the large vibrissae on the contralateral face. In studies of rat FASD models, prenatal and postnatal alcohol exposures significantly reduced the total area, individual barrels and septal portion of the PMBSF. Here we provide further evidence for barrel field modification following prenatal chronic alcohol exposure (PAE) in C57BL/6J mice at early adulthood (postnatal day [PND] 56). Pregnant mice were exposed to alcohol, through oral gavage (chronic alcohol, CA, group), on gestational days 7 – 16. Two control groups, an oral gavage sucrose control (chronic alcohol control, CAc, group) and a non-treated control (NTc group), were also examined. At PND 56 the left cerebral hemisphere of mice from each group were manually flattened, sectioned parallel to the pial surface and reacted for cytochrome oxidase. We found reductions in the mean area of the PMBSF enclosure, total mean area of the PMBSF barrels, mean areas of the individual PMBSF barrels and mean area of the septal portion of the PMBSF in the CA group, but these differences were not significantly different from controls. Specific individual barrels showed significant reductions in size with PAE. Although reductions in size were observed across barrel rows in the CA group compared to controls, significant reductions in barrel sizes were only observed in barrel rows D and E. This seems to

indicate that PAE hinders PMBSF development, which may explain the reason for the sensory-motor delays in children exposed to prenatal alcohol.

1.6.3. Lack of changes to the cerebellar cortex of C57BL/6J mice at early adulthood (56 days post-natal) following chronic prenatal alcohol exposure:

We examined the effect of chronic prenatal alcohol exposure on the architecture and neurochemistry of the vermal cerebellar cortex of C57BL/6J mice exposed to prenatal alcohol once they had reached 56 days post-natal. Pregnant mice were exposed to alcohol, through oral gavage, on gestational days 7 – 16, with recorded blood alcohol concentrations averaging 1.84 mg/ml (chronic alcohol group, CA). Two control groups, an oral gavage sucrose control group (chronic alcohol control group, CAc) and a non-treated control group (NTc), were also examined. At 56 days post-natal, the pups from each group were sacrificed and the cerebellum sectioned in a sagittal plane, with sections stained for Nissl (cresyl violet) or immunostained for the calcium-binding proteins parvalbumin, calbindin and calretinin, labelling specific neuronal structures within the cerebellar cortex. The overall architecture and neurochemistry of the vermal cerebellar cortex did not differ between the experimental groups. Stereological quantification of the density of Nissl cell bodies and parvalbumin stained neurons in the molecular layer of the cerebellar cortex did not differ between experimental groups. In addition, the stereological estimation of area and volume of the Purkinje cells immunolabelled with calbindin did not differ between groups. Thus, despite the known deleterious effects of alcohol exposure on the developing nervous system, no specific differences were observed in the current study. This lack of variation is discussed in relation to the timing of

exposure to alcohol and cerebellar development and the potential systems-specific effects of prenatal alcohol exposure.

1.6.4. Changes in the cholinergic, catecholaminergic, orexinergic and serotonergic neurons forming part of the sleep systems of adult mice exposed to intrauterine alcohol:

We examined the effect of chronic prenatal alcohol exposure on certain neurons involved with the sleep-wake cycle of C57BL/6J mice exposed to prenatal alcohol once they had reached 56 days post-natal. Pregnant mice were exposed to alcohol, through oral gavage, on gestational days 7 – 16, with recorded blood alcohol concentrations averaging 1.84 mg/ml (chronic alcohol group, CA). Two control groups, an oral gavage sucrose control group (chronic alcohol control group, CAc) and a non-treated control group (NTc), were also examined. At 56 days post-natal, the pups from each group were sacrificed and the whole brain sectioned in a coronal plane and immunolabelled for cholineacetyltransferase (ChAT), tyrosine hydroxylase (TH), serotonin (5HT), and orexin-A (OxA) which labels cholinergic, catecholaminergic, serotonergic and orexinergic neurons respectively. The overall nuclear organization and neuronal morphology were identical in all three groups studied, and resemble that reported for laboratory rodents. Quantification of the numbers of ChAT immunopositive (+) neurons of the pons, the TH+ neurons of the pons and the OxA+ neurons of the hypothalamus showed no statistically significant difference between the three experimental groups. The stereologically estimated areas and volumes of OxA+ neurons in the CA group were statistically significantly larger than the groups not exposed to prenatal alcohol, but the ChAT+ neurons in the CA

group were statistically significantly smaller. No statistically significant difference was found in the area and volume of TH+ neurons between the three experimental groups. These differences are discussed in relation to the sleep disorders recorded in children with fetal alcohol spectrum disorder.

CHAPTER TWO: Neurogenesis in the hippocampus of C57BL/6J mice at early adulthood (56 days post-natal) following chronic prenatal alcohol exposure

2.1. Introduction:

Neurogenesis is the process of the generation of new neural cells from proliferating adult stem cells, and this process persists throughout life in most mammals (Barlow and Targum, 2007; Gil-Perotin et al., 2009; Patzke et al., 2015; Lazarov and Hollands, 2016; Opendak et al., 2016). Within the hippocampus, adult hippocampal neurogenesis begins with the progenitor or stem cells found in the subgranular zone (SGZ), which is located deep to the granule cell layer (GCL) of the dentate gyrus. The pluripotent stem cells in the SGZ undergo proliferation, with some of the newly born cells remaining as progenitor stem cells, some differentiating into glia cells, while some differentiate into neurons (Gil-Perotin et al., 2009). The cells destined to become neurons migrate a short distance to the GCL and eventually integrate into the existing hippocampal circuitry where they augment hippocampal functions (Barlow and Targum, 2007; Gil-Perotin et al., 2009). The neurogenic activity in the hippocampal dentate gyrus can be readily modulated by both internal (growth factors, neurotransmitters and humoral factors) and external factors (drugs, environmental and social conditions, stress, starvation and physical activity) (Shors et al., 2012; Song et al., 2012; Cameron and Glover, 2015; Opendak et al., 2016).

Fetal exposure to alcohol has been shown to impact neurogenesis during brain development and maturation, causing neurodevelopmental and neurobehavioural problems that are termed fetal alcohol syndrome (FAS) (Famy et al., 1998; Sulik,

2005; Niccols, 2007; Gil-Mohapel et al., 2010, 2011; Incerti et al., 2010). Memory impairment and learning difficulties have been reported in children with FAS (Uecker and Nadel, 1996), pointing towards pathology of the hippocampus, a brain region involved in the formation and retrieval of memories (Gil-Mohapel et al., 2010). Fetal alcohol exposure appears to cause a reduction in the volume of hippocampus, which is thought to result from either an overall reduction in cell proliferation or an increase in cell death or both, leading to impairments in memory functions (Archibald et al., 2001; Autti-Rämö, 2002; Klintsova et al., 2007; Gil-Mohapel et al., 2010). Significant reductions in the numbers of proliferative cells and immature neurons in the hippocampus were reported in alcohol-exposed 7-day old mice (Ieraci and Herrera, 2007), as well as in mice models exposed to either chronic or binge alcohol paradigms during the fetal stage (Nixon and Crews, 2002). In addition, prenatal administration of alcohol in rats has been shown to decrease neuron numbers in the dentate gyrus of hippocampus (Miller, 1995). In contrast, postnatal administering of alcohol resulted in a significant increase in neuron numbers in the rodent dentate gyrus (Miller, 1995), complicating the interpretation of the effects of alcohol on the hippocampus. Some studies argue that such an increase is simply a compensatory process driven by the destructive effect of alcohol on the dentate gyrus (Pawlak et al., 2002; Zharkovsky et al., 2003; Åberg et al., 2005), while other studies reported the opposite effect (Miller, 1995; Nixon and Crews, 2002), and yet others report no effect (Wozniak et al., 2004; Klintsova et al., 2007; Helfer et al., 2009).

The presentation of FAS-related defects depends on the gestational day of alcohol exposure, but does not depend on the mode of exposure (Sulik et al., 1981; Webster et al., 1983; Cudd, 2005). Thus, several different experimental designs have been used to evaluate the effects of alcohol on the hippocampus (Sulik et al., 1981;

Webster et al., 1983; Nixon and Crews, 2002; Pawlak et al., 2002; Cudd, 2005; Redila et al., 2006; Zagron and Weinstock, 2006; Ieraci and Herrera, 2007). Recently, Gil-Mohapel et al. (2014) found that prenatal alcohol exposure had no effect on the process of hippocampal cell proliferation and neuronal generation in adolescent (post-natal days 31-35) or older (post-natal days 378-394) rats, but the rate of neuronal generation was significantly reduced. Given the somewhat contradictory range of findings, the present study aimed to provide further experimental data by investigating the effect of prenatal alcohol exposure, using oral-gavage, on adult hippocampal neurogenesis of mice at early adulthood (post-natal day 56).

2.2. Materials and methods:

2.2.1. Breeding and prenatal ethanol exposure:

All animals were treated and used according to the guidelines of the University of the Witwatersrand Animal Ethics Committee (Clearance No. 2012/15/2B), which parallel those of the National Institutes of Health (NIH) for the care and use of animals in scientific experimentation. 12 week-old female C57BL/6J mice (*Mus musculus*) were allocated into three experimental groups: Chronic Alcohol exposure (CA), control for Chronic Alcohol exposure (CAc), and a Non-Treatment control group (NTc). For effective mating, 1–2 female mice were introduced into the cage of a C57BL/6J male mouse for 12 hours, which was considered gestational day 0 (GD 0). In all, a total of 14 female mice (4–5 mice assigned to each experimental group) and 8 male mice were used to generate the required numbers of pups used in the present study.

For the CA group, each pregnant mouse received a dose of 7.5 µl/g of 50 % alcohol in distilled water (5.9 g/kg) per day (Haycock and Ramsay, 2009; Knezovich and Ramsay, 2012) for 10 consecutive days by oral gavage, starting from GD 7 (Webster et al., 1980; Sulik et al., 1981; Webster et al., 1983; Choi et al., 2005; Redila et al., 2006; Parnell et al., 2009), while each pregnant mouse in the CAc group received an equivalent dose of isocaloric sucrose (704 g/L) by oral gavage over the same period (Haycock and Ramsay, 2009; Knezovich and Ramsay, 2012). To control for the possible influence of post-traumatic stress in the pregnant mice, pregnant mice in the NTc group did not undergo any oral gavage. Food and water was provided *ad libitum* to the mice, except in the control groups (CAc and NTc), where it was withheld for two hours post-gavage in order to partially mimic the anorectic effect of alcohol (Haycock and Ramsay, 2009). The pups were weaned 21 days after birth and then the male and female pups separated. Three pups of the same sex from each experimental group were kept in separate cages (cage dimensions: 200 x 200 x 300 mm) with adequate food and water supplies until post-natal day (PND) 56.

2.2.2. Blood alcohol concentration assay in the pregnant mice:

On the last day (10^{th} day) of oral gavage (GD 16), a small lesion was made at the site of the saphenous vein on the left hind legs of all the pregnant mice in the CA and CAc experimental groups. The saphenous bleeding procedure was performed on the pregnant mice in the sucrose group in order to mimic the effects of the bleeding on the alcohol exposed pregnant mice. The non-treatment pregnant mice served as controls for the possible effects of the bleeding and/or the oral gavage procedures. 50 µl of blood was drawn into heparinized capillary tubes at 30 min post-gavage

(Bielawski and Abel, 1997) to determine the blood alcohol concentration (BAC). The blood samples from the FAS model and the sucrose control were stored at 4°C overnight after which they were centrifuged with Vivaspin500 100 µm membrane tubes (Biotech, South Africa) for 30 min before the serum was extracted and the BAC analyzed using an EnzyChrom™ Ethanol Assay Kit (BioVision, South Africa). The pregnant mice belonging to the CA group that were administered alcohol had an average BAC of 1.84 mg/ml (s.e. = 0.39), which is above the pharmacologically significant level of 1 mg/ml reported by Rhodes et al. (2005) and Sulik (2005).

2.2.3. Sacrifice and tissue processing:

At PND 56, when the prenatally-alcohol-exposed mice reached adulthood, a total number of six mice (n = 6) from each experimental group (1–2 mice randomly selected from each litter set) were weighed and then euthanized (Eutha-naze 1 ml/kg, contains sodium pentobarbitone 100 mg/ml, intra-peritoneally) before being perfused trans-cardially with 0.9% cold (4°C) saline followed immediately by cold 4% paraformaldehyde in 0.1 M phosphate buffer (PB). The brain was removed from the skull, weighed and post-fixed for 24 h in 4% paraformaldehyde in 0.1 M PB at 4°C. The brains were then cryoprotected by immersion in 30 % buffered sucrose solution in 0.1 M PB at 4°C until they equilibrated. The left cerebral hemisphere of all 18 individual mice was dissected from the remainder of the brain, frozen in crushed dry ice, and sectioned in a sagittal plane at 50 µm thickness using a sliding microtome. A one in three series of sections was stained for Nissl substance (cresyl violet) to reveal cytoarchitectural features, Ki-67 immunostaining, and doublecortin (DCX) immunostaining. The Nissl sections were mounted on 0.5% gelatine-coated slides,

dried overnight, cleared in a 1:1 mixture of 100% ethanol and 100% chloroform and stained with 1% cresyl violet. The other sections were used for free-floating Ki-67 and DCX immunohistochemistry.

2.2.4. Immunohistochemistry protocol:

The sections used for immunohistochemical staining were initially incubated in a solution containing 1.6% of 30% H_2O_2, 49.2% methanol and 49.2% 0.1M PB solution, for 30 min to reduce endogenous peroxidase activity, which was followed by three 10 min rinses in 0.1M PB. To block unspecific binding sites the sections were then pre-incubated for 2 h, at room temperature, in blocking buffer (3% normal goat serum or 3% normal rabbit serum, 2% bovine serum albumin and 0.25% Triton X-100 in 0.1 M PB). Thereafter, the sections were incubated for 48 h at 4°C in the primary antibody solution (1:1000, rabbit anti-Ki-67, NCL-Ki-67p Dako in blocking buffer or 1:300, goat anti-doublecortin, DCX, SC-18 Santa Cruz Biotech in blocking buffer) under gentle agitation. After incubation the sections were rinsed for 10 min in 0.1 M PB three times and then incubated in a secondary antibody solution (1:1000 dilution of biotinylated goat anti-rabbit IgG, BA1000, 3% normal goat serum, and 2% bovine serum albumin in 0.1 M PB or 1:1000 dilution of biotinylated rabbit anti-goat IgG, BA 5000, Vector Labs, in 3% normal rabbit serum and 2% bovine serum albumin in 0.1 M PB) for 2 h at room temperature. This was followed by three 10 min rinses in 0.1 M PB, after which sections were incubated for 1 h in an avidin-biotin solution (1:125; Vector Labs), followed by a further three 10 min rinses in 0.1 M PB. Sections were then placed in a solution containing 0.05% diaminobenzidine (DAB) in 0.1 M PB for 5 min, followed by the addition of 3.3 µl of 30% hydrogen peroxide per 1 ml

of DAB solution. Chromatic precipitation was visually monitored under a low power stereomicroscope until the background stain was at a level that would allow for accurate architectonic matching to the Nissl sections without obscuring the immunopositive structures. Development was stopped by placing sections in 0.1 M PB for 10 min, followed by two more 10 min rinses in this solution. Sections were then mounted on 0.5% gelatine coated glass slides, dried overnight, dehydrated in a graded series of alcohols, cleared in xylene and coverslipped with DPX. To rule out non-specific staining of the immunohistochemical protocol, we ran tests on sections where we omitted the primary antibody, and sections where we omitted the secondary antibody. In both cases no staining was observed.

2.2.5. Quantification of cell numbers and statistical analysis

The Nissl stained sections were used to determine and qualitatively compare the distribution of cells in the hippocampus between experimental groups. Digital photomicrographs of these cell distributions were captured using Zeiss Axioshop and Axiovision software. No pixilation adjustments or manipulation of the captured images was undertaken, except for the adjustment of contrast, brightness, and levels using Adobe Photoshop 7.

To quantify the number of Ki-67 immunolabelled cells in the left hippocampus of each mouse, we exhaustively counted all positively immunolabelled cells with a clearly defined nuclear boundary observed in the SGZ along the whole length of the dentate gyrus using a 40x objective (Erasso et al., 2012) on an Axiovision light microscope. The total number of labelled cells in the left dentate gyrus of each brain was determined by multiplying the number of labelled cells counted by three (Mouton

et al., 2012). To reduce bias, the Ki-67 immunolabelled nuclei were counted again under blinded conditions in a sub-sample after a two-week interval. No significant differences were observed between the counts recorded in the two time intervals, and thus only the total counts are presented.

For the quantification of DCX immunopositive cells, a modified unbiased stereological procedure was used as described previously by Segi-Nishida et al. (2008), Malberg et al. (2000) and Noori and Fornal (2011). Immunopositive DCX cells in the SGZ of the dentate gyrus were counted at 40x magnification using an Olympus BX-60 light microscope equipped with a video camera. Cells were included if the cells lay within, or touched, the SGZ. The SGZ was defined as the area from one cell diameter within the GCL from the hilus-GCL border and two cell diameters below the hilus-GCL border (Eriksson et al., 1998). Cells were excluded if the cell was more than two cell diameters from the GCL, focusing through the thickness of the section according to optical dissector principle (Gundersen et al., 1988; West, 1993; Coggeshall and Lekan, 1996) to avoid errors due to oversampling. Similar to the Ki-67 analysis, every section was counted throughout the whole length of the hippocampus and the sum was multiplied by 3 to provide an estimate of the total number of immunopositive DCX cells in the left hippocampus of each mouse (Mouton et al., 2012).

An analysis of variance was performed on the data to evaluate group (CA, CAc and NTc) differences in mean Ki-67 or DCX counts. All statistical analyses were performed using SPSS Inc programme (version 22.0). A significance level of 5% was used as an indicator of a significant difference for all the statistical analyses.

2.3. Results:

2.3.1. General observations on the body, brain, and patterns of adult neurogenesis:

The pups that experienced chronic prenatal alcohol exposure (CA group) showed no overt signs of FAS, in that no craniofacial abnormalities were readily apparent and there was no evident reduction in overall body mass. At the time of sacrifice, the average body masses of the mice were: CA male – 18.96 g (s.d. 2.75 g), CA female – 15.31 g (s.d. 1.05 g); CAc male – 20.53 g (s.d. 1.14 g), CAc female – 16.06 g (s.d. 0.63 g); NTc male – 19.93 g (s.d. 0.98 g), NTc female – 17.86 g (s.d. 2.43 g). No statistically significant differences were observed between experimental groups in terms of body mass.

In addition, there were no observable differences in the general morphology of the brains of mice treated with alcohol (CA group), sucrose (CAc group) or the non-treated control group (NTc). The average brain masses recorded for each group were: CA male – 0.406 g (s.d. 0.015 g), CA female – 0.397 g (s.d. 0.009 g); CAc male – 0.409 g (s.d. 0.009 g), CAc female – 0.388 g (s.d. 0.009 g); NTc male – 0.403 g (s.d. 0.008 g), NTc female – 0.393 g (s.d. 0.012 g). No statistically significant differences were observed between groups in terms of brain mass. In addition, Nissl staining revealed no observable abnormalities in the neuronal distribution pattern in the brains of all the experimental mice, and specifically so in the dentate gyrus of the hippocampus (Fig. 2.1).

For all mice studied there were no marked differences in the shape or size of the Ki-67 immunopositive cells in either the subgranular layer of the dentate gyrus or the subventricular zone of the lateral ventricle. In all 18 individual mice, irrespective of the experimental group, we found that the distribution of cells immunopositive for Ki-

67 was very similar. We observed Ki-67 immunopositive cells in two distinct proliferative regions – the dentate gyrus of the hippocampus, and the subventricular zone of the lateral ventricle (Figs. 2.2, 2.3). A distinct subgranular zone, located between the granular cell layer and the hilus of the dentate gyrus of the hippocampus was evident in all mice examined (Fig. 2.2). Numerous Ki-67 immunopositive cells were observed in the subventricular zone of the lateral ventricle in all the mice studied. From the SVZ two streams of Ki-67 immunopositive cells could be observed, one that ran dorsal and then rostral to the caudate nucleus, and one that ran caudal to the caudate nucleus (Fig. 2.3). The stream that ran dorsal and anterior to the caudate nucleus was observed to turn, in a rostral direction, into the olfactory tract to infuse the olfactory bulb with Ki-67 immunopositive neurons (Fig. 2.3). The stream that ran caudal to the caudate nucleus was observed to extend ventrally to the anterior commissure, from where it made a lateral extension around the globus pallidus towards the piriform cortex.

In all 18 mice investigated, the distribution of cells immunopositive for DCX was very similar. A distinct subgranular zone, located between the granular cell layer and the hilus of the dentate gyrus in the hippocampus, was evident displaying DCX immunopositive cells (Fig. 2.2). The majority of these DCX positive cells exhibited processes that extended into the molecular layer of the dentate gyrus. In all mice clusters of DCX positive cells and processes were present in the subventricular zone (SVZ) with the highest density of immunolabelled structures observed towards the rostral end of the lateral ventricle (Fig. 2.3). The labelled cells were characterized by relatively short unipolar and/or bipolar processes. From the SVZ a stream of DCX immunopositive cells could be observed – the rostral migratory stream (RMS). DCX immunopositive cells were found between the rostrodorsal aspects of the caudate

nucleus and the subcortical white matter, as well as on the caudal aspect of the caudate nucleus. At the rostroventral pole of the caudate nucleus, the “stream” of immunolabelled cells turned in a rostral direction with the stream ending in the olfactory bulb (Fig. 2.3). The DCX immunopositive cells in the RMS were often obscured by the numerous tangentially oriented fibres of the stream, but when readily viewable were found to be fusiform in shape, small in size and displayed bipolar processes. The DCX immunopositive cells and processes found along the caudal aspect of the caudate nucleus were observed to join the RMS where it turned to enter the olfactory bulb.

In the main olfactory bulb (MOB) DCX immunoreactivity was evident in all layers in all mice. The majority of DCX-expressing cells were located in the granular cell layer (GCL), exhibiting radially orientated DCX-positive cells and processes. Most of these cells were bipolar and ovoid in shape. The external plexiform layer of the olfactory bulb (EPL) presented with distinct radial fibres, while the glomerular layer (GL) displayed sparsely distributed DCX immunopositive cells that presumably represent periglomerular cells (Fig. 2.3). In addition to these two main regions of DCX immunopositive structures, cells were observed in layer II of the piriform cortex, and the occasional cell was observed in the amygdala. Weakly labelled DCX immunopositive neurons were occasionally observed in the rostral half of the cerebral neocortex in some individuals.

2.3.2. Quantification of proliferative cells (Ki-67 immunopositive) in the dentate gyrus of the hippocampus:

Our quantitative analysis of the numbers of Ki-67 immunopositive cells, presumably proliferative cells, in the dentate gyrus of the left hippocampus of mice from the three different experimental groups revealed a distinct homogeneity in numbers between individuals in the same group, and between groups. For the CA group, the average number of Ki-67 immunopositive cells was 1653.5 (s.e. 126.3), for the CAc group it was 1622.5 (s.e. 123.1) and for the NTc group it was 1349.0 (s.e. 90.3) (Fig. 2.4A). Thus, while there is a trend for the two groups that underwent oral gavage procedures, irrespective of the presence of ethanol, to have higher numbers of proliferative cells in the dentate gyrus, statistical analyses using analysis of variance and post-hoc pairwise comparisons revealed that the higher number of proliferative cells in the CA group was not statistically significantly different from the CAc group ($p = 0.980$) or the NTc group ($p = 0.178$). A comparison between CAc and NTc groups was also not statistically significantly different ($p = 0.241$).

2.3.3. Quantification of immature neurons (DCX immunopositive) in the dentate gyrus of the hippocampus:

In contrast to the quantification of Ki-67 immunopositive cells, our quantification of the numbers of DCX immunopositive cells, presumably immature neurons, in the left hippocampus of mice from the three experimental groups did reveal significant inter-group differences. For the CA group, the average number of DCX immunopositive cells was 10 441.0 (s.e. 913.7), for the CAc group it was 15 238.5 (s.e. 1019.8) and for the NTc group it was 19 963.0 (s.e. 817.3) (Fig. 2.4B).

Thus, it is apparent that the group exposed to prenatal alcohol, the CA group, had substantially lower numbers of DCX immunopositive cells in the dentate gyrus. Statistical analyses confirmed that the estimated number of DCX immunopositive cells was significantly lower in the CA group when compared to the CAc group ($p = 0.006$) or the NTc group ($p < 0.0001$), but there was not statistically significant difference between the CAc and NTc groups ($p = 0.404$).

Figure 2.1: Photomicrographs of the dorsal left hippocampus of the mouse in the sagittal plane, showing the general morphology of the dentate gyrus (**DG**) and cornu ammonis (**CA1**, **CA3**) regions in the three different groups analyzed in the present study, the group exposed to chronic prenatal alcohol (**CA**) (**A**), the prenatal gavage control group (**CAc**) (**B**) and the non-treated control group (**NTc**) (**C**). Note the lack of observable differences in the structure of these hippocampal regions between groups. In all images dorsal is to the top and rostral to the left. Scale bar in **C** = 500 µm and applies to all.

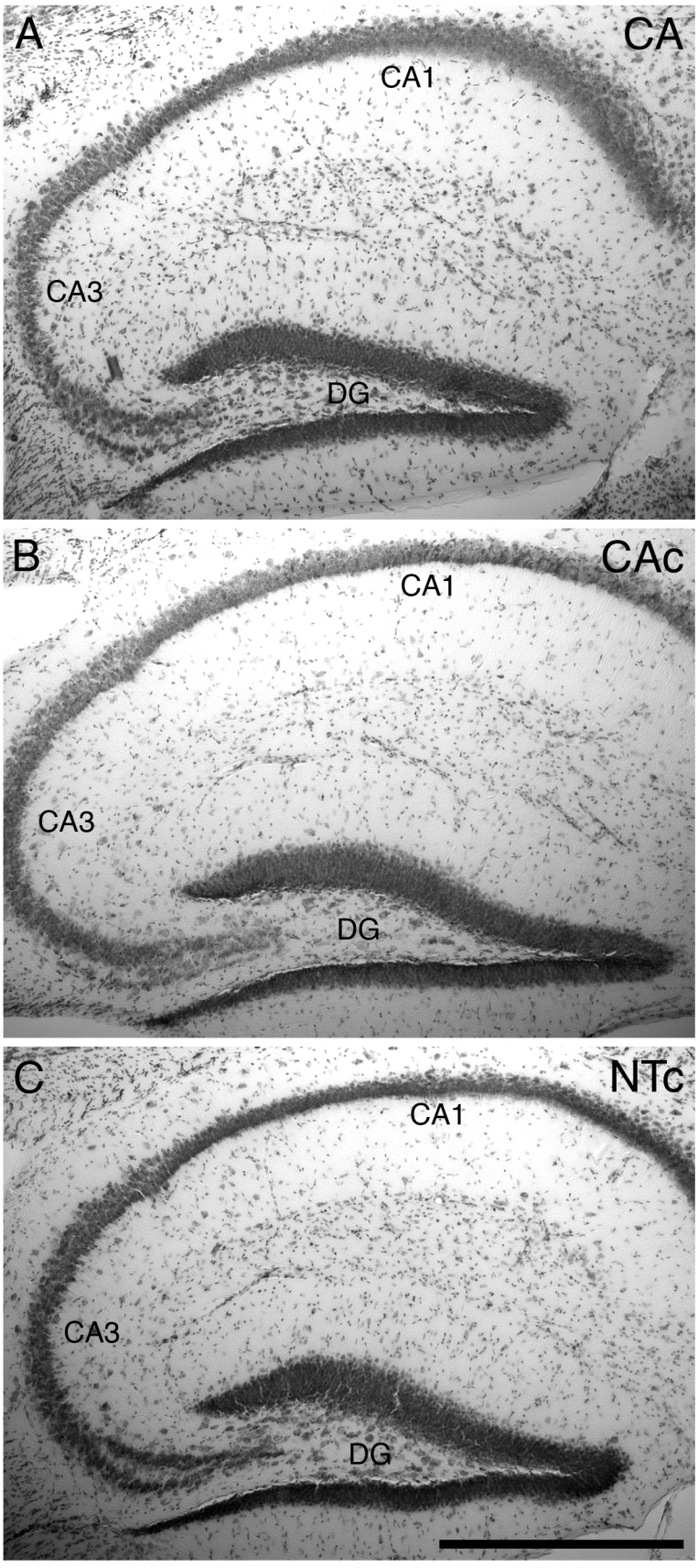
A
CA
CA1
CA3
DG
B
CAc
CA1
CA3
DG
C
NTc
CA1
CA3
DG

Figure 2.2: Photomicrographs of the dorsal left hippocampus of the mouse in the sagittal plane immunostained for **Ki-67** (**A**, **C**, **E**) or doublecortin (**DCX**) (**B**, **D**, **F**) in the three different groups analyzed in the present study, the group exposed to chronic prenatal alcohol (**CA**) (**A**, **B**), the prenatal gavage control group (**CAc**) (**C**, **D**) and the non-treated control group (**NTc**) (**E**, **F**). The insets in the upper right corner of each image represent higher magnification photomicrographs of each region to demonstrate cellular morphology. Qualitatively, the density of both Ki-67 and DCX immunostained cells and structures appears similar, but quantification (see Fig. 4) revealed differences. In all images dorsal is to the top and rostral to the left. Scale bar in **F** = 500 µm and applies to **A** – **F**. Scale bar in inset **E** = 100 µm, and applies to all insets.

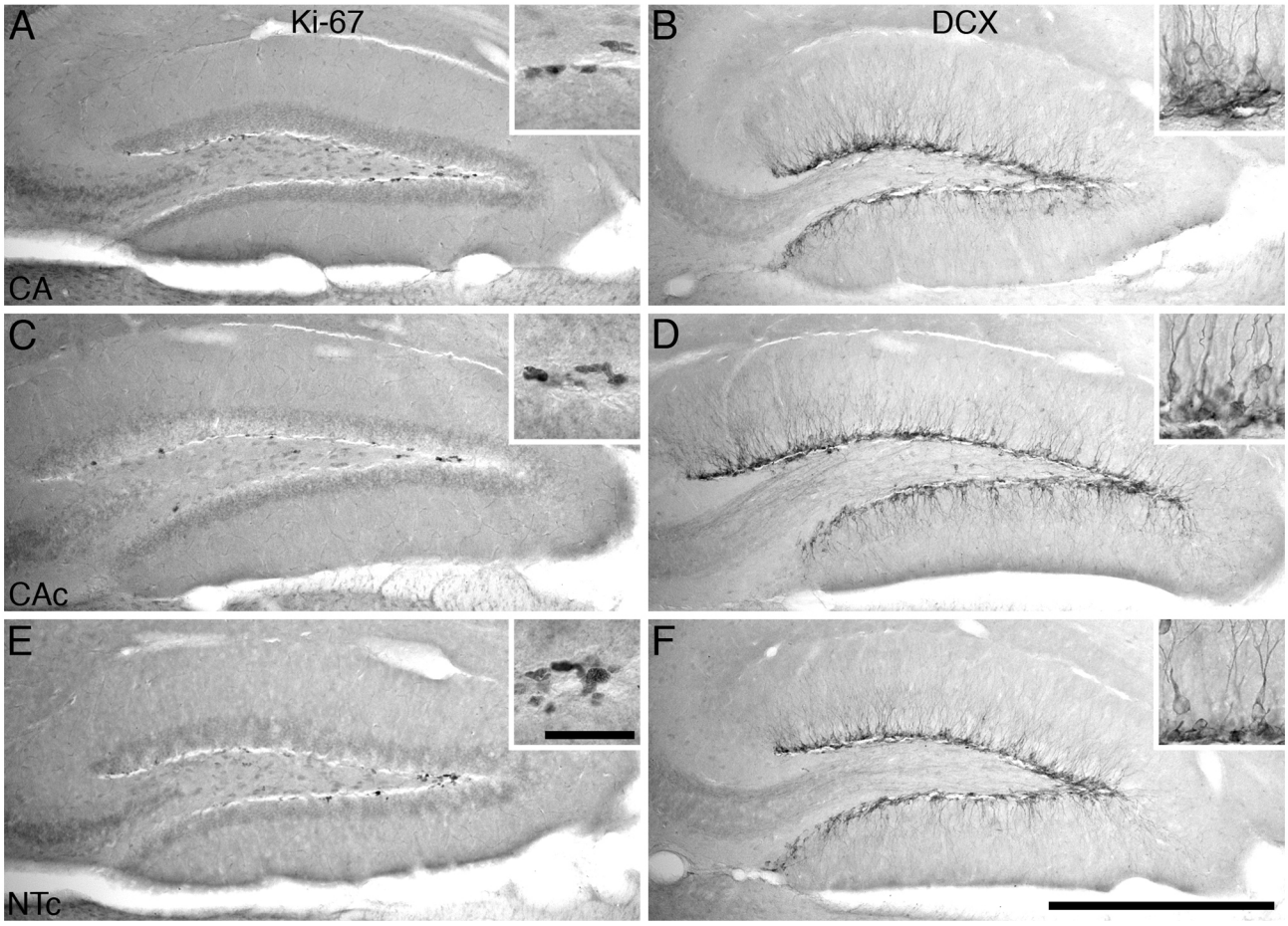
A
Ki-67
B
DCX
CA
C
D
CAc
E
F
NTc

Figure 2.3: Photomicrographs of Ki-67 (**A**, **B**) and doublecortin (DCX) (**C**, **D**) immunostained sections showing different aspects of the rostral migratory stream (**RMS**) in the mice studied. **A**. Ki-67 immunostained cells of the **RMS** rostral to the caudate nucleus (**C**) and the flexure of this stream as it enters the olfactory bulb (**OB**). Scale bar in **A** = 500 µm. **B**. Higher power photomicrograph of Ki-67 immunostained cells in the **RMS** showing their typical clustered appearance. Scale bar in **B** = 100 µm. **C**. DCX immunostained structures in the subventricular zone (**SVZ**) of the lateral ventricle (**LV**) located caudal and dorsal to the caudate nucleus (**C**), and giving rise to the **RMS**. Scale bar in **C** = 250 µm. **D**. DCX immunostained cells and dendrites surrounding the glomeruli found in the glomerular layer (**GL**) of the olfactory bulb. Scale bar in **D** = 100 µm. In all images dorsal is to the top and rostral to the left.

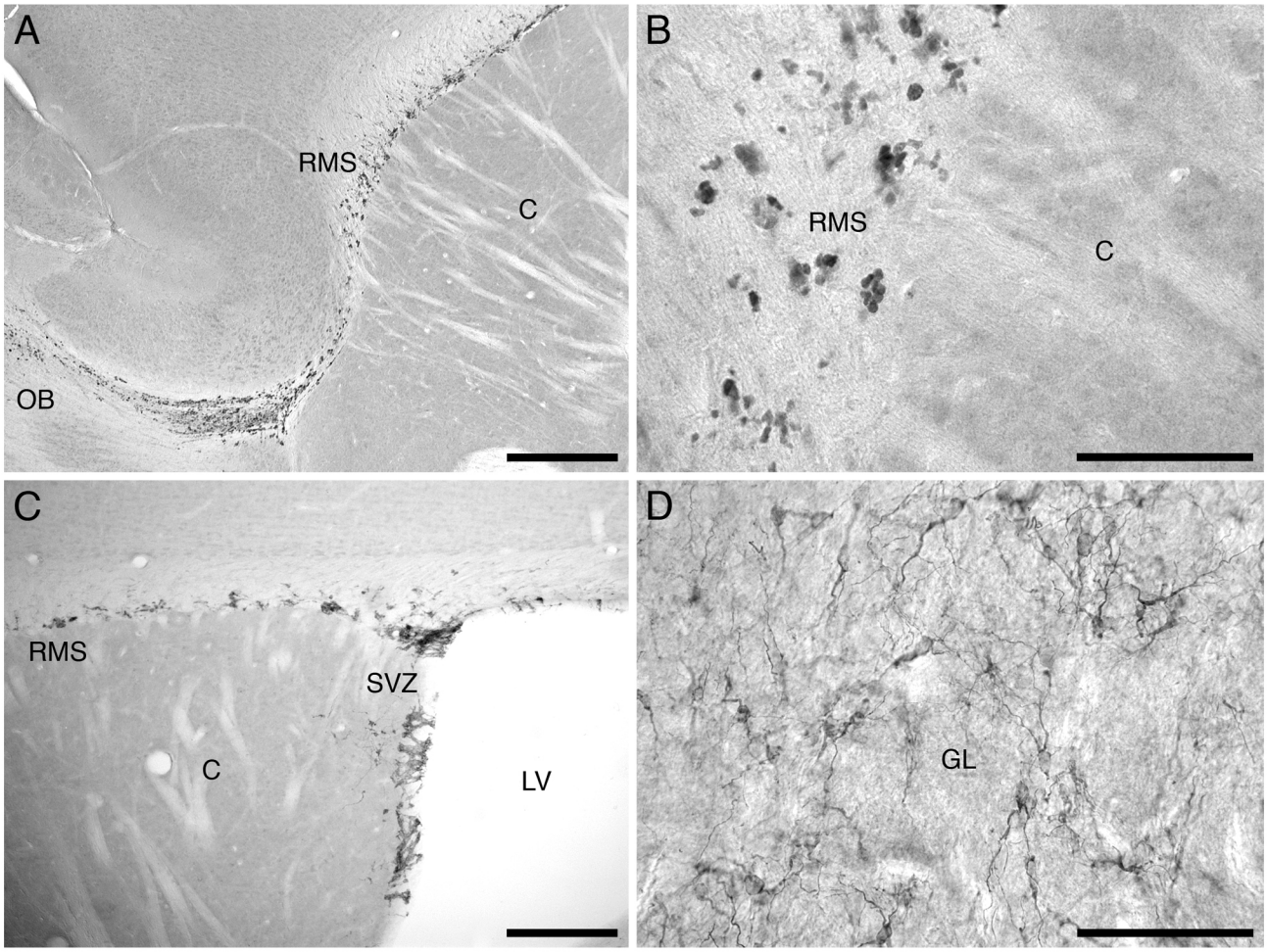
A
RMS
C
OB
B
RMS
C
C
RMS
SVZ
C
LV
D
GL

Figure 2.4: Graphs showing the average numbers of Ki-67 (**A**) and doublecortin (DCX) (**B**) immunoreactive cells in the left hippocampus of three different groups (n = 6 per group) analyzed in the present study, the group exposed to chronic prenatal alcohol (**CA**), the prenatal gavage control group (**CAc**) and the non-treated control group (**NTc**). Note that while the two groups that underwent gavage treatment (**CA** and **CAc**) appear to have slightly higher numbers of Ki-67 immunoreactive cells than the untreated group (**NTc**) (**A**), these are not statistically significant differences. The number of DCX immunoreactive cells (**B**) was statistically significantly (*****) lower in the **CA** group compared to the two control groups (**CAc** and **NTc**). The vertical bars represent standard error bars.

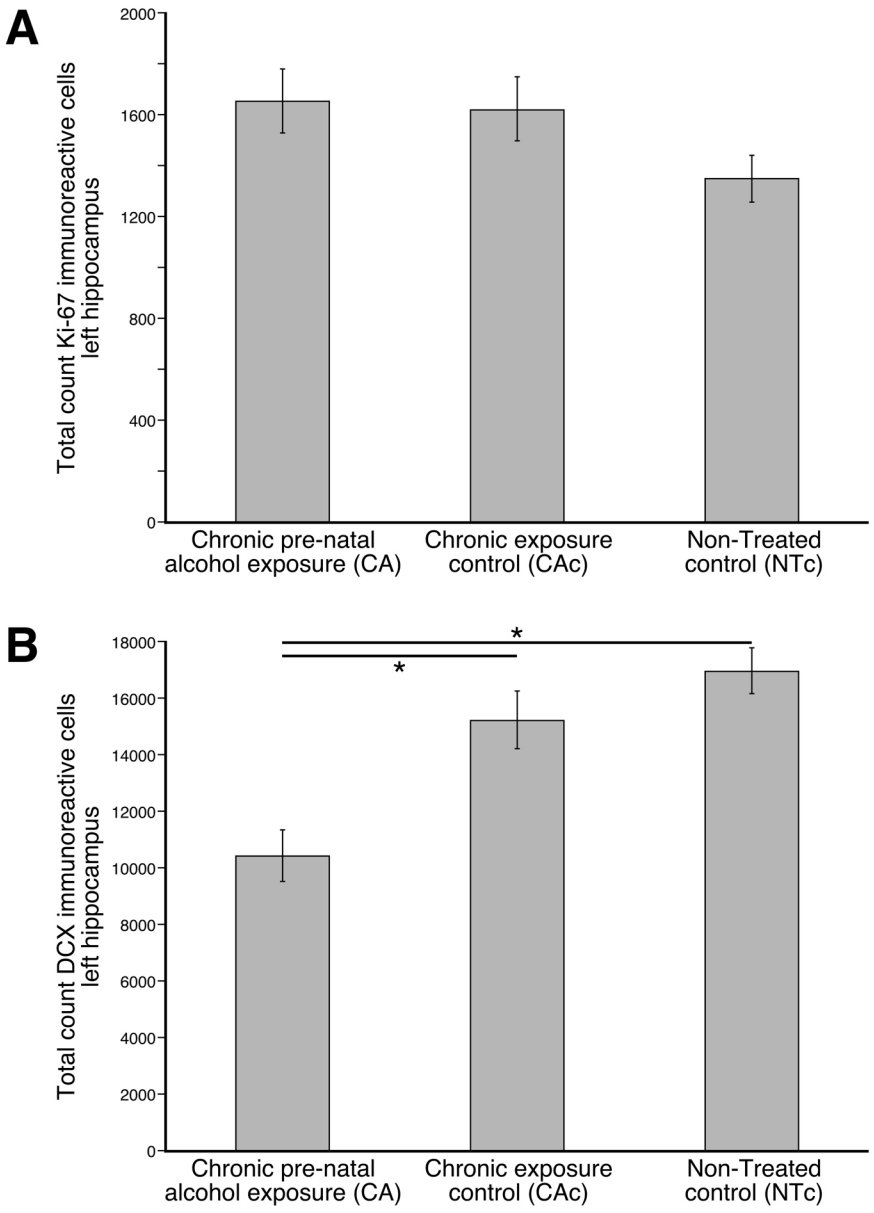
A
Total count Ki-67 immunoreactive cells left hippocampus
2000
1600
1200
800
400
0
Chronic pre-natal alcohol exposure (CA)
Chronic exposure control (CAc)
Non-Treated control (NTc)
B
Total count DCX immunoreactive cells left hippocampus
18000
16000
14000
12000
10000
8000
6000
4000
2000
0
*
*
Chronic pre-natal alcohol exposure (CA)
Chronic exposure control (CAc)
Non-Treated control (NTc)

2.4. Discussion:

In the present study, the effect of chronic prenatal ethanol exposure, using an oral gavage method, on the process of adult neurogenesis was explored in C57BL/6J mice at postnatal day 56. The fetal mice were exposed to maternal blood alcohol concentrations (BAC) slightly above those considered pharmacologically significant (Rhodes et al., 2005; Sulik, 2005) from gestational days 7 – 16 inclusive (10 days in total), which appears to be equivalent to the later stages of the first trimester and the early stages of the second trimester of humans (Patten et al., 2014). Our results indicate that the location of cells associated with adult neurogenesis, and their distribution throughout the brain, does not appear to be affected by this prenatal alcohol exposure. In addition, the rate of proliferation of newly born cells in the dentate gyrus of the hippocampus does not appear to be affected, but the numbers of immature hippocampal neurons in the dentate gyrus is significantly lower in the mice exposed to ethanol compared to the control groups.

2.4.1. Methodological considerations:

In this study, we utilized a chronic alcohol paradigm using an oral gavage method to develop a fetal alcohol spectrum disorder (FASD) mouse model. The oral gavage method was utilized to ensure that the pregnant mice consumed adequate doses of alcohol of pharmacological significance (Rhodes et al., 2005; Sulik, 2005), and to maintain uniform alcohol consumption amongst the pregnant mice (Åberg et al., 2005; Gil-Mohapel et al., 2014). The average BAC level obtained from the pregnant mice in this study was slightly higher than the pharmacologically significant level reported by Miller (1995), Rhodes et al. (2005) and Sulik (2005). Precautionary

measures, as described by Turner et al. (2011), were taken during the oral gavage procedure in order to reduce stress in the pregnant mothers. In addition, the pregnant mothers were housed alone, weighed daily and blood samples were collected only on the last day of either alcohol or sucrose administration. Subsequently, the weaned litters from these pregnant mice were housed in groups of three per cage. These precautions were necessary because it has been reported that many factors can impact adult hippocampal neurogenesis (Gould et al., 1998; Lee et al., 2000; Malberg et al., 2000; Åberg et al., 2005).

2.4.2. Distribution of Ki-67 and doublecortin (DCX) immunopositive cells:

Across mammals, the endogenous proteins Ki-67 and DCX have been shown to be accurate markers of cells at two different phases in the process of adult neurogenesis, the proliferative phase (Ki-67) and the immature neuron phase (DCX) (Balthazart and Ball, 2014). In mammals generally, and in mice specifically, two proliferative regions, the subventricular and subgranular zone, are consistently reported. The cells within the subventricular zone migrate through the rostral migratory stream, around the caudate nucleus, to invest mostly in the olfactory bulb, but may also enter other brain regions, such as the piriform cortex, neocortex and amygdaloid complex (Gil-Perotin et al., 2009). The cells of the subgranular zone migrate a short distance to the granular layer of the dentate gyrus of the hippocampus, where many of these cells become integrated into the hippocampal circuitry (Pawlak et al., 2002; Åberg et al., 2005). During the migratory phase, the proliferative cells (immunopositive to Ki-67 antibodies) become immature migrating neurons (immunopositive to DCX antibodies). This general pattern of adult neurogenesis did not appear to be affected by the prenatal ethanol exposure in the mice studied, with

the overall pattern of adult neurogenesis being identical across experimental groups, and to previous studies of adult neurogenesis in mice (Klintsova et al., 2007).

2.4.3. Quantification of proliferative (Ki-67 immunoreactive) cells in the dentate gyrus of the hippocampus:

Our quantification of proliferative cells, those immunostained with Ki-67, in the left dentate gyrus of the mice revealed numbers in the range of 1300 – 1650, which is comparable to the numbers of proliferative cells reported previously in C57BL/6J mice (Fuss et al., 2010; Nada et al., 2010); however, we did not find any statistically significant effect of prenatal ethanol exposure on the numbers of proliferative cells in the dentate gyrus. This finding is in agreement with previous reports indicating that postnatal alcohol exposure does not have an effect on the rate of cell proliferation in the dentate gyrus of hippocampus, especially at early adulthood in laboratory rodent models (Wozniak et al., 2004; Klintsova et al., 2007; Helfer et al., 2009; Gil-Mohapel et al., 2014). In contrast, in senescent Sprague-Dawley rats subjected to prenatal alcohol exposure a decrease in proliferation rates was observed (Gil-Mohapel et al., 2014). Thus, our study corroborates previous reports (Choi et al., 2005; Ieraci and Herrera, 2007; Klintsova et al., 2007; Gil-Mohapel et al., 2014) indicating that the deleterious effect of prenatal alcohol exposure could be less noticeable during early adulthood, or indeed that this exposure had no specific effect on the proliferation of cells within the early adult hippocampus.

Despite this, the number of Ki-67 immunoreactive cells in the hippocampi of the two experimental groups that underwent oral gavage was higher (by ~300 cells, or 1.2 times, on average), though not statistically significantly, than the non-treated

control group. It is important to note that there are several contradictory reports on the effect of alcohol on the dentate gyrus (Miller, 1995; Nixon and Crews, 2002; Pawlak et al., 2002; Zharkovsky et al., 2003; Redila et al., 2006; Ieraci and Herrera, 2007). In some cases, an increase in cell proliferation is thought to be a compensatory mechanism for a significant increase in cell death in the dentate gyrus due to the damaging effect of alcohol (Pawlak et al., 2002; Zharkovsky et al., 2003; Åberg et al., 2005), although we did not examine cell death in the current study so cannot confirm this hypothesis. It has been shown that factors, such as chronic stress during the development of the brain, may cause a permanent change in the rate of cell proliferation in the hippocampus (Gould et al., 1998; Lee et al., 2000; Malberg et al., 2000; Mirescu et al., 2004; Åberg et al., 2005; Lemaire et al., 2006; Ieraci and Herrera, 2007). In the present study, the use of the oral gavage method for delivery of the alcohol, may have caused, epigenetically through maternal stress, the slight, but non-significant, increase in cell proliferation rates observed in the two groups that underwent this treatment.

2.4.4. Quantification of immature (DCX immunoreactive) neurons in the dentate gyrus of the hippocampus:

Our quantification of immature neurons, those immunostained with DCX, in the left dentate gyrus of the mice revealed numbers in the range of 10 000 – 20 000, which is comparable to the numbers of immature neurons reported previously in C57BL/6J mice (Fuss et al., 2010; Nada et al., 2010); however, unlike the proliferative cells, we did find a statistically significant reduction in the number of immature neurons (50 – 70% the number of control groups) in the dentate gyrus of the mice exposed to prenatal alcohol when compared to both control groups (for which

there was no statistically significant difference). In rats at postnatal day 35, prenatal ethanol exposure did not affect the number of neurons in the dentate gyrus (Miller, 1995; Gil-Mohapel et al., 2014), but reduced the number of neurons in the CA1 region (Miller, 1995), but in aged rats (postnatal day 386) a reduction in the number of immature neurons was observed in the dentate gyrus (Gil-Mohapel et al., 2014). Thus, while there are some varying results, it does appear that the deleterious effect of prenatal alcohol exposure on the number of immature neurons only becomes significantly detectable by early adulthood.

Although there was not a statistically significant reduction in the number of immature neurons in the sucrose gavage control group (CAc) compared to the non-treated control group (NTc), the average number of immature neurons in the dentate gyrus of the CAc group was approximately 75% that of the non-treated group, indicating, as with the proliferative cell numbers, that the process of oral gavage may have induced maternal stress leading to an epigenetic effect on the production of immature neurons, a result observed previously using specific stress interventions (Gil-Mohapel et al., 2014). However, despite this potential stress-related reduction in immature neurons, it is clear that the prenatal alcohol exposure performed on the mice studied here does have a significant effect on the rate of conversion of proliferative cells into immature neurons and the survival of these neurons.

2.4.5. Potential functional correlates of decreased numbers of immature hippocampal neurons:

The dentate gyrus is thought to function as a pattern separator, a neural process that allows the distinct representation of overlapping or similar inputs within this

circuitry (Treves et al., 2008; Sahay et al., 2011). Ablation of adult neurogenesis in the dentate gyrus leads to an impairment in the ability of an organism to undertake pattern separation (Sahay et al., 2011; Clelland et al., 2009; Tronel et al., 2010), while increasing the rate of adult hippocampal neurogenesis improves pattern separation (Sahay et al., 2011). These findings have led to the memory resolution hypothesis, which indicates that the broadly tuned, young neurons, those that are identified with DCX immunostaining, interact with the specifically tuned mature neurons to increase the fidelity of spatial and contextual discrimination (Aimone et al., 2011).

The results of the current investigation indicate that in FASD children there is a potential downregulation of the number of immature neurons in the dentate gyrus. This appears to correlate with reports of executive dysfunctions and the inability to recall more objects than in normal children in FASD children (Zimmerberg et al., 1991; Connor et al., 2000; Fuglestad et al., 2015). In addition, the ability to recall acquired information (retrospective memory) (Willoughby et al., 2008), to perform delayed intentions (prospective memory) (Kliegel et al., 2008) and to temporarily store and handle information (working memory) (Burden et al., 2005) were similarly dysfunctional in children that were exposed to prenatal alcohol. These are indications that learning and memory are adversely affected after exposure to prenatal alcohol (Kaemingk et al., 2003; Lewis et al., 2016; Mattson and Roebuck, 2002), and that this in part may be the result of potentially fewer immature neurons within the hippocampus of FASD children, as observed in the current mouse model.

CHAPTER THREE: Changes to the somatosensory barrel cortex in C57BL/6J mice at early adulthood (56 days post-natal) following chronic prenatal alcohol exposure

3.1. Introduction:

Children with fetal alcohol spectrum disorder (FASD) are known to have impaired sensory processing skills, including sensory-motor problems associated with tactile sensitivity impairment (Streissguth et al., 1990; Coles et al., 2002; Oladehin et al., 2007; Franklin et al., 2008; Jirikowic et al., 2009; Carr et al., 2010). These impaired sensory sensitivities are associated with neuropsychological and behavioural effects (Carr et al., 2010; Mattson et al., 2011). Studies in animal models of FASD have indicated that these deficits may be caused by altered expression of genes associated with neural plasticity (Medina and Krahe, 2008). In rodent models of FASD, one region of the cerebral cortex, the barrel field, is a readily identified region that, due to its consistency in appearance, can be used to evaluate the potentially detrimental effects of prenatal alcohol exposure.

The barrel field in the cerebral neocortex of rodents is found within the primary somatosensory cortex (Welker and Woolsey, 1974). Each barrel processes sensory information from 1 – 3 facial vibrissae, and within the barrel field, the posterior medial barrel subfield (PMBSF) contains barrels where tactile information from the prominent vibrissae on the contralateral side of the face of a rodent is processed (Welker and Woolsey, 1974; Oladehin et al., 2007). The barrels of the PMBSF develop postnatally (McCandlish et al., 1989; Oladehin et al., 2007), at a time when motor skills arising from explorative activities (walking, running, climbing

and jumping) and behavioural changes (rearing, grooming, and feeding) are observed (Altman and Sudarshan, 1975; Rice and van der Loos, 1977; Richmond and Sachs, 1980; Markus and Petit, 1987; Whishaw et al., 1992; Seelke et al., 2012).

In studies of rat FASD models, prenatal and postnatal alcohol exposure significantly reduced the total area of the PMBSF, the area of individual PMBSF barrels, and the septal area (the area within the PMBSF barrel not occupied by the individual barrels) (Margret et al., 2005; Chappell et al., 2007; Oladehin et al., 2007); however, there was no disruption to the organisation of the PMBSF, and of the number of barrels within this subfield. Interestingly, the appearance of the PMBSF barrels was delayed by a few days following prenatal alcohol exposure (Margret et al., 2006). To our knowledge, the only previous study of the effect of chronic prenatal alcohol exposure on the barrel field in a mouse model of FASD was undertaken by Powrozek and Zhou (2005), were the barrel field was examined at post-natal day 7 and showed similar results to that observed in rats. The present study therefore aims to provide further experimental data on the modification of the cortical barrels by investigating the effect of prenatal alcohol exposure on C57BL/6J mice at early adulthood (PND 56) using a chronic alcohol exposure paradigm.

3.2. Materials and methods:

3.2.1. Breeding and prenatal ethanol exposure:

All animals were treated and used according to the guidelines of the University of the Witwatersrand Animal Ethics Committee (Clearance No. 2012/15/2B), which parallel those of the NIH for the care and use of animals in scientific experimentation. 12 week-old female C57BL/6J mice (*Mus musculus*) were

allocated into three experimental groups: Chronic Alcohol exposure (CA), control for Chronic Alcohol exposure (CAc), and a Non-Treatment control group (NTc). For effective mating, 1–2 female mice were introduced into the cage of a C57BL/6J male mouse for 12 hours, which was considered gestational day 0 (GD 0). In all, a total of 14 female mice (4–5 mice assigned to each experimental group) and 8 male mice were used to generate the required numbers of pups used in the present study.

For the CA group, each pregnant mouse received a dose of 7.5 µl/g of 50 % alcohol in distilled water (5.9 g/kg) per day (Webster et al., 1983; Haycock and Ramsay, 2009; Knezovich and Ramsay, 2012) for 10 consecutive days by oral gavage, starting from GD 7 (Webster et al., 1980, 1983; Sulik et al., 1981; Choi et al., 2005; Redila et al., 2006; Parnell et al., 2009), while each pregnant mouse in the CAc group received an equivalent dose of isocaloric sucrose (704 g/L) by oral gavage over the same period (Haycock and Ramsay, 2009; Knezovich and Ramsay, 2012). To control for the possible influence of post-traumatic stress in the pregnant mice, pregnant mice in the NTc group did not undergo any oral gavage. Food and water was provided *ad libitum* to the mice, except in the control groups (CAc and NTc), where it was withheld for two hours post-gavage in order to partially mimic the anorectic effect of alcohol (Haycock and Ramsay, 2009). The pups were weaned 21 days after birth and then the male and female pups separated. Three pups of the same sex from each experimental group were kept in separate cages (cage dimensions: 200 x 200 x 300 mm) with adequate food and water until post-natal day (PND) 56.

3.2.2. Blood alcohol concentration assay in the pregnant mice:

On the last day (10th day) of oral gavage (GD 16), a small lesion was made at the site of the saphenous vein on the left hind legs of all the pregnant mice in the two experimental (alcohol and sucrose) groups. The saphenous bleeding procedure was performed on the pregnant mice in the sucrose group in order to mimic the effects of the bleeding on the alcohol exposed pregnant mice. The non-treatment pregnant mice served as controls for the possible effects of the bleeding and/or the oral gavage procedures. 50 µl of blood was drawn into heparinized capillary tubes at 30 min post-gavage (Bielawski and Abel, 1997) to determine the blood alcohol concentration (BAC). The blood samples from the FAS model and the sucrose control were stored at 4°C overnight after which they were centrifuged with Vivaspin500 100 µm membrane tubes (Biotech, South Africa) for 30 min before the serum was extracted and the BAC analyzed using an EnzyChrom™ Ethanol Assay Kit (BioVision, South Africa). The pregnant mice belonging to the CA group that were administered alcohol had an average BAC of 1.84 mg/ml (s.e. = 0.39), which is above the pharmacologically significant level of 1 mg/ml reported by Rhodes et al. (2005) and Sulik (2005).

3.2.3. Sacrifice and tissue processing:

At PND 56, when the prenatally-alcohol-exposed mice reached adulthood, a total number of six mice (n = 6) from each experimental group (1–2 mice randomly selected from each litter set) were weighed and then euthanized (Eutha-naze 1 ml/kg, contains sodium pentobarbitone 100 mg/ml, delivered intra-peritoneally) before being perfused trans-cardially with 0.9% cold (4°C) saline followed immediately by cold

4% paraformaldehyde in 0.1 M phosphate buffer (PB). The brain was removed from the skull, weighed and post-fixed for 24 h in 4% paraformaldehyde in 0.1 M PB at 4°C. The left cerebral hemisphere of all 18 individual mice was prepared for cytochrome oxidase (CO) staining according to Wong-Riley (1979), Tootell and Silverman (1985) and Seelke et al. (2012). The cerebral hemisphere was carefully dissected away from the remainder of the brain by cutting along the acute angles of the curvature of the cortex, manually flattened between two glass slides and cyroprotected in 30 % sucrose for 24 hours at 4°C before being frozen on to the microtome stage where they were sectioned at 50 µm in the plane of the pial surface. The sections were subsequently placed in 1 % solution of cobalt chloride and 10% sucrose for 20 mins, and then rinsed three times in 0.1M PB for 10 mins each. The sections were then incubated in CO solution (in a 200 ml 0.1 M PB mixture: 100 mg cytochrome oxidase [Sigma, C2506], 50 mg diaminobenzidine, 20 g sucrose and a visible amount of catalase [Sigma C-10] at 37 °C for 2-6 hours). Chromatic precipitation was visually monitored under a low power stereomicroscope until a desirable staining level was achieved. Subsequently, the sections were rinsed three times in 0.1 M PB for 10 mins each and then mounted on a 0.5 % gelatine coated glass slide, allowed to dry overnight, dehydrated in a graded series of alcohols, cleared in xylene for 1 h and then cover-slipped with DPX mounting medium.

3.2.4. Determination of barrel sizes and statistical analysis:

Aligning of the PMBSF barrels and quantitative analyses were performed as described by Margret et al. (2005), Chappell et al. (2007) and Oladehin et al. (2007). The PMBSF barrels, indicated by 4 straddler barrels (α-δ), 4 barrels in distal row A, 4

in row B, 5 in row C, 5 in row D, and 5 in row E, from serial sections were aligned using the blood vessels that appear as white circles on the sections using a camera lucida attached to a stereomicroscope at 4 times magnification. The position of blood vessels in the brain sections aided in aligning the barrels, preventing duplication or misalignment. The outlines of the barrels were carefully traced on firmly secured white paper using a camera lucida attached to the microscope. This was performed to reconstruct a single image of all 27-PMBSF barrels, which were identified in one to three sections. The paper tracings were subsequently scanned at 300 dpi before the size of individual PMBSF barrels and the PMBSF enclosure were carefully measured using ImageJ software. From the data, the average total septal area of the PMBSF barrels was calculated by subtracting the total area of PMBSF barrels from the total area of PMBSF enclosure. In addition, barrel-to-barrel comparisons were performed across all experimental groups in order to reveal any size differences in the individual barrels. The measured parameters are illustrated in Figure 3.1.

An intra-observer reliability test was performed to determine reliability of the measurements. A Lin's Concordance Correlation Coefficient was used as a measure of precision and accuracy between four different measurements taken independently at three weeks intervals. The results of the test showed almost perfect agreement (0.9910) in accordance with Landis and Koch (1977). In addition, an analysis of variance (ANOVA) was performed on the data to evaluate group (CA, CAc and NTc) differences in mean sizes of individual PMBSF barrels, average total area of PMBSF barrels, average total area of PMBSF enclosures or average total septal area. Where the ANOVA was significant, a post-hoc analysis was further performed using Tukey's pairwise comparison test to determine where significant differences exist. All statistical analyses were performed using SPSS Inc programme (version 22.0). A

significance level of 5% was used as an indicator of significance difference for all the statistical analyses.

3.3. Results:

3.3.1. General observations on the body and brain:

The pups that experienced chronic prenatal alcohol exposure (CA group) showed no overt signs of FAS, in that no craniofacial abnormalities were readily apparent and there was no evident reduction in overall body mass. At the time of sacrifice, the average body masses of the mice were: CA male – 18.33 g (s.d. 2.08 g), CA female – 15.17 g (s.d. 0.58 g); CAc male – 20.33 g (s.d. 0.76 g), CAc female – 16.00 g (s.d. 0.76 g); NTc male – 19.50 g (s.d. 0.50 g), NTc female – 15.33 g (s.d. 0.29 g). No statistically significant differences were observed between experimental groups in terms of body mass when mice of the same sex were compared.

In addition, there were no observable differences in the general morphology of the brains of mice treated with alcohol (CA group), sucrose (CAc group) or the non-treated control group (NTc). The average brain masses recorded for each group were: CA male – 0.403 g (s.d. 0.006 g), CA female – 0.393 g (s.d. 0.012 g); CAc male – 0.417 g (s.d. 0.012 g), CAc female – 0.390 g (s.d. 0.010 g); NTc male – 0.407 g (s.d. 0.012 g), NTc female – 0.393 g (s.d. 0.012 g). No statistically significant differences were observed between groups in terms of brain mass.

3.3.2. General appearance and organization of the PMBSF:

All 27-PMBSF barrels were present in all the mice used in this study. The PMBSF barrels appeared darkly CO reactive with no distorted boundaries or

disruptions to the organization of the barrels, and appeared typical of that reported generally for mice (Woolsey and van der Loos, 1970; Simons and Woolsey, 1979) (Fig. 3.1). In the mice investigated in the current study, we could readily identify all PMBSF barrels normally found in mice, with five distinct barrel rows, and the PMBSF being sharply distinct from the adjacent cortex on three sides, the posterior, posteromedial and posterolateral borders, but the anterior border was less distinct. On the posteromedial border of the PMBSF the four distinct large straddler barrels (α-δ) were evident, 4 barrels in lateral row A, 4 barrels in row B, 5 barrels in row C, 5 barrels in row D, and 5 barrels in the most medial row E were readily observed. The size of the barrels decreased steadily from the posteromedial straddler barrels to the anterolateral barrels of the subfield.

3.3.3. Average area of the PMBSF enclosure:

In the non-treated control mice (NTc group), the average area of the PMBSF enclosure was 1.279 mm^2 (s.e. 0.019). In the gavage control mice (CAc group), the average area of the PMBSF enclosure was 1.310 mm^2 (s.e. 0.037), while in the mice exposed to chronic prenatal alcohol (CA group), the average area of the PMBSF enclosure was 1.244 mm^2 (s.e. 0.046) (Fig. 3.2A, Table 3.1). Thus, the size of the PMBSF enclosure was slightly smaller in the mice exposed to prenatal alcohol than in the two control groups, but this difference was not statistically significant ($p = 0.44$). The size of the PMBSF enclosure reported here is similar to that measured previously in other strains of mice (e.g. Woolsey and van der Loos, 1970).

3.3.4. Total average area of the PMBSF barrels:

The total area of the PMBSF barrels was calculated by summing the areas of the 27 individual barrels in each mouse. The average PMBSF barrel area in the NTc mice was 0.750 mm^2 (s.e. 0.019), in the CAc mice it was 0.790 mm^2 (s.e. 0.031) and in the CA mice exposed to prenatal alcohol it was 0.733 mm^2 (s.e. 0.028) (Fig. 3.2B, Table 3.1). Thus, the total area of the PMBSF barrels was slightly smaller in the mice exposed to prenatal alcohol than in the two control groups, but this difference was not statistically significant ($p = 0.31$).

3.3.5. Average areas of the individual PMBSF barrels:

By summing and averaging the areas of each individual barrel for each group, we calculated an average individual PMBSF barrel area that was compared across groups. Thus, all barrels measured in the 6 mice in the NTc groups were summed (162 PMBSF barrels in total) and averaged, with the same being done for the CAc and CA groups (each of which had 162 barrels in total). The average individual PMBSF barrel area in the NTc mice was 0.028 mm^2 (s.e. 0.001), in the CAc mice it was 0.029 mm^2 (s.e. 0.001) and in the CA mice exposed to prenatal alcohol it was 0.027 mm^2 (s.e. 0.001) (Fig. 3.2C, Table 3.1). Thus, the average area of the individual PMBSF barrels was slightly smaller in the mice exposed to prenatal alcohol than in the two control groups, but this difference was not statistically significant ($p = 0.12$).

As the individual barrels are readily identified across individuals, and have a specific nomenclature, we examined whether there were specific individual barrels that showed significant changes in size with the prenatal alcohol exposure. The average area of individual PMBSF barrels in the CA group was 0.027 μm^2, which was

smaller, but not significantly, than the average areas of the barrels in the CAc group (0.029 μm^2) and the NTc group (0.028 μm^2) (Table 3.2). When comparing the alcohol exposed CA group to the sucrose gavage control CAc group, we found that 20 of the 27 (~74%) readily identifiable PMBSF barrels were smaller in the CA group compared to the CAc group (Table 3.2, Fig. 3.3A). Overall, the average size of the CA barrels were 93.96% of the CAc barrel (Table 3.2). When comparing the alcohol exposed CA group to the non-treated control NTc group, we found that 14 of the 27 (~52%) readily identifiable PMBSF barrels were smaller in the CA group compared to the NTc group (Table 3.2, Fig. 3.3B). The average size of the CA barrels was 98.91% of the NTc barrels (Table 3.2). Although reductions in size were observed across most barrel rows, including the straddler barrels, the most substantial reductions in barrel sizes were observed in barrel rows D and E (Fig. 3.3A,B; Table 3.2). This is evident by comparison of the mean sizes of barrels in the experimental groups for barrels located in rows D and E. The mean barrel size was significantly reduced in CA when compared to CAc (in row D: $p = 0.01$ and in row E: $p = 0.002$). A frequency distribution plot of the average area of the individual PMBSF barrels showed that the distribution, based on area, of the individual PMBSF barrels in the CA group was skewed to the lower end of the range, while the barrel areas in the two control groups were skewed to the higher end of the range (Fig. 3.3C).

3.3.6. Average area of the septal portion of the PMBSF:

The average size of the septal portion of the PMBSF was calculated by subtracting the summed areas of the individual barrels from the area of the total PMBSF enclosure. In the NTc mice the average septal area was 0.520 mm^2 (s.e. 0.012), in the CAc mice the average septal area was 0.524 mm^2 (s.e. 0.021), and in the

ethanol exposed CA mice the average septal area was 0.512 mm^2 (s.e. 0.024) (Fig. 3.2D, Table 3.1). As with the other measures, the average septal area was smaller in the mice exposed to prenatal alcohol compared to the two control groups, but this reduction in size was not statistically significant ($p = 0.87$).

Table 3.1: A table detailing the calculated mean and standard error of mean for the measured PMBSF barrels

Experimental groups	Average total area of PMBSF barrels (mm^2)		Average area of individual PMBSF barrel (mm^2)		Average total area enclosed by the PMBSF barrels (mm^2)		Average septal area of PMBSF barrels (mm^2)	
	Mean	Standard error	Mean	Standard error	Mean	Standard error	Mean	Standard error
CA	0.733	0.028	0.027	0.001	1.244	0.046	0.512	0.024
CAc	0.790	0.031	0.029	0.001	1.310	0.037	0.524	0.021
NTc	0.750	0.019	0.028	0.001	1.279	0.019	0.520	0.012

Table 3.2: Barrel-to-barrel comparisons of the average size of individual PMBSF barrels as well as the percentage change in the mean size of PMBSF barrels of the mice exposed to prenatal alcohol (CA) compared to the sucrose gavage control (CAc) and non-treatment controls (NTc).

Individual PMBSF barrel	Average area of individual PMBSF barrel (mm^2)			Percentage change CA/CAc (%)	Percentage change CA/NTc (%)
	CA	CAc	NTc		
A1	0.017	0.021	0.020	80.95	85.00
A2	0.017	0.016	0.018	106.25	94.44
A3	0.015	0.017	0.016	88.24	93.75
A4	0.012	0.013	0.012	92.31	100.00
B1	0.033	0.030	0.032	110.00	103.13
B2	0.027	0.031	0.025	87.10	108.00
B3	0.023	0.024	0.021	95.83	109.52
B4	0.019	0.015	0.015	126.67	126.67
C1	0.038	0.041	0.041	92.68	92.68
C2	0.035	0.037	0.033	94.59	106.06
C3	0.030	0.032	0.030	93.75	100.00
C4	0.026	0.027	0.026	96.30	100.00
C5	0.026	0.022	0.020	118.18	130.00
D1	0.038	0.041	0.042	92.68	90.48
D2	0.032	0.037	0.036	86.49	88.89
D3	0.029	0.038	0.032	76.32	90.63
D4	0.028	0.034	0.030	82.35	93.33
D5	0.028	0.031	0.024	90.32	116.67
E1	0.028	0.036	0.034	77.78	82.35
E2	0.025	0.032	0.029	78.13	86.21
E3	0.025	0.032	0.028	78.13	89.29
E4	0.027	0.033	0.027	81.82	100.00
E5	0.026	0.030	0.025	86.67	104.00
α	0.030	0.030	0.035	100.00	85.71
β	0.034	0.035	0.040	97.14	85.00
γ	0.038	0.036	0.033	105.56	115.15
δ	0.029	0.024	0.031	120.83	93.55
Average	0.027	0.029	0.028	93.96	98.91

Figure 3.1: Diagrams showing (**A**) the nomenclature used for the barrels within the posterior-medial barrel subfield (**PMBSF**), (**B**) the measurement made to calculate the area of the enclosure of the PMBSF, (**C**) the measurements made to obtain data for individual barrel areas, and when combined the total area of the PMBSF, and (**D**) the measurement made to define the septal area of the PMBSF. M – medial, R – rostral.

Barrel Nomenclature

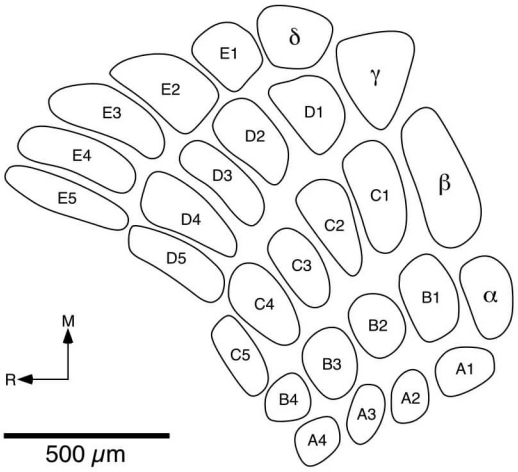

PMBSF enclosure

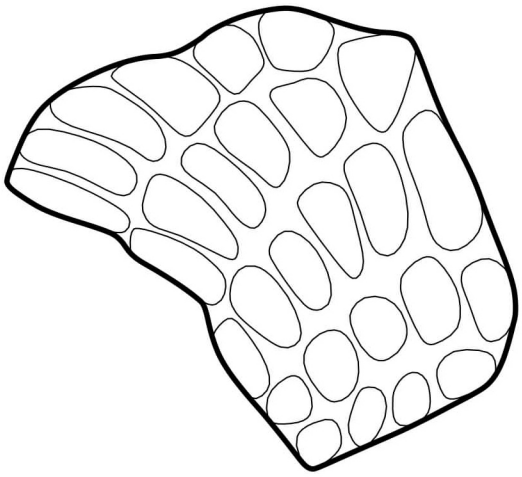

PMBSF total area

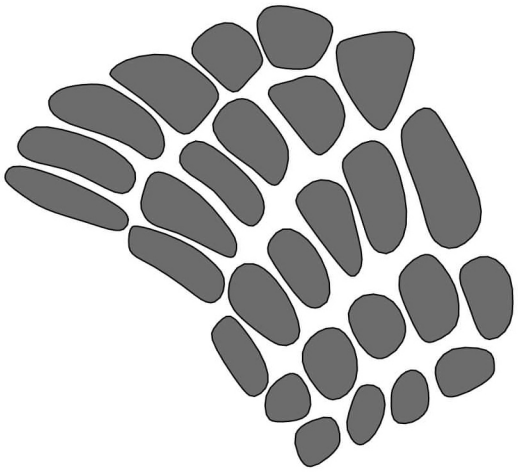

PMBSF septal area

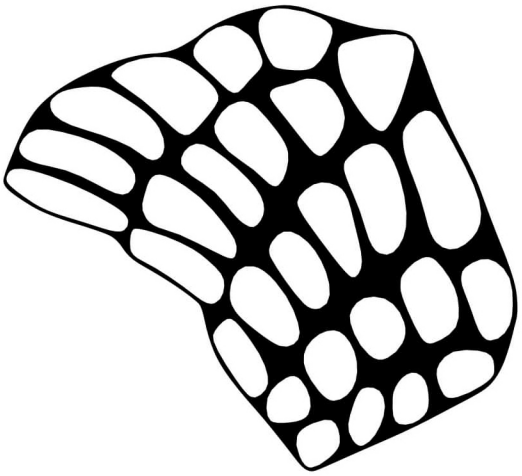

Figure 3.2: Bar charts showing (**A**) the average total area of the PMBSF enclosure, (**B**) the average total area of PMBSF barrels, (**C**) the average area of individual PMBSF barrels, and (**D**) the average septal area within the PMBSF enclosure, in the brains of three different groups (n = 6 per group) analyzed in the present study, the group exposed to chronic prenatal alcohol (**CA**), the prenatal gavage control group (**CAc**) and the non-treated control group (**NTc**). Note that while for all measurements made the average values for the CA group are smaller than the two control groups, these are not statistically significant differences.

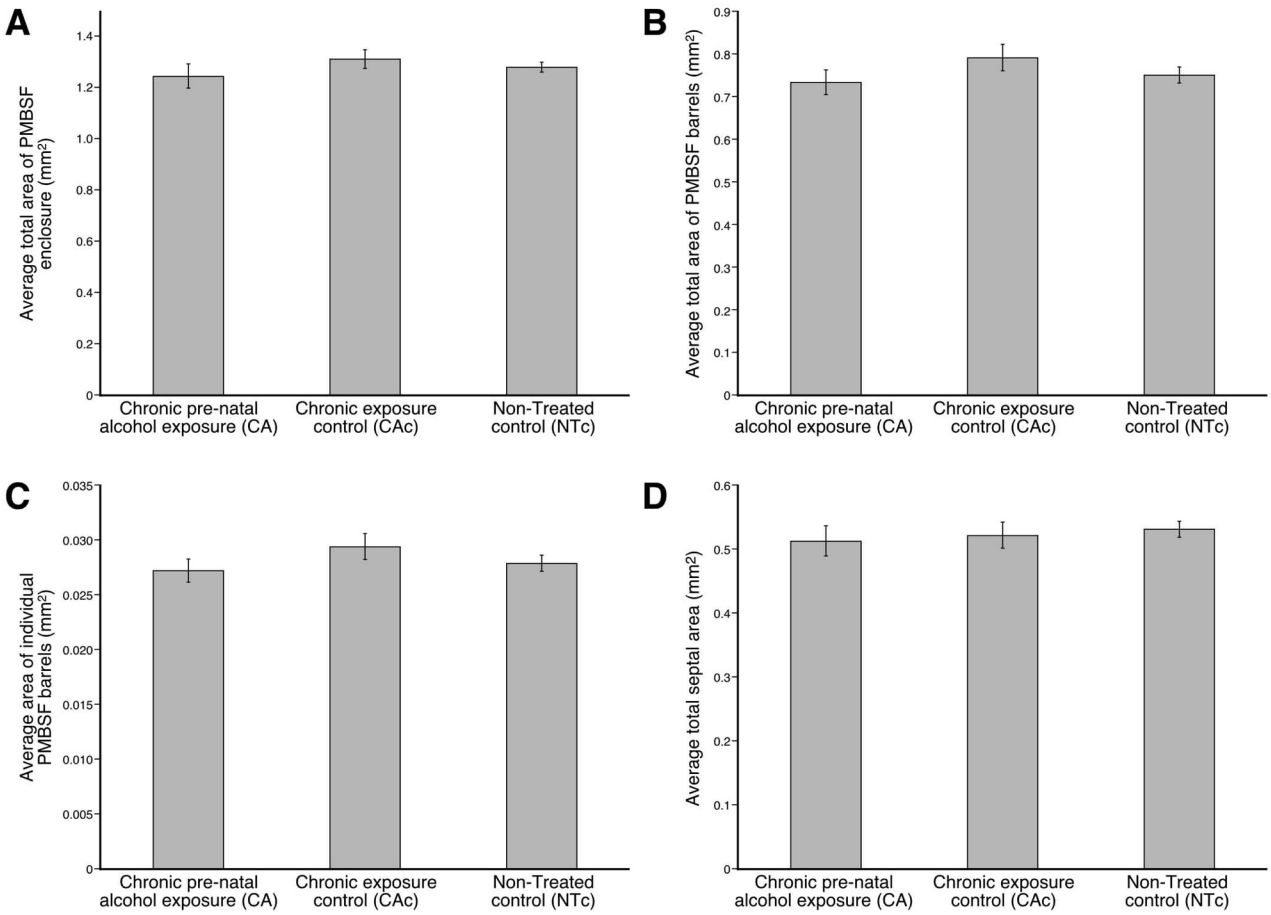
A
Average total area of PMBSF enclosure (mm²)
1.4
1.2
1.0
0.8
0.6
0.4
0.2
0
Chronic pre-natal alcohol exposure (CA)
Chronic exposure control (CAc)
Non-Treated control (NTc)
B
Average total area of PMBSF barrels (mm²)
0.9
0.8
0.7
0.6
0.5
0.4
0.3
0.2
0.1
0
Chronic pre-natal alcohol exposure (CA)
Chronic exposure control (CAc)
Non-Treated control (NTc)
C
Average area of individual PMBSF barrels (mm²)
0.035
0.030
0.025
0.020
0.015
0.010
0.005
0
Chronic pre-natal alcohol exposure (CA)
Chronic exposure control (CAc)
Non-Treated control (NTc)
D
Average total septal area (mm²)
0.6
0.5
0.4
0.3
0.2
0.1
0
Chronic pre-natal alcohol exposure (CA)
Chronic exposure control (CAc)
Non-Treated control (NTc)

Figure 3.3: The outlines of the PMBSF in **A** and **B** illustrate the comparisons in area of individual barrels in the PMBSF barrel field of the group exposed to prenatal alcohol (CA) in comparison to the sucrose gavage control group (**A**) and the non-treated control group (**B**). Note that for several of the individual barrels substantial reductions in size (expressed as a percentage) were evident, although there are several barrels that also show no change. (**C**) A bar chart showing the frequency distributions of areas of individual PMBSF barrels in the three different groups (n = 6 per group) analyzed in the present study, the group exposed to chronic prenatal alcohol (**CA**), the prenatal gavage control group (**CAc**) and the non-treated control group (**NTc**). This graph shows that the PMBSF barrel size in the alcohol exposed group (**CA**) group has a tendency to show smaller mean areas than in the **CAc** or **NTc** control groups, although these differences are not statistically significant.

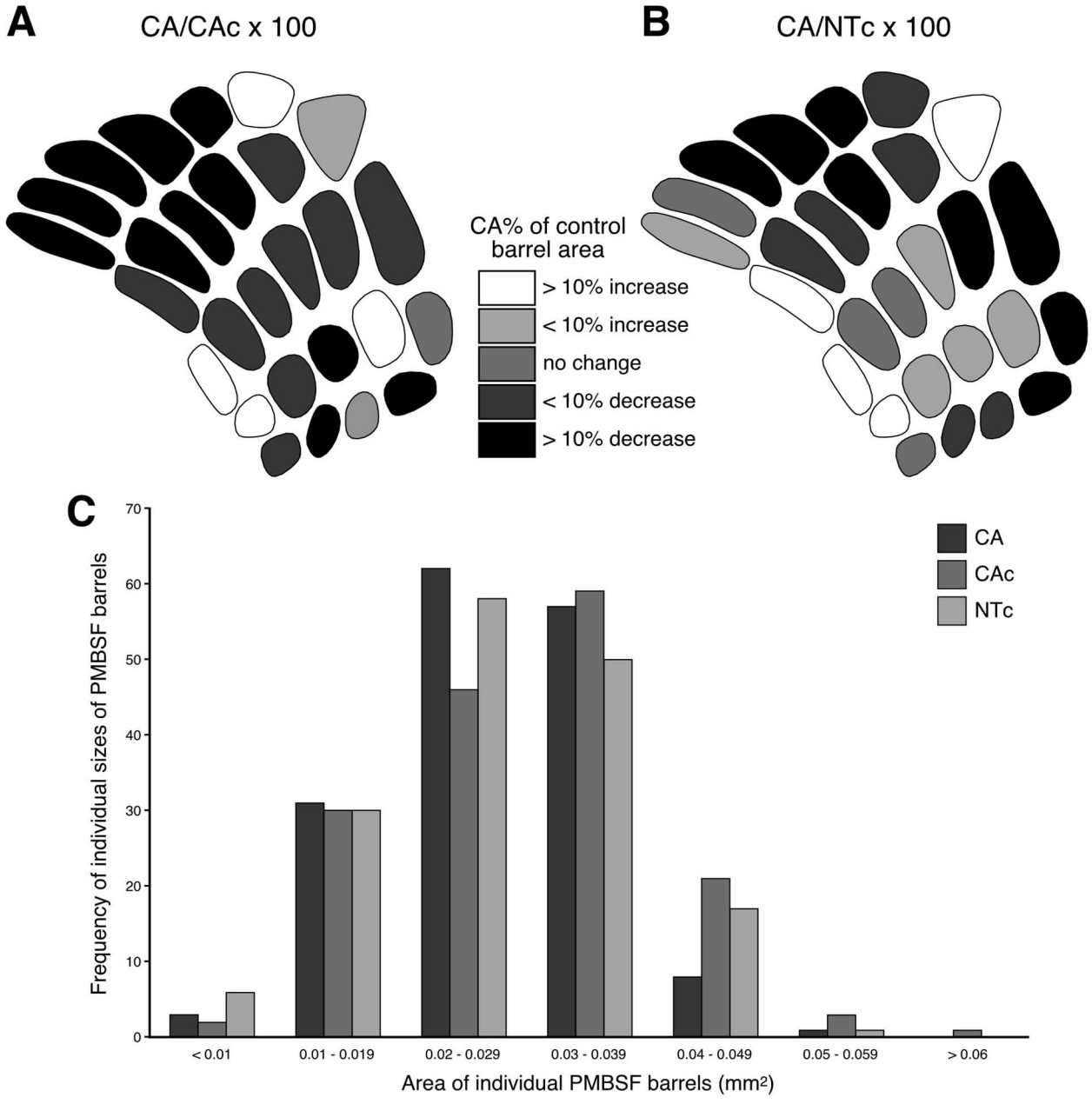
A
CA/CAc x 100
B
CA/NTc x 100
CA% of control barrel area
> 10% increase
< 10% increase
no change
< 10% decrease
> 10% decrease
C
CA
CAc
NTc
Frequency of individual sizes of PMBSF barrels
0
10
20
30
40
50
60
70
< 0.01
0.01 - 0.019
0.02 - 0.029
0.03 - 0.039
0.04 - 0.049
0.05 - 0.059
> 0.06
Area of individual PMBSF barrels (mm2)

3.4. Discussion:

The present study investigated the effect of alcohol administered prenatally from gestational days 7 – 16 on the total size of the PMBSF barrels, the area of the PMBSF enclosure and the PMBSF septal area in the somatosensory cortex of an adult mouse model of FASD. The present study found no statistically significant differences in the mean sizes of these measured parameters, although there was a general trend for decreases in these parameters in the group of mice exposed to prenatal alcohol when compared to controls. Despite this, specific individual barrels were substantially reduced in size, but these were limited in number and mostly found in the barrel rows D and E. These findings, while exhibiting similar trends, are different to those previously reported in rats and mice (Margret et al., 2005; Powrozek and Zhou, 2005; Oladehin et al., 2007; Chappell et al., 2007) where it was found that statistically significant reductions in the average total area of the PMBSF barrels, the average size of individual PMBSF barrels, the area of PMBSF barrel enclosure, and the septal area of the PMBSF, were observed; however, it should be noted that Chappell et al. (2007) found no significant difference in the septal area of the PMBSF following prenatal alcohol exposure, which is similar to what was observed in the present study. Despite these differences, the general observations in both rat and mice exposed to a prenatal alcohol regime are consistent, in that there are reductions in the amount of cortex devoted to processing tactile information. However, the differences between studies may be due to the models used (i.e. rat vs mouse), or in the precise paradigms of prenatal alcohol exposure and their relationship to process of cortical development in the different animal models.

It is well documented that the developing cerebral cortex is highly susceptible to alcohol teratogenicity (Maier et al., 1999; Livy et al., 2001; Maier and West, 2003; Tran and Kelly, 2003; Oladehin et al., 2007). The differences observed in the present and previous studies showing reductions in the mean size of the PMBSF barrel enclosure and the septal area could be attributed to differences in cortical circuitry or neural projections to the barrels (Welker and Woolsey, 1974; Senft and Woolsey, 1991; Kim and Ebner, 1999; Gil et al., 2002; Molnár et al., 2003; Chappell et al., 2007; Oladehin et al., 2007; Seelke et al., 2012). It is possible that prenatal alcohol exposure may have varying effects on the septal circuitry as studies have shown that thalamocortical projections and dendrites of pyramidal neurons in the somatosensory cortex are similarly susceptible to damage by alcohol (Galofré et al., 1987; Al-Rabiai and Miller, 1989; Rice, 1995; Chappell et al., 2007; Oladehin et al., 2007).

In a comparison of the same barrels across the experimental groups the present study found that approximately 65 % of the barrels in the alcohol exposed group were smaller in size than in the control groups, while only a small proportion of the barrels in the alcohol exposed group had sizes larger than the controls. Although there was no significant difference when a barrel-to-barrel comparison was performed between the alcohol group and controls, there does appear to be a strong trend related to alcohol exposure. Our findings indicate that prenatal alcohol exposure may have differential effects on the developing individual barrels. Chappell et al. (2007) also reported that the size of a significant number of barrels, although not all, in their alcohol exposed group were reduced when compared to the controls. It was also found that the anterior barrels were more vulnerable to alcohol than the barrels located posteriorly in juvenile and senescent rats (Chappell et al., 2007). The report by Chappell et al. (2007) is similar to the findings of the present study except that the reductions in the sizes of

the barrels in the prenatally alcohol exposed mice were not significantly different from the controls and we found that the more medially located barrels, rather than those located anteriorly, were the ones most strongly affected in the mice. This may reflect a model animal difference, or may reflect a difference in the alcohol exposure regime.

Alcohol has been shown to inflict damage through the disruptions of cortical organisation, altering DNA sequences, protein structures, and inducing cell death (Granato et al., 1995; Miller, 1996, 2006; Ikonomidou et al., 2000; Climent et al., 2002; Heaton et al., 2003; Moore et al., 2004; Oladehin et al., 2007). In addition, thalamocortical and corticocortical connections have shown to be altered by alcohol, potentially explaining somatosensory anomalies associated with FAS (Rice, 1995; Oladehin et al., 2007). In the present study, and in previous studies of rat barrel cortex following prenatal exposure to alcohol (Margret et al., 2005, 2006; Chappell et al., 2007; Oladehin et al., 2007), no change to the overall organization of the PMBSF was noted. This indicates that despite the specific differences found regarding individual barrels and other parameters measured, the global organization of the PMBSF, in terms of barrel numbers and topography, is preserved and maintained into adulthood irrespective of the variations in the gestational period during which the pups were exposed to alcohol.

In conclusion, the present findings, along with previous reports, indicate that there may be reductions in the amount of the cortex devoted to processing somatosensory input following prenatal exposure to alcohol in both mice and rats models of FASD. Given that it is known that FASD children experience sensory-motor problems due to impaired tactile sensitivity that are often co-expressed with

neuropsychological and behavioural problems (Streissguth et al., 1990; Coles et al., 2002; Oladehin et al., 2007; Franklin et al., 2008; Jirikowic et al., 2009; Carr et al., 2010; Mattson et al., 2011), it would seem reasonable to conclude that the somatosensory cortex located on the post-central gyrus of FASD children may be somewhat reduced in size. Thus, there may be lower numbers of neurons and perturbed connectivity of the somatosensory cortex in FASD children that may underlie these problems. Further investigations into the microconnectivity of the barrels in the FASD rodent models, counts of neurons, and neurochemistry of the barrel neurons, along with imaging studies in FASD humans, may reveal more specific details regarding the deleterious outcomes of prenatal alcohol exposure, and may suggest potential therapeutic interventions.

CHAPTER FOUR: Lack of changes to the cerebellar cortex of C57BL/6J mice at early adulthood (56 days post-natal) following chronic prenatal alcohol exposure

4.1. Introduction:

Several reports have shown a high susceptibility of the cerebellum to alcohol toxicity causing irreversible damages (Li et al., 2002; Sullivan et al., 2002; Burd et al., 2003; Luo, 2015). Fetal alcohol syndrome (FAS) children show overt signs of motor developmental defects, including fine- and gross-motor skills (Powrozek and Zhou, 2005), as well as skills that are dependent on sensory inputs such as reaction time to stimuli, and generally motor tasks are significantly delayed (Abel, 1984; Streissguth et al., 1984; Powrozek and Zhou, 2005; Oladehin et al., 2007). In a study investigating balance coordination in FAS children, there was no compensation for balance deficits when the sensory inputs such as visual or vestibular input was altered in the experimental tasks (Roebuck et al., 1998a,b). In the brain of FAS subjects, a reduction in the volume of cerebellar white matter was reported by Spottiswoode et al. (2011) and autopsy studies on subjects exposed to prenatal alcohol consistently report changes to the general brain morphology, especially the cerebellum (Clarren and Smith, 1978; Wisniewski et al. 1983). The results of the autopsy studies are similar to MR imaging studies of living subjects, which demonstrated striking neuroanatomical changes in the cerebellar vermis (Riley et al., 1995; Mattson et al., 1996; Sowell et al., 1996). In addition, similar cerebellar defects in rat and mouse models of FAS have been reported (Miller and Robertson, 1993; Maier et. al., 1999).

The cerebellum is thought to be involved in a multitude of functions, many of which relate to movement. One of the basic functional actions of the cerebellum is the learning and execution of instructions for movements, ensuring co-ordination of the force, extent, and duration of the contraction of muscles in both planned and unplanned movements (e.g. D'Angelo et al., 2011; Martinez, 2014). The three layered cerebellar cortex shows a specific and iterative circuitry across the cerebellum that is related to the functional aspects of the cerebellum. One of the intrinsic attributes of this iterated cerebellar cortical circuitry is inhibition, and various inhibitory aspects of this circuit can be revealed with immunohistochemical staining for the calcium-binding proteins parvalbumin, calbindin and calretinin (e.g. Rogers, 1989; Celio, 1990; Resibois and Rogers, 1992). Calcium ions within the intracellular neuronal matrix are important for normal functioning (Wierzba-Bobrowicz et al., 2011) as these ions regulate the release of neurotransmitters and hormones, maintain axonal action potentials, enzymatic action and gene transcriptions (Braun, 1990; Wierzba-Bobrowicz et al., 2011). Intra-neuronal calcium ions are actively regulated by specific proteins, the calcium-binding proteins, such as parvalbumin, calbindin, calretinin and calmodulin (Sloviter et al., 1991; Yew et al., 1997; Wierzba-Bobrowicz et al., 2011).

As different cerebellar neurons express specific calcium-binding proteins (Rogers, 1989; Celio, 1990; Resibois and Rogers, 1992; Collins et al., 2005; Wierzba-Bobrowicz et al., 2011) it is believed that a slight alteration to the expression of some of these proteins could indicate a neuropathology (Sloviter et al., 1991; Yew et al., 1997). Due to the motor deficits present in FAS children and the specific localization of the calcium-binding proteins in the cerebellar cortex, in the present study we investigated the qualitative distribution of the calcium-binding proteins parvalbumin, calbindin and calretinin in the cerebellar cortex of 56 day-old C57BL/6J mice

following exposure to a chronic prenatal alcohol regime. In addition, we quantified the density of neurons, those stained with cresyl violet and immunostained with parvalbumin, in the molecular layer of the vermal cerebellar cortex, and the volume of the Purkinje cells in the vermal cerebellar cortex.

4.2. Materials and methods:

4.2.1. Breeding and prenatal ethanol exposure:

All animals were treated and used according to the guidelines of the University of the Witwatersrand Animal Ethics Committee (Clearance No. 2012/15/2B), which parallel those of the NIH for the care and use of animals in scientific experimentation. 12 week-old female C57BL/6J mice (*Mus musculus*) were allocated into three experimental groups: Chronic Alcohol exposure (CA), control for Chronic Alcohol exposure (CAc), and a Non-Treatment control group (NTc). For effective mating, 1–2 female mice were introduced into the cage of a C57BL/6J male mouse for 12 hours, which was considered gestational day 0 (GD 0). In all, a total of 14 female mice (4–5 mice assigned to each experimental group) and 8 male mice were used to generate the required numbers of pups used in the present study.

For the CA group, each pregnant mouse received a dose of 7.5 µl/g of 50 % alcohol in distilled water (5.9 g/kg) per day (Haycock and Ramsay, 2009; Knezovich and Ramsay, 2012) for 10 consecutive days by oral gavage, starting from GD 7 (Webster et al., 1980; Sulik et al., 1981; Webster et al., 1983; Choi et al., 2005; Redila et al., 2006; Parnell et al., 2009), while each pregnant mouse in the CAc group received an equivalent dose of isocaloric sucrose (704 g/L) by oral gavage over the

same period (Haycock and Ramsay, 2009; Knezovich and Ramsay, 2012). To control for the possible influence of stress induced by the gavage method in the pregnant mice, pregnant mice in the NTc group did not undergo any oral gavage. Food and water was provided *ad libitum* to the mice, except in the control groups (CAc and NTc), where it was withheld for two hours post-gavage in order to partially mimic the anorectic effect of alcohol (Haycock and Ramsay, 2009). The pups were weaned 21 days after birth and then the male and female pups separated. Three pups of the same sex from each experimental group were kept in separate cages (cage dimensions: 200 x 200 x 300 mm) with adequate food and water supplies until post-natal day (PND) 56.

4.2.2. Blood alcohol concentration assay in the pregnant mice:

On the last day (10th day) of oral gavage (GD 16), a small lesion was made at the site of the saphenous vein on the left hind legs of all the pregnant mice in the CA and CAc experimental groups. The saphenous bleeding procedure was performed on the pregnant mice in the sucrose group in order to mimic the effects of the bleeding on the alcohol exposed pregnant mice. The non-treatment pregnant mice served as controls for the possible effects of the bleeding and/or the oral gavage procedures. 50 µl of blood was drawn into heparinized capillary tubes at 30 min post-gavage (Bielawski and Abel, 1997) to determine the blood alcohol concentration (BAC). The blood samples from the FAS model and the sucrose control were stored at 4°C overnight after which they were centrifuged with Vivaspin500 100 µm membrane tubes (Biotech, South Africa) for 30 min before the serum was extracted and the BAC analyzed using an EnzyChrom™ Ethanol Assay Kit (BioVision, South Africa). The

pregnant mice belonging to the CA group that were administered alcohol had an average BAC of 1.84 mg/ml (s.e. = 0.39), which is above the pharmacologically significant level of 1 mg/ml reported by Rhodes et al. (2005) and Sulik (2005).

4.2.3. Sacrifice and tissue processing:

At PND 56, when the prenatally-alcohol-exposed mice reached adulthood, a total number of six mice (n = 6) from each experimental group (1–2 mice randomly selected from each litter set) were weighed and then euthanized (Eutha-naze 1 ml/kg, contains sodium pentobarbitone 100 mg/ml, intra-peritoneally) before being perfused trans-cardially with 0.9% cold (4°C) saline followed immediately by cold 4% paraformaldehyde in 0.1 M phosphate buffer (PB). The brain was removed from the skull, weighed and post-fixed for 24 h in 4% paraformaldehyde in 0.1 M PB at 4°C. The brains were then cryoprotected by immersion in 30 % buffered sucrose solution in 0.1 M PB at 4°C until they equilibrated. The left cerebellar hemisphere of all 18 individual mice was dissected from the remainder of the brain, frozen in crushed dry ice, and sectioned in a sagittal plane at 50 µm thickness using a sliding microtome. A one in four series of sections was stained for Nissl substance (cresyl violet) to reveal cytoarchitectural features while the other sections were prepared for immunostaining with parvalbumin (PV), calretinin (CR) and calbindin (CB) antibodies. The Nissl sections were mounted on 0.5% gelatine-coated slides, dried overnight, cleared in a 1:1 mixture of 100% ethanol and 100% chloroform and stained with 1% cresyl violet.

4.2.4. Immunostaining protocol:

The sections used for immunohistochemical staining were initially incubated in a solution containing 1.6% of 30% H_2O_2, 49.2% methanol and 49.2% 0.1M PB solution, for 30 min to reduce endogenous peroxidase activity, which was followed by three 10 min rinses in 0.1M PB. To block non-specific binding sites the sections were then pre-incubated for 2 h, at room temperature, in blocking buffer (made up of 3% normal goat serum, 2% bovine serum albumin and 0.25% Triton X-100 in 0.1 M PB). Thereafter, the sections were incubated for 48 h at 4°C in the primary antibody solution (made up of the blocking buffer plus the appropriate dilution of each antibody) under gentle agitation. To reveal parvalbumin, calbindin and calretinin containing neurons and neuronal structures, we used anti-parvalbumin (PV) (PV28, Swant, raised in rabbit), anti-calbindin (CB) (CB38a, Swant, raised in rabbit), and anti-calretinin (CR) (7699/3H, Swant, raised in rabbit), all at a dilution of 1:10000.

After incubation in the primary antibody solution, the sections were rinsed for 10 min in 0.1 M PB three times and then incubated in a secondary antibody solution made up of a 1:1000 dilution of biotinylated anti-rabbit IgG (BA1000, Vector Labs), 3% normal goat serum, and 2% bovine serum albumin in 0.1 M PB for 2 h at room temperature. This was followed by three 10 min rinses in 0.1 M PB, after which sections were incubated for 1 h in an avidin-biotin solution (1:125; Vector Labs), followed by a further three 10 min rinses in 0.1 M PB. Sections were then placed in a solution containing 0.05% diaminobenzidine (DAB) in 0.1 M PB for 5 min, followed by the addition of 3.3 µl of 30% hydrogen peroxide per 1 ml of DAB solution. Chromatic precipitation was visually monitored under a low power stereomicroscope until the background stain was at a level that would allow for accurate architectonic

matching to the Nissl sections without obscuring the immunopositive structures. Development was stopped by placing sections in 0.1 M PB for 10 min, followed by two more 10 min rinses in this solution. Sections were then mounted on 0.5% gelatine coated glass slides, dried overnight, dehydrated in a graded series of alcohols, cleared in xylene and coverslipped with DPX. To rule out non-specific staining of the immunohistochemical protocol, we ran tests on sections where we omitted the primary antibody, and sections where we omitted the secondary antibody. In both cases no staining was observed.

4.2.5. Qualitative, quantitative and statistical analysis:

For qualitative comparison the stained sections were examined under both low and high power light microscopy. Digital photomicrographs were captured using Zeiss Axioshop and Axiovision software. No pixelation adjustments or manipulation of the captured images was undertaken, except for the adjustment of contrast, brightness, and levels using Adobe Photoshop 7.

For the quantification of the density of Nissl cell bodies and immunopositive PV neurons within the molecular layer of the vermal cerebellar cortex, an unbiased design based systematic random sampling stereological protocol was employed. We used a MicroBrightfield (MBF) (Colchester, Vermont, USA) system with three plane motorised stage, Zeiss.Z2 Vario Axioimager and StereoInvestigator software (MBF, version 11.08.1; 64-bit). Initially we measured the thickness of the molecular layer of the cerebellar cortex and obtained an average for each group to assist in maintaining consistency with stereological parameters across the groups. Separate pilot studies for each of Nissl and PV stains from each experimental group, were then conducted to

optimise sampling parameters, such as the counting frame and sampling grid sizes, and achieve a coefficient of error (CE) below 0.1 (Gundersen et al., 1988; West et al., 1991; Dell et al., 2016). At this point we would like to acknowledge that while every effort was made to obtain a CE below 0.1, this was not always achieved mostly due to a limited number of countable sections in those instances. In addition we measured the tissue section thickness at every 10^{th} sampling site and the vertical guard zone was determined according to tissue thickness to avoid errors/biases due to sectioning artifacts (West et. al., 1991; Dell et al., 2016). We decided to maintain consistency amongst sampling parameters between the groups studied for both Nissl and PV stained tissue to reduce unfavourable stereological estimation biases. Table 4.1 provides a detailed summary of the parameters that were used in the current study.

To estimate the total number of Nissl cell bodies and PV+ neurons within a consistently defined region of interest (ROI), we used the 'Optical Fractionator' probe and the following equation (West et al., 1991; Dell et al., 2016):

$$N = Q / (SSF \times ASF \times TSF)$$

Where *N* was the total estimated neuronal number, *Q* was the number of neurons counted, *SSF* was the fraction of the sections sampled, ASF was the area sub fraction (which is calculated by the ratio of the size of the counting frame to the size of the sampling grid), and TSF was the thickness sub fraction (which is calculated by the ratio of the disector height relative to the section thickness).

The densities reported for Nissl cell bodies and PV+ neurons were calculated by multiplying the ROI area by the section thickness, and then using the generated volume as the denominator to estimate neuronal density. To determine neuronal sizes of the calbindin stained Purkinje cells, we used the 'Nucleator' probe. For all

individuals counted these probes were used concurrently while maintaining strict criteria, e.g. only neurons with complete cell bodies were counted, and obeying all commonly known stereological rules.

An analysis of variance (ANOVA) was performed to determine if there was significant variation in the mean Nissl or parvalbumin immunopositive neuronal densities in the molecular layer of the vermal cerebellum as well as the area and volume of Purkinje cells in the vermal cerebellum between the three experimental groups (CA, CAc and NTc). Where the ANOVA was significant, a Post hoc analysis was further performed using Tukey's pairwise comparison test to determine where significant differences exist. All statistical analyses were performed using SPSS Inc programme (version 22.0). A significance level of 5% was used as an indicator of significant differences for all statistical analyses.

Table 4.1: Stereological parameters used for estimating cell densities and volumes in the molecular layer and Purkinje cell layer of the vermal cerebellar cortex. CA – chronic alcohol group, CAc – control for chronic alcohol group, NTc – non-treated control group, CE – coefficient of error, CB – calbindin, PV – parvalbumin.

Experimental group	Stain	Counting frame size (µm)	Sampling grid size (µm)	Disector height (µm)	Section thickness (µm)	Average mounted thickness (µm)	Guard zones (µm)	Section interval	Average number of sections	Average number of sampling sites	Average CE (Gundersen m = 1)
Nissl stain – density of cells in molecular layer											
CA	Nissl	75x75	75x75	15	50	19.6	2	4	6	28.0	0.07
CAc	Nissl	75x75	75x75	16	50	20.4	2	4	6	27.7	0.07
NTc	Nissl	75x75	75x75	11	50	19.6	2	4	6	27.7	0.07
Parvalbumin immunostain – density of cells in molecular layer											
CA	PV	75 x 75	75 x 75	17	50	21.9	2	4	6	28.0	0.15
CAc	PV	75 x 75	75 x 75	18	50	23.1	2	4	6	27.5	0.16
NTc	PV	75 x 75	75 x 75	17	50	21.7	2	4	6	29.0	0.16
Calbindin immunostain – Purkinje cell volumes											
CA	CB	75 x 75	75 x 75	16	50	20.8	2	4	6	68.5	0.10
CAc	CB	75 x 75	75 x 75	18	50	22.6	2	4	6	71.7	0.09
NTc	CB	75 x 75	75 x 75	17	50	22.1	2	4	6	59.2	0.10

4.3. Results:

4.3.1. General observations on the body and brain:

The pups that experienced chronic prenatal alcohol exposure (CA group) showed no overt signs of FAS, in that no craniofacial abnormalities were readily apparent and there was no evident reduction in overall body mass. At the time of sacrifice, the average body masses of the mice were: CA male – 20.67 g (s.d. 1.53 g), CA female – 15.00 g (s.d. 0.71 g); CAc male – 19.75 g (s.d. 0.35 g), CAc female – 16.13 g (s.d. 0.25 g); NTc male – 19.88 g (s.d. 0.63 g), NTc female – 15.25 g (s.d. 0.35 g). There were no observable differences in the general morphology of the brains of mice treated with alcohol (CA group), sucrose (CAc group) or the non-treated control group (NTc). The average brain masses recorded for each group were: CA male – 0.418 g (s.d. 0.017 g), CA female – 0.395 g (s.d. 0.007 g); CAc male – 0.405 g (s.d. 0.007 g), CAc female – 0.385 g (s.d. 0.006 g); NTc male – 0.405 g (s.d. 0.006 g), NTc female – 0.390 g (s.d. 0.014 g). No statistically significant differences were observed between experimental groups in terms of body or brain mass when mice of the same sex were compared.

4.3.2. Cytoarchitecture of the cerebellar cortex:

Staining with cresyl violet revealed that the mice from all three experimental groups evinced the typical three-layered cerebellar cortex, made up of the molecular layer (layer I), the Purkinje cell layer (layer II) and the granule cell layer (layer III) (Fig. 4.1A, 4.1E, 4.1I). Throughout the molecular layer moderately intensely stained cells, presumably basket and stellate cells, were observed. Large palely stained cells,

presumably Purkinje cells, formed a monolayer immediately deep to the molecular layer. Deep to the Purkinje cell layer, a high density of intensely stained small round cells, presumably granule cells, formed the granule cell layer. When examined at high magnification, in addition to granule cells, Golgi-type II cells, Lugaro cells and occasional unipolar brush cells could be observed. Thus, the mice from all three experimental groups presented with a cerebellar cortical architecture that could be described as typical for laboratory rodents.

4.3.3. Parvalbumin immunoreactive (PV+) structures in the cerebellar cortex:

Within the molecular layer of the cerebellar cortex, the soma of both stellate and basket cells were moderately intensely immunoreactive to the parvalbumin antibody (Fig. 4.1B, 4.1F, 4.1J) in mice from all three experimental groups. The primary, but not the secondary, dendrites of the stellate and basket cells were also observed to be PV+. A significant proportion of the Purkinje cells were weak to moderately intensely immunoreactive to the parvalbumin antibody (Fig. 4.1B, 4.1F, 4.1J) in mice from all three experimental groups. The main dendrites of the Purkinje cells were also PV+, but only in close apposition to the cells, within one cell width of the Purkinje cell soma. Surrounding the Purkinje cells, intensely immunoreactive axons emanating from the granule cells, presumably those going on to form the parallel fibres were stained, but no obvious parallel fibres were stained in the molecular layer. No PV+ structures, apart from axons emanating from the granule cells, were observed in the granule cell layer of mice from any of the experimental groups. Thus, no distinct qualitative differences could be observed for parvalbumin

immunoreactive structures in the cerebellar cortex across the three experimental groups (Fig. 4.1B, 4.1F, 4.1J).

4.3.4. Calbindin immunoreactive (CB+) structures in the cerebellar cortex:

The soma and major dendrites of the Purkinje cells were intensely immunoreactive to the calbindin antibody (Fig. 4.1C, 4.1G, 4.1K) in mice from all three experimental groups. The large soma of the Purkinje cells exhibited the typical monolayer appearance between the molecular and granule layers of the cerebellar cortex. From the superficial aspect of the Purkinje cell soma, a single large, but highly ramified, dendrite was observed to emerge and invest into the molecular cell layer through to the pial surface (Fig. 4.1C, 4.1G, 4.1K). Within the molecular layer the extensively branched and bouton dense climbing fibres, closely associated with the major dendrites of the Purkinje cells, were also intensely CB+. In the granule cell layer, the region of the climbing fibre axons that did not contain boutons, and the exiting axons of the Purkinje cells were both intensely CB+. The occasional palely CB+ Golgi-type II cell could be observed in the granule cell layer in mice from all three experimental groups. Thus, no distinct qualitative differences could be observed for calbindin immunoreactive structures in the cerebellar cortex across the three experimental groups (Fig. 4.1C, 4.1G, 4.1K).

4.3.5. Calretinin immunoreactive (CR+) structures in the cerebellar cortex

A number of neural structures within the cerebellar cortex, from all mice from the three experimental groups, were CR+ (Fig. 4.1D, 4.1H, 4.1L). Within the

molecular layer a high density of CR+ boutons could be observed throughout the layer, but it is not possible to associate these with any specific neural structure. The Purkinje cell layer appeared to have a complete absence of CR immunoreactivity. Within the granule cell layer the vast majority of granule cells exhibited a moderately intense CR immunoreactivity. In some regions of the cerebellar cortex, clearly CR+ Golgi-type II cells, Lugaro neurons and unipolar brush cells were observed, but this was in limited regions of the cortex and mostly associated with regions where the intensity of CR immunoreactivity in the granule cells was lower. No distinct qualitative differences could be observed for calretinin immunoreactive structures in the cerebellar cortex across the three experimental groups (Fig. 4.1D, 4.1H, 4.1L).

4.3.6. Quantification of cell densities of Nissl stained and parvalbumin immunoreactive cells in the molecular layer of the vermal cerebellar cortex:

The quantitative analysis of the cell densities of Nissl stained neurons in the molecular layer of the vermal cerebellar cortex of mice from the three different experimental groups revealed a distinct homogeneity in densities between individuals in the same group, and between groups. For the CA group, the average cell densities of Nissl stained neurons was 0.0115 cells/μm^3 (s.e. 0.0006), for the CAc group it was 0.0103 cells/μm^3 (s.e. 0.0005) and for the NTc group it was 0.0111 cells/μm^3 (s.e. 0.0007) (Fig. 4.2A). While there is a trend for the CA to have slightly higher cell density than the CAc and the NTc groups, analysis of variance and post-hoc pairwise comparisons revealed that the cell density of Nissl stained neurons in the CA group was not statistically significantly different from the CAc group ($p = 0.339$) or the NTc

group (p = 0.896). A comparison between CAc and NTc groups was also not statistically significantly different (p = 0.583).

For the quantitative analysis of the cell densities of parvalbumin immunoreactive (PV+) neurons in the molecular layer of the vermal cerebellar cortex of mice from the three different experimental groups, stereological analysis revealed a distinct homogeneity in the densities of PV+ neurons in the molecular layer between individuals in the same group, and between groups (Fig. 4.2B). For the CA group, the average density of PV+ neurons was 0.0021 cells/μm^3 (s.e. 0.0002) for the CAc group it was 0.0016 cells/μm^3 (s.e. 0.0002) and for the NTc group it was 0.0019 cells/μm^3 (s.e. 0.0003) (Fig. 4.2A). While there is a trend for the CA to have a slightly higher cell density than the CAc and the NTc groups (Fig. 4.2B), analysis of variance and post-hoc pairwise comparisons revealed that the cell density of PV+ neurons in the CA group was not statistically significantly different from the CAc group (p = 0.424) or the NTc group (p = 0.853). A comparison between CAc and NTc groups was also not statistically significantly different (p = 0.741).

4.3.7. Quantification of Purkinje cell areas and volumes in the vermal cerebellar cortex:

In terms of average somal area of the calbindin immunoreactive (CB+) Purkinje cells of the vermal cerebellar cortex, the CA group had an average somal area of 208.2 μm^2 (s.e. 2.5), for the CAc group it was 205.6 μm^2 (s.e. 2.0.) and for the NTc group it was 212.3 μm^2 (s.e. 1.9) (Fig. 4.2C). Statistical analyses using analysis of variance and post-hoc pairwise comparisons revealed that the somal area of the CB+ Purkinje cells in the CA group was not statistically significantly different from those

of the CAc group (p = 0.676) and the NTc group (p = 0.369). A comparison of Purkinje cell areas between the CAc and NTc groups was not statistically significantly different (p = 0.073). In regards to average Purkinje cell volume, the CA group exhibited Purkinje cells with an average volume of 2406.02 μm^3 (s.e. 42.2), for the CAc group it was 2340.1 μm^3 (s.e. 33.7) and for the NTc group it was 2440.4 μm^3 (s.e. 31.6) (Fig. 4.2D). Statistical analyses revealed that the volumes of the CB+ Purkinje cells in the CA group was not statistically significantly different from the Purkinje cell volumes of the CAc group (p = 0.409) and the NTc group (p = 0.783). A comparison of the somal volumes between the CAc and NTc groups was not statistically significantly different (p = 0.127).

Figure 4.1: Photomicrographs of Nissl stained (**A**, **E**, **I**), parvalbumin (**B**, **F**, **J**), calbindin (**C**, **G**, **K**), and calretinin (**D**, **H**, **L**) immunostained vermal cerebellar cortex of 56 day-old C57BL/6J mice following exposure to a chronic prenatal alcohol regime *via* oral gavage (**A** – **D**, **CA**), oral gavage control (**E** – **H**, **CAc**), and non-treated control (**I** – **L**, **NTc**). No overt variation in the cytoarchitecture, or immunolocalization of the calcium-binding proteins, was observed. Scale bar in **H** = 200 µm and applies to all. In all images the pial surface is towards the top of the image.

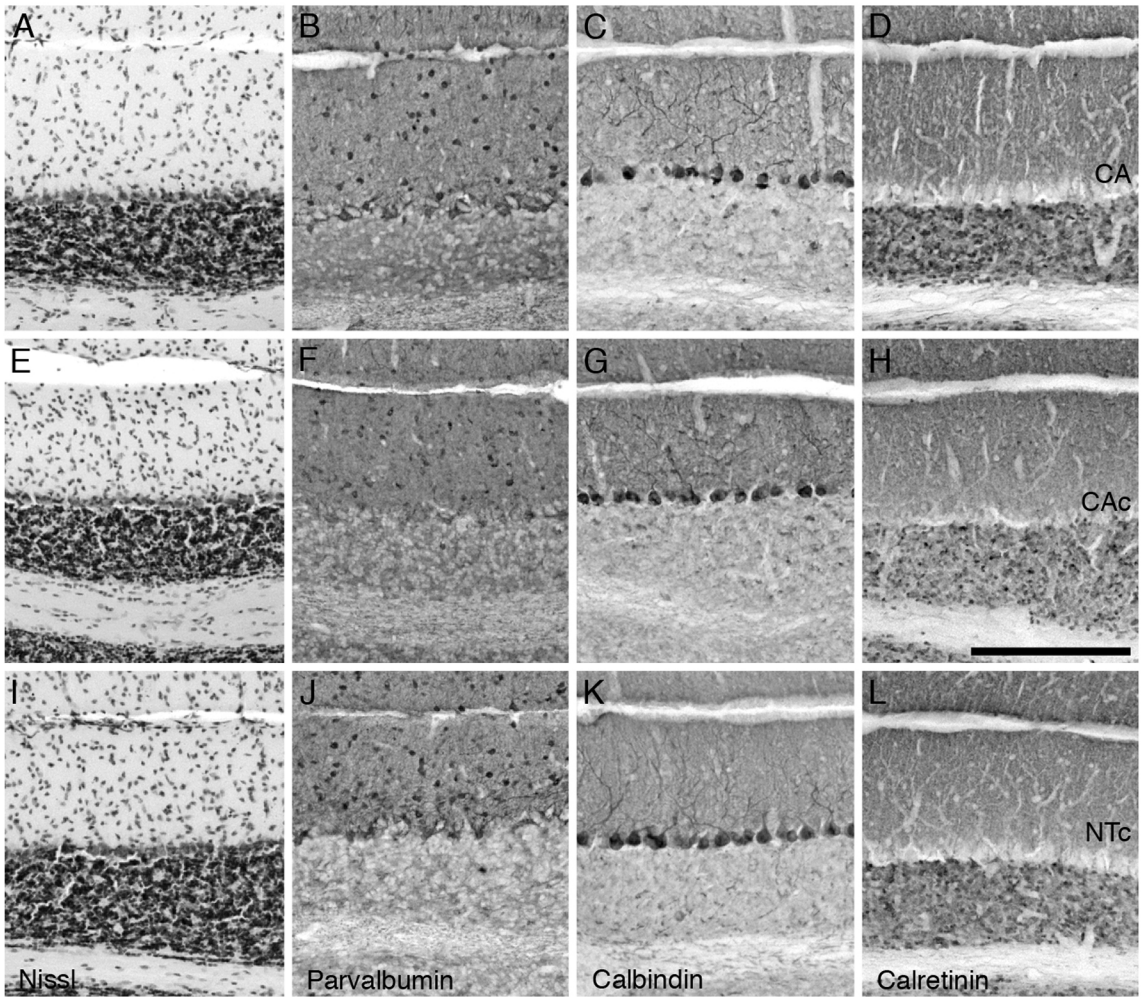
A
B
C
D
CA
E
F
G
H
CAc
I
J
K
L
NTc
Nissl
Parvalbumin
Calbindin
Calretinin

Figure 4.2: Graphs showing the average densities of Nissl stained (**A**) and parvalbumin immunoreactive (**B**) neurons in the molecular layer of the vermal cerebellar cortex, and the average area (**C**) and volume (**D**) of Purkinje cells from the same region of the three different experimental groups (n = 6 per group) analyzed in the present study: the group exposed to chronic prenatal alcohol (**CA**); the prenatal gavage control group (**CAc**); and the non-treated control group (**NTc**). Note the lack of any statistically significant differences in any of these parameters across all three experimental groups.

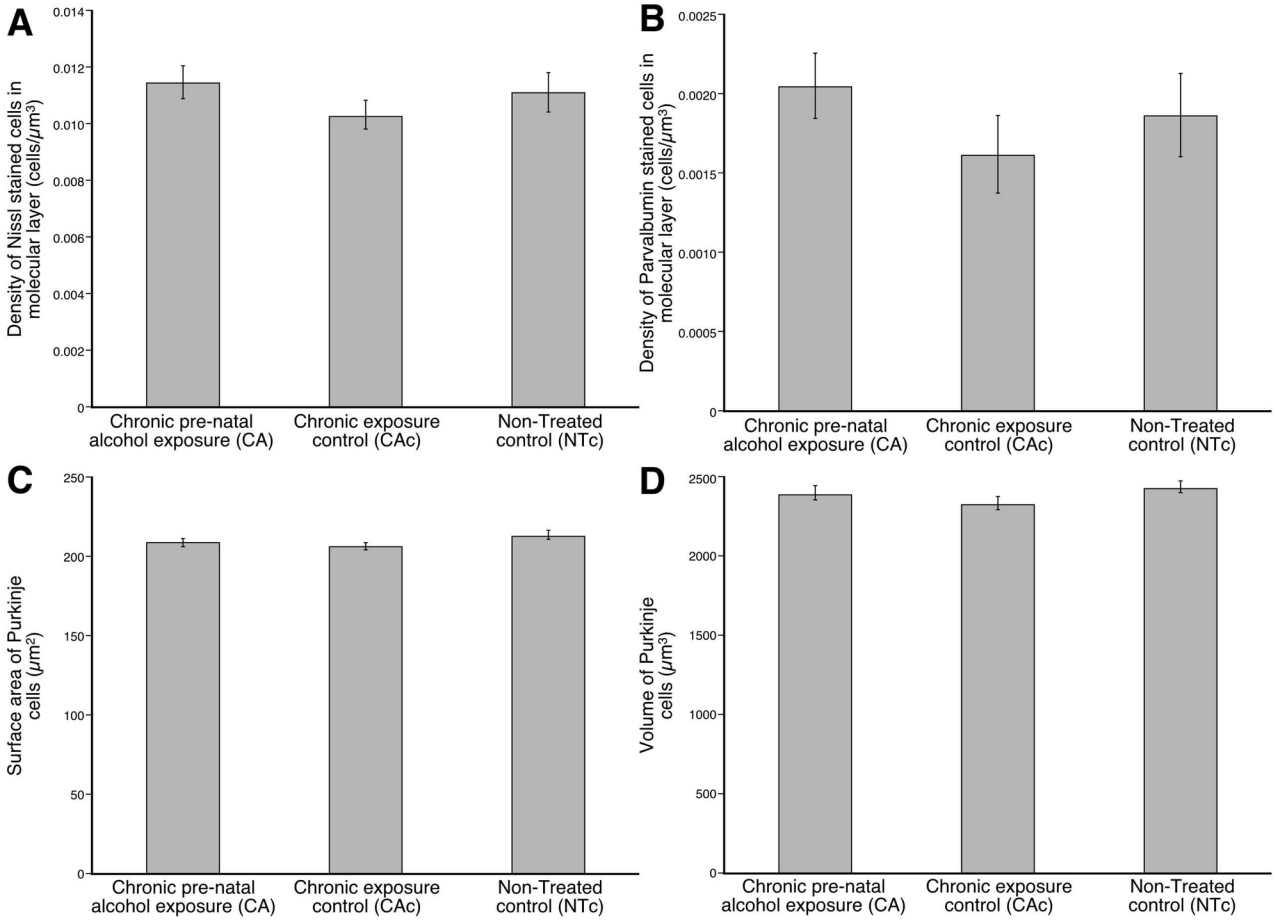
A
Density of Nissl stained cells in molecular layer (cells/μm^3)
0.014
0.012
0.010
0.008
0.006
0.004
0.002
0
Chronic pre-natal alcohol exposure (CA)
Chronic exposure control (CAc)
Non-Treated control (NTc)
B
Density of Parvalbumin stained cells in molecular layer (cells/μm^3)
0.0025
0.0020
0.0015
0.0010
0.0005
0
Chronic pre-natal alcohol exposure (CA)
Chronic exposure control (CAc)
Non-Treated control (NTc)
C
Surface area of Purkinje cells (μm^2)
250
200
150
100
50
0
Chronic pre-natal alcohol exposure (CA)
Chronic exposure control (CAc)
Non-Treated control (NTc)
D
Volume of Purkinje cells (μm^3)
2500
2000
1500
1000
500
0
Chronic pre-natal alcohol exposure (CA)
Chronic exposure control (CAc)
Non-Treated control (NTc)

4.4. Discussion:

Despite earlier observations demonstrating cerebellar structural deficits with associated behavioural problems in FASD children and rodent models (Abel, 1984; Streissguth et al., 1984; Miller and Robertson, 1993; Riley et al., 1995; Mattson et al., 1996; Sowell et al., 1996; Maier et. al., 1999; Powrozek and Zhou, 2005; Oladehin et al., 2007; Roebuck et al., 1998a,b; Spottiswoode et al., 2011), in the current anatomical study of the vermal cerebellar cortex no changes in either the structure or immunolocalization of the calcium-binding proteins was observed. This lack of substantive differences was supported with both qualitative and quantitative examination of the vermal cerebellum. In addition, with the same mice, significant differences in the process of adult neurogenesis (see Chapter 2), the structure of the barrel cortex (see Chapter 3), and the sleep systems (see Chapter 5), were observed, meaning that it appears reasonable to conclude, that, at least for the alcohol exposure regime used herein, the cerebellar cortex appears to be spared from damage. This lack of change in the architecture and neurochemistry of the vermal cerebellar cortex is of interest, as much of the remainder of the mouse brain was affected by exposure to prenatal alcohol.

One possibility is that the timing of alcohol exposure did not coincide with the development of the cerebellar cortex, but does coincide with the development of other parts of the brain, allowing the cerebellar cortex to be spared from damage. In the chronic prenatal alcohol exposure regime used herein, the *in utero* pups were exposed to alcohol from gestational (or post-conception) day 7 to gestational day 16. Previous reports indicate that the peak of generation of cells forming both Purkinje cells and the cells of the deep cerebellar nuclei in the mouse occurs during gestational days 10 to 11 (Clancy et al., 2001). Thus, the timing of peak neuronal birth rates in the

cerebellum in the mouse clearly overlaps with the period when the *in utero* mice pups in the current study were exposed to alcohol. Interestingly, the peak development periods for the dentate gyrus (gestational day 14), the layers of the cerebral cortex (gestational days 12 to 16), the hypothalamus (gestational days 12.5 – 13), and the pons (gestational days 10 – 13.5) (Clancy et al., 2001) also all overlap with the period of *in utero* alcohol exposure and all showed deficits (see earlier Chapters). Previous studies of the effect of alcohol on the structure of the cerebellum in rats have shown that the effect of alcohol exposure was substantially more evident when the pups were exposed to alcohol postnatally (Klintsova et al., 1999). Thus, while the timing of alcohol exposure in the current study does overlap with the peak of neurogenesis in the cerebellum of the mouse (Clancy et al., 2001), it appears that this exposure may have occurred too early to inculcate significant changes in the architecture and neurochemistry of the cerebellar cortex. Interestingly, using the same alcohol exposure regime did not affect the locus coeruleus of the mice studied, but affected the pontine cholinergic neurons that are found in almost the same location as the locus coeruleus neurons (see Chapter 5). Thus, there appears to be some specificity to the deleterious effects of alcohol exposure on different parts of the brain, and in order to introduce specific effects in model animals, the exposure to alcohol must be undertaken at specific developmental times, making the generation of a generalized rodent model of Fetal Alcohol Spectrum Disorder (FASD) a complex task.

Alternatively, the motor deficits observed in both FASD children and rodent models of FASD, may involve portions of the motor systems not directly associated with the cerebellar cortex. For example, although not studied herein, the thalamocortical and striatal portions of the motor system, or the deep cerebellar nuclei, may have been affected. It would be of interest to examine all portions of the

brain involved in motor control in more detail to determine whether the lack of changes observed for the cerebellar cortex are a common feature of the motor systems, indicating that in order to develop motor disorders the exposure to alcohol must be specifically timed (Klintsova et al., 1999), or whether the timing of alcohol exposure can differentially affect the various portions of the motor control systems of the brain. Despite the negative findings of the current study, this analysis has raised two interesting avenues for future work: (1) vary the timing of alcohol exposure to determine whether timing is the crucial aspect for producing deficits in the cerebellar cortex; and (2) examine the motor systems more broadly throughout the brain to determine whether there is specificity of the deleterious effects of developmental alcohol exposure associated with different exposure times. While these two possibilities can be worked on simultaneously, the amount of work required is significant; however, this type of work will lead to a clearer understanding of the effects of alcohol on the developing mammalian brain, including that of humans, and may present opportunities to develop interventions that could improve the quality of life of children exposed to alcohol.

CHAPTER FIVE: Changes in the cholinergic, catecholaminergic, orexinergic and serotonergic neurons forming part of the sleep systems of adult mice exposed to intrauterine alcohol

5.1. Introduction:

Adequate quality sleep, especially in children, is important for the development of the brain (Chen et al., 2012; Ipsiroglu et al., 2013). Certain neural functions such as learning, cognition, motor activities, attention, alertness, as well as brain growth and metabolic activities, are only performed effectively if there has been adequate sleep (Chen et al., 2012; Ipsiroglu et al., 2013). Sleep problems are often observed in concert with neurodevelopmental conditions such as autism (Malow et al., 2006), attention deficit hyperactivity disorders (Cortese et al., 2009) and fetal alcohol syndrome (FAS) (Streissguth et al., 2004; May et al., 2009; Olson et al., 2009; Chen et al., 2012; Ipsiroglu et al., 2013). Children with FAS show an unwillingness to go to bed (Meltzer and Mindell, 2004; Wengel et al., 2011), experience short sleep duration (Jan et al., 2010; Wengel et al., 2011), and experience sleep anxiety and frequent sleep disruptions (Haydon et al., 2009; Wengel et al., 2011). Morever, FAS children report night terrors (Durmer and Dinges, 2005), exhibit sleep walking (Randazzo et al., 1998), daytime tiredness (Lancioni et al., 1999), and suppressed sensory information processing (Wengel et al., 2011) when compared to neurotypical children.

The neural systems that control and regulate sleep are comprised of neurons, in specific nuclear clusters in the basal forebrain, hypothalamus and pons, which

produce a variety of neurotransmitters. These neurons depolarize in specific patterns during wake, slow wave sleep (SWS) and rapid eye movement sleep (REM) (Datta and MacLean, 2007; Lyamin et al., 2008; Takahashi et al., 2010; Dell et al., 2012; Bhagwandin et al., 2013; Petrovic et al., 2013). Briefly, the GABAergic neurons of the basal forebrain are sleep promoters, whereas the cholinergic neurons of the basal forebrain are part of the arousal system. Hypothalamic orexinergic and histaminergic neurons are associated with arousal, while the midbrain/pontine cholinergic neurons are associated with wake and REM sleep. The GABAergic neurons of the midbrain/pons inhibit the activity of the serotonergic and noradrenergic neurons in this region, with the noradrenergic and serotonergic neurons being active during wake and SWS, but inactive during REM.

Due to the relationship of these neuronal groups to the sleep-wake cycle, it may be that the anatomy of these neuronal systems differ from neurotypical in FAS children with sleep disorders; however, to the author's knowledge, there appear to be no reports that directly correlate the morphological changes in the sleep centres in FAS subjects that are known to experience sleep disorders. In order to determine whether morphological changes in the neural systems involved in the production and regulation of sleep may be correlated to the sleep disorders observed in FAS children, we targeted for investigation the organization, morphology and numbers of pontine cholinergic (laterodorsal tegmental and pedunculopontine nuclei), pontine catecholaminergic (locus coeruelus complex), hypothalamic orexinergic and midbrain serotonergic (dorsal raphe) neurons of 56 day old C57BL/6J mice following exposure to prenatal alcohol. In addition to qualitative examination of these neurons involved in sleep, stereological analysis of neuronal numbers and neuronal size was undertaken for the cholinergic laterodorsal tegmental nucleus (LDT) and pedunculopontine

tegmental nucleus (PPT), the noradrenergic locus coeruleus complex (LC) and the orexinergic neurons of the hypothalamus.

5.2. Materials and methods:

5.2.1. Breeding and prenatal ethanol exposure

All animals were treated and used according to the guidelines of the University of the Witwatersrand Animal Ethics Committee (Clearance No. 2012/15/2B), which parallel those of the NIH for the care and use of animals in scientific experimentation. Female C57BL/6J mice (*Mus musculus*), twelve weeks of age, were allocated into three experimental groups: Chronic Alcohol exposure (CA), control for Chronic Alcohol exposure (CAc), and a Non-Treatment control group (NTc). For effective mating, 1–2 female mice were introduced into the cage of a C57BL/6J male mouse for 12 hours, which was considered gestational day 0 (GD 0). In all, a total of 14 female mice (4–5 mice assigned to each experimental group) and 8 male mice were used to generate the required numbers of pups used in the present study.

For the CA group, each pregnant mouse received a dose of 7.5 µl/g of 50 % alcohol in distilled water (5.9 g/kg) per day (Haycock and Ramsay, 2009; Knezovich and Ramsay, 2012) for 10 consecutive days by oral gavage, starting from GD 7 (Webster et al., 1980; Sulik et al., 1981; Webster et al., 1983; Choi et al., 2005; Redila et al., 2006; Parnell et al., 2009), while each pregnant mouse in the CAc group received an equivalent dose of isocaloric sucrose (704 g/L) by oral gavage over the same period (Haycock and Ramsay, 2009; Knezovich and Ramsay, 2012). To control

for the possible influence of post-traumatic stress in the pregnant mice, pregnant mice in the NTc group did not undergo any oral gavage. Food and water was provided *ad libitum* to the mice, except in the control groups (CAc and NTc), where it was withheld for two hours post-gavage in order to partially mimic the anorectic effect of alcohol (Haycock and Ramsay, 2009). The pups were weaned 21 days after birth and then the male and female pups separated. Three pups of the same sex from each experimental group were kept in separate cages (cage dimensions: 200 x 200 x 300 mm) with adequate food and water supplies until post-natal day (PND) 56.

5.2.2. Blood alcohol concentration assay in the pregnant mice:

On the last day (10^{th} day) of oral gavage (GD 16), a small lesion was made at the site of the saphenous vein on the left hind legs of all the pregnant mice in the CA and CAc experimental groups. The saphenous bleeding procedure was performed on the pregnant mice in the sucrose group in order to mimic the effects of the bleeding on the alcohol exposed pregnant mice. The non-treatment pregnant mice served as controls for the possible effects of the bleeding and/or the oral gavage procedures. 50 µl of blood was drawn into heparinized capillary tubes at 30 min post-gavage (Bielawski and Abel, 1997) to determine the blood alcohol concentration (BAC). The blood samples from the FAS model and the sucrose control were stored at 4°C overnight after which they were centrifuged with Vivaspin500 100 µm membrane tubes (Biotech, South Africa) for 30 min before the serum was extracted and the BAC analyzed using an EnzyChrom™ Ethanol Assay Kit (BioVision, South Africa). The pregnant mice belonging to the CA group that were administered alcohol had an

average BAC of 1.84 mg/ml (s.e. = 0.39), which is above the pharmacologically significant level of 1 mg/ml reported by Rhodes et al. (2005) and Sulik (2005).

5.2.3. Sacrifice and tissue processing:

At PND 56, when the prenatally-alcohol-exposed mice reached adulthood, a total number of six mice (n = 6) from each experimental group (1–2 mice randomly selected from each litter set) were weighed and then euthanized (Eutha-naze 1 ml/kg, contains sodium pentobarbitone 100 mg/ml, intra-peritoneally) before being perfused trans-cardially with 0.9% cold (4°C) saline followed immediately by cold 4% paraformaldehyde in 0.1 M phosphate buffer (PB). The brain was removed from the skull, weighed and post-fixed for 24 h in 4% paraformaldehyde in 0.1 M PB at 4°C. The brains were then cryoprotected by immersion in 30 % buffered sucrose solution in 0.1 M PB at 4°C until they equilibrated. The diencephalon and pons was dissected from the remainder of the brain for all 18 individual mice and was then frozen in crushed dry ice, and sectioned in a coronal plane at 50 µm thickness using a sliding microtome. A one in four series of sections was taken. The first series of sections, stained for Nissl substance to reveal cytoarchitectural features, was mounted on 0.5% gelatine-coated slides, dried overnight, cleared overnight in a 1:1 mixture of 100% ethanol and 100% chloroform and stained with 1% cresyl violet in H_2O. The second series of sections was immunostained with an antibody to cholineacetyltransferase (ChAT, AB144P, Chemicon, raised in goat) to reveal cholinergic neurons, and the third series was immunostained with an antibody to tyrosine hydroxylase (TH, AB151, Chemicon, raised in rabbit) to reveal catecholaminergic neurons. The fourth series of sections was divided at the level of the posterior commissure. All sections

rostral to the posterior commissure were immunostained with an antibody to orexin-A (OxA, AB3704, Merck-Millipore, raised in rabbit) to reveal the hypothalamic orexinergic neurons, while all sections caudal to the posterior commissure were immunostained with an antibody to serotonin (5HT, AB938, Chemicon, raised in rabbit) to reveal the serotonergic neurons.

5.2.4. Immunostaining protocol:

All sections used for immunohistochemical staining were initially incubated in a solution containing 1.6% of 30% H_2O_2, 49.2% methanol and 49.2% 0.1M PB solution, for 30 min to reduce endogenous peroxidase activity, which was followed by three 10 min rinses in 0.1M PB. To block non-specific binding sites the sections were then preincubated at room temperature for 2 h in a blocking buffer solution containing 3% normal serum (normal rabbit serum, NRS, Chemicon, for ChAT sections, and normal goat serum, NGS, Chemicon, for the remaining sections), 2% bovine serum albumin (BSA, Sigma) and 0.25% Triton X-100 (Merck) in 0.1M PB. The sections were then placed in a primary antibody solution (blocking buffer with correctly diluted primary antibody) and incubated at 4°C for 48 hours under gentle shaking. To reveal cholinergic neurons, anti-cholineacetyltransferase (ChAT) at a dilution of 1:3000 was used. To reveal putative catecholaminergic neurons, anti-tyrosine hydroxylase (TH) was used at a dilution of 1:3000. To reveal serotonergic neurons, anti-serotonin (5-HT) at a dilution of 1:5000 was used. To reveal orexinergic neurons, anti-orexin-A (OxA) at a dilution of 1:3000 was used.

This was followed by three 10 min rinses in 0.1M PB, after which the sections were incubated in a secondary antibody solution for 2 h at room temperature. The

secondary antibody solution contained a 1:1000 dilution of biotinylated anti-goat IgG (BA-5000, Vector labs, for ChAT sections) or biotinylated anti-rabbit IgG (BA-1000, Vector Labs, for the remaining sections) in a solution containing 3% NGS/NRS and 2% BSA in 0.1M PB. This was followed by three 10 min rinses in 0.1M PB after which the sections were incubated in AB solution (Vector Labs) for 1 h. After three further 10 min rinses in 0.1M PB, the sections were placed in a solution of 0.05% diaminobenzidine in 0.1M PB for five minutes (1 ml/section), followed by the addition of 3 µl of 30% H_2O_2 to the solution in which each section was immersed. The precipitation process was stopped by immersing the sections in 0.1M PB and then rinsing them twice more in 0.1M PB. To check for non-specific staining from the immunohistochemistry protocol, we omitted the primary antibody and the secondary antibody in selected sections, which produced no evident staining. The sections were then mounted on 0.5% gelatine coated glass slides, dried overnight, dehydrated in a graded series of alcohols, cleared in xylene and coverslipped with DPX.

5.2.5. Qualitative and quantitative determination of cell numbers and statistical analysis:

The distribution of immunopositive cells was compared qualitatively between the experimental groups using both low and higher power light microscopy. Digital photomicrographs of these cells were captured using Zeiss Axioshop and Axiovision software. No pixelation adjustments or manipulation of the captured images was undertaken, except for the adjustment of contrast, brightness, and levels using Adobe Photoshop 7.

For the quantification of Chat+, TH+ and OxA+ cells, an unbiased design based systematic random sampling stereological protocol was employed. We used a MicroBrightfield (MBF) (Colchester, Vermont, USA) system with three plane motorised stage, Zeiss.Z2 vario axioimager and StereoInvestigator software (MBF, version 11.08.1; 64-bit). Separate pilot studies for each immunohistochemical stain for each group, were conducted to optimise sampling parameters, such as the counting frame and sampling grid sizes, and achieve a coefficient of error (CE) below 0.1 (Gundersen et al., 1988; West et al., 1991; Dell et al., 2016). At this point we would like to acknowledge that while every effort was made to obtain a CE below 0.1, this was not always achieved mostly due to a limited number of countable sections in those instances. In addition we measured the tissue section thickness at every 10^{th} sampling site and the vertical guard zone was determined according to tissue thickness to avoid errors/biases due to sectioning artifacts (West et. al., 1991; Dell et al., 2016). We decided to maintain consistency amongst sampling parameters between the groups studied for each neuroanatomical region to reduce unfavourable stereological estimation biases. Table 5.1 provides a detailed summary of the parameters used for each neuroanatomical region and between the groups in the current study.

To estimate the total number of pontine Chat+ neurons (LDT and PPT), pontine locus coeruleus TH+ neurons and hypothalamic OxA+ neurons, we used the 'Optical Fractionator' probe and the following equation (West et al., 1991; Dell et al., 2016):

$$N = Q / (SSF \times ASF \times TSF)$$

Where *N* was the total estimated neuronal number, *Q* was the number of neurons counted, *SSF* was the fraction of the sections sampled, ASF was the area sub

fraction (which is calculated by the ratio of the size of the counting frame to the size of the sampling grid), and TSF was the thickness sub fraction (which is calculated by the ratio of the disector height relative to the section thickness).

To determine neuronal sizes, we used the 'Nucleator'probe. For all individuals counted these probes were used concurrently while maintaining strict criteria, e.g. only neurons with complete cell bodies were counted, and obeying all commonly known stereological rules.

An analysis of variance (ANOVA) was performed to determine if there was a significant variation in the mean ChAT+, TH+, or OxA+ neuronal counts, areas and volumes of all the experimental groups (CA, CAc and NTc). Where the ANOVA was significant, a Post hoc analysis was further performed using Tukey's pairwise comparison test to determine where significant differences exist. All statistical analyses were performed using SPSS Inc programme (version 22.0). A significance level of 5% was used as an indicator of significant differences for all statistical analyses.

Table 5.1: Stereological parameters used for estimating cell numbers and sizes in the various nuclei quantified in the current study. CA – chronic alcohol group, CAc – control for chronic alcohol group, NTc – non-treated control group, CE – coefficient of error.

Experimental group	Antibody	Counting frame size (µm)	Grid frame size (µm)	Disector height (µm)	Section thickness (µm)	Average mounted thickness (µm)	Guard zones (µm)	Section interval	Average number of sections	Average number of sampling sites	Average CE (Gundersen m = 1)
Cholinergic neurons of the laterodorsal tegmental (LDT) and pedunculopontine tegmental (PPT) nuclei											
CA	ChAT	300 x 300	300 x 300	11	50	17.6	2	4	10.2	159.4	0.07
CAc	ChAT	300 x 300	300 x 300	11	50	16.8	2	4	11.3	182.2	0.08
NTc	ChAT	300 x 300	300 x 300	11	50	16.7	2	4	12.8	180.6	0.07
Noradrenergic neurons of the locus coeruleus complex											
CA	TH	375 x 375	375 x 375	11	50	16.3	2	4	5.2	60.8	0.14
CAc	TH	375 x 375	375 x 375	11	50	17.5	2	4	4.8	68.2	0.15
NTc	TH	375 x 375	375 x 375	11	50	17.6	2	4	5.5	66.3	0.17
Orexinergic neurons of the hypothalamus											
CA	OxA	375 x 375	375 x 375	13	50	18.2	2	4	4.4	60.6	0.13
CAc	OxA	375 x 375	375 x 375	13	50	20.9	2	4	4.2	51.3	0.14
NTc	OxA	375 x 375	375 x 375	13	50	18.4	2	4	4.0	102.0	0.14

5.3. Results:

5.3.1. General observations on the body and brain:

The pups that experienced chronic prenatal alcohol exposure (CA group) showed no overt signs of FAS, in that no craniofacial abnormalities were readily apparent and there was no evident reduction in overall body mass. At the time of sacrifice, the average body masses of the mice were: CA male – 19.75 g (s.d. 1.06 g), CA female – 15.13 g (s.d. 1.11 g); CAc male – 19.88 g (s.d. 0.85 g), CAc female – 16.00 g (s.d. 0.50 g); NTc male – 20.25 g (s.d. 1.50 g), NTc female – 15.63 g (s.d. 0.48 g). In addition, there were no observable differences in the general morphology of the brains of mice treated with alcohol (CA group), sucrose (CAc group) or the non-treated control group (NTc). The average brain masses recorded for each group were: CA male – 0.420 g (s.d. 0.028 g), CA female – 0.398 g (s.d. 0.005 g); CAc male – 0.408 g (s.d. 0.005 g), CAc female – 0.388 g (s.d. 0.006 g); NTc male – 0.403 g (s.d. 0.005 g), NTc female – 0.390 g (s.d. 0.014 g). No statistically significant differences were observed between experimental groups in terms of body or brain mass when mice of the same sex were compared.

5.3.2. Cholinergic neurons of the laterodorsal tegmental and pedunculopontine nuclei:

For all mice in all three experimental groups, there were no marked differences in the location and morphology of the ChAT+ neurons within the pedunculopontine (PPT) and the laterodorsal (LDT) nuclei. The ChAT+ neurons forming the PPT were located within the dorsal aspect of the pontine tegmentum extending from the

ventrolateral border of the periaqueductal/periventricular grey matter to the superior cerebellar peduncle (Fig. 5.1). A moderate to high density of ChAT+ neurons were observed in this region. Within the periventricular grey matter, caudal to the oculomotor nucleus, a moderate to high density of ChAT+ neurons were designated as those forming the LDT nucleus (Fig. 5.1). The ventrolateral border of the LDT neurons was contiguous with the dorsomedial border of the PPT nucleus, the only reason to separate these two nuclei being the transition from the periventricular grey matter to the pontine tegmentum. The PPT and LDT ChAT+ neurons exhibited a variety of somal shapes due to being multipolar (Fig. 5.1).

Our quantitative analysis of the numbers of ChAT+ neurons in the LDT and PPT in the brain of mice from the three different experimental groups revealed a distinct homogeneity in numbers between individuals in the same group, and between groups. For the CA group, the average number of ChAT+ neurons was 1741.4 (s.e. 276.8), for the CAc group it was 1844.3 (s.e. 312.7) and for the NTc group it was 2091.9 (s.e. 405.2) (Fig. 5.2A). While there is a trend for the CA and CAc groups to have less ChAT+ neurons than the NTc group, these were not statistically significant differences. Analysis of variance and post-hoc pairwise comparisons revealed that the lower number of ChAT+ neurons in the CA group was not statistically significantly different from the CAc group ($p = 0.977$) or the NTc group ($p = 0.763$). A comparison between CAc and NTc groups was also not statistically significantly different ($p = 0.872$).

In terms of average somal area, the CA group had an average somal area of 89.7 μm^2 (s.e. 1.0), for the CAc group it was 95.0 μm^2 (s.e. 0.7) and for the NTc group it was 92.9 μm^2 (s.e. 0.8) (Fig. 5.3A). Statistical analyses using analysis of variance and

post-hoc pairwise comparisons revealed that the smaller somal area of the ChAT+ neurons in the CA group was statistically significantly smaller than the CAc group (p = 0.000) and the NTc group (p = 0.017). A comparison of somal areas between the CAc and NTc groups was not statistically significantly different (p = 0.170). In regards to average somal volume, the CA group exhibited an average somal volume of 707.5 μm^3 (s.e. 12.5), for the CAc group it was 763.9 μm^3 (s.e. 8.9) and for the NTc group it was 739.4 μm^3 (s.e. 9.4) (Fig. 5.3B). Statistical analyses revealed that the smaller somal volumes of the ChAT+ neurons in the CA group was statistically significantly smaller than the somal volumes of the CAc group (p = 0.000), but not significantly different from the NTc group (p = 0.070). A comparison of the somal volumes between the CAc and NTc groups was not statistically significantly different (p = 0.208). Thus, for the pontine cholinergic neurons, the only substantive difference observed between the groups was the reduction in size, by around 5 – 10%, of the soma in the group exposed to prenatal alcohol.

5.3.3. Catecholaminergic neurons of the locus coeruleus complex:

For all mice in all three experimental groups, there were no marked differences in the location and morphology of the TH+ neurons within the locus coeruleus complex. Within the pontine region a large number of TH+ neurons forming the locus coeruleus complex were readily observed (Fig. 5.4). The locus coeruleus complex could be subdivided into five nuclei, these being: the subcoeruleus compact portion (A7sc), subcoeruleus diffuse portion (A7d), locus coeruleus compact portion (A6c), fifth arcuate nucleus (A5), and the dorsolateral division of locus coeruleus (A4). Within the dorsal portion of the pontine tegmentum adjacent to the

ventrolateral region of the periaqueductal grey matter, a tightly packed cluster of TH+ neurons represented the A7 compact portion of the LC. This division is the same as what was previously described as the subcoeruleus (Dahlström and Fuxe, 1964; Olson and Fuxe, 1972). Ventral and lateral to the A7sc, a diffusely organized aggregation of TH+ neurons formed the A7d nuclear complex (Fig. 5.4). These neurons are located both medially and laterally around the trigeminal motor nucleus (Vmot). Within the lateral portion of the periventricular grey matter a tightly packed, moderate to high density of TH+ neurons were assigned to the A6c nucleus (Fig. 5.4). The neurons of this group were found adjacent to the wall of the fourth ventricle, stretching across the periventricular grey matter to its lateral edge as seen in the laboratory rat (Dahlström and Fuxe, 1964). In the ventrolateral pontine tegmentum lateral to the superior olivary nucleus and lateral to Vmot and A7d, a small cluster of TH+ neurons formed the A5 nucleus. These neurons formed a rough meshlike dendritic network around the ascending fascicles located within the ventrolateral pontine tegmentum. Immediately adjacent to the wall of the fourth ventricle, in the dorsolateral portion of the periaqueductal grey matter, a very dense, but small cluster of TH+ neurons represent the A4 nucleus. All neurons throughout the locus coeruleus complex showed a similar variety of somal shapes and all were multipolar.

Our quantitative analysis of the numbers of TH+ neurons in the A7 and A7 nuclei of the locus coeruleus complex from the three different experimental groups revealed a distinct homogeneity in numbers between individuals in the same group, and between groups (Fig. 5.2B). For the CA group, the average number of TH+ neurons was 549.9 (s.e. 113.6), for the CAc group it was 510.2 (s.e. 60.6) and for the NTc group it was 512.8 (s.e. 104.4) (Fig. 5.2B). While the number of TH+ neurons is highest in the CA group, statistical analyses using analysis of variance and post-hoc

pairwise comparisons revealed that the number of TH+ neurons in the CA group was not statistically significantly different from the CAc group ($p = 0.952$) or the NTc group ($p = 0.958$). A comparison between CAc and NTc groups was also not statistically significantly different ($p = 0.999$).

In terms of average somal area, the CA group had an average somal area of 111.1 μm^2 (s.e. 1.9), for the CAc group it was 115.5 μm^2 (s.e. 1.9) and for the NTc group it was 114.1 μm^2 (s.e. 2.5) (Fig. 5.3C). Statistical analyses using analysis of variance and post-hoc pairwise comparisons revealed that the average somal areas of the TH+ neurons in the CA group was not statistically significantly different from the CAc group ($p = 0.305$) or the NTc group ($p = 0.578$). A comparison between CAc and NTc groups was also not statistically significantly different ($p = 0.884$). In regards to average somal volume, the CA group exhibited an average somal volume of 955.5 μm^3 (s.e. 25.2), for the CAc group it was 1011.3 μm^3 (s.e. 25.6) and for the NTc group it was 1007.1 μm^3 (s.e. 33.7) (Fig. 5.3D). Statistical analyses revealed that the average somal volume of the TH+ neurons in the CA group was not statistically significantly different from the CAc group ($p = 0.340$) or the NTc group ($p = 0.397$). A comparison between CAc and NTc groups was similarly not statistically significantly different ($p = 0.994$). Thus, for the neurons of the locus coeruleus complex, no differences in nuclear organization, neuronal morphology, neuronal numbers, or somal size was detected between the three experimental groups investigated.

5.3.4. Serotonergic neurons of the dorsal raphe nuclear complex:

For all mice in all three experimental groups, there were no marked differences in the location and morphology of the 5-HT+ neurons within the dorsal

raphe nuclear complex (Fig. 5.5). Within the 5HT+ neuronal region designated as the dorsal raphe nuclear complex there were six distinct nuclei, these being: the dorsal raphe interfascicular (DRif) nucleus, dorsal raphe ventral (DRv) nucleus, dorsal raphe dorsal (DRd) nucleus, dorsal raphe lateral (DRl) nucleus, dorsal raphe peripheral (DRp) nucleus and the dorsal raphe caudal (DRc) nucleus (Fig. 5). These six nuclei were found, for the most part, within the periaqueductal and periventricular grey matter from the level of the oculomotor nucleus to the trigeminal motor nucleus. The DRif was located between the two medial longitudinal fasciculi and exhibited a high density of oval shaped, mostly bipolar, 5HT+ neurons (Fig. 5.5). The DRv was found immediately dorsal to the DRif between and just caudal to the oculomotor nuclei. The DRv exhibited a high density of oval shaped, mostly bipolar, 5HT+ neurons. Immediately dorsal to DRv and ventral to the inferior border of the cerebral aqueduct a high-density cluster of oval shaped, mostly bipolar, 5HT+ neurons was designated as the DRd nucleus. A moderate density of 5HT+ neurons representing the DRp, were located in the ventrolateral portion of the periaqueductal grey matter lateral to the DRd and DRv. Some neurons of the DRp were found in the adjacent tegmentum and were the only ones found outside the periaqueductal grey matter. The 5HT+ neurons of the DRl were located dorsolateral to the DRd and adjacent to the ventrolateral edges of the cerebral aqueduct in a low to moderate density. The neurons of the DRp, DRl and DRc nuclei were readily distinguishable from the DRif, DRv and DRd nuclei since they were substantially larger and multipolar (Fig. 5.5B, 5.5D, 5.5F). As we followed the DRl caudally, where the cerebral aqueduct opened into the fourth ventricle and the DRd, DRv and DRif nuclei finished, the neurons of the DRl formed an arc across the midline of the dorsal portion of the periventricular grey matter. This caudal arc of the DRl was classified as the DRc nucleus. Thus, for the neurons of the

dorsal raphe complex, no differences in nuclear organization or neuronal morphology was detected between the three experimental groups investigated.

5.3.5. Orexinergic neurons of the hypothalamus:

For all mice in all three experimental groups, there were no marked differences in the location and morphology of the OxA+ neurons within the hypothalamus (Fig. 5.6). Within this aggregation of OxA+ hypothalamic neurons we could identify three distinct clusters – a main cluster (Mc), a zona incerta cluster (Zic) and an optic tract cluster (Otc) (Fig. 5.6). The main cluster (Mc) was identified as a large group of densely packed OxA+ neurons located lateral to the third ventricle in the perifornical region, with a moderate number of neuronal cell bodies extending medially from this area into the dorsomedial hypothalamus and a larger number extending into the lateral hypothalamic areas. From the main cluster a group of OxA+ neurons extended laterally into the region of the zona incerta (Zic) (Fig. 5.6). This cluster had a lower density of OxA+ neurons. The third cluster, the optic tract cluster (Otc) extended ventrolaterally from the main cluster to the ventrolateral region of the hypothalamus adjacent to the optic tract. This cluster exhibited a moderate to low density of OxA+ neurons (Fig. 5.6). All the OxA+ neurons were multipolar and exhibited a variety of somal shapes.

Our quantitative analysis of the numbers of OxA+ neurons in the hypothalamus of the three different experimental groups revealed a distinct homogeneity in numbers between individuals in the same group, and between groups. For the CA group, the average number of OxA+ neurons was 840.1 (s.e. 115.6), for the CAc group it was 762.6 (s.e. 107.4) and for the NTc group it was 684.8 (s.e. 131.4) (Fig. 5.2C). The

number of OxA+ neurons was highest in the CA group, but statistical analyses using analysis of variance and post-hoc pairwise comparisons revealed that the number of OxA+ neurons in the CA group was not statistically significantly different from the CAc group ($p = 0.892$) or the NTc group ($p = 0.639$). A comparison between CAc and NTc groups was also not statistically significantly different ($p = 0.891$).

In terms of average somal area, the OxA+ neurons in the CA group had an average somal area of 63.3 μm^2 (s.e. 1.3), for the CAc group it was 58.9 μm^2 (s.e. 1.3) and for the NTc group it was 55.8 μm^2 (s.e. 1.1) (Fig. 5.3E). Statistical analyses using analysis of variance and post-hoc pairwise comparisons revealed that the OxA+ somal areas in the CA group were statistically significantly larger than the OxA+ neurons of the CAc group ($p = 0.026$) and the NTc group ($p = 0.000$). A comparison of somal area between the CAc and NTc groups was not statistically significantly different ($p = 0.165$) (Fig. 5.3E). In regards to average somal volume, the OxA+ neurons in the CA group exhibited an average somal volume of 426.3 μm^3 (s.e. 13.1), for the CAc group it was 379.3 μm^3 (s.e. 12.5) and for the NTc group it was 350.9 μm^3 (s.e. 10.9) (Fig. 5.3F). Similar to the somal area, statistical analyses revealed that the somal volume in the OxA+ neurons in the CA group was statistically significantly larger than the OxA+ neurons of the CAc group ($p = 0.030$) and the NTc group ($p = 0.000$). A comparison of somal volume between CAc and NTc groups was not statistically significantly different ($p = 0.217$) (Fig. 5.3F). Thus, for the hypothalamic orexinergic neurons, the only substantive difference observed between the groups was the increase in size, by around 7 – 20%, of the soma in the group exposed to prenatal alcohol.

Figure 5.1: Lower (**A**, **C**, **E**) and higher (**B**, **D**, **F**) magnification photomicrographs of the laterodorsal tegmental (**LDT**, **B**, **D**, **F**) and pedunculopontine (**PPT**) nuclei of the mouse in the coronal plane immunostained for cholineacetyltransferase (ChAT) in the three different groups analyzed in the present study, the group exposed to chronic prenatal alcohol (**CA**) (**A**, **B**), the prenatal gavage control group (**CAc**) (**C**, **D**) and the non-treated control group (**NTc**) (**E**, **F**). The nuclear organization and number of ChAT immunostained cells was similar between groups, but the soma of the neurons in the **CA** group, exposed to chronic prenatal alcohol, were statistically significantly smaller than the two control groups (**CAc** and **NTc**). In all images dorsal is to the top and medial to the left. Scale bar in **E** = 250 µm and applies to **A**, **C** and **E**, scale bar in **F** = 100 µm and applies to **B**, **D** and **F**.

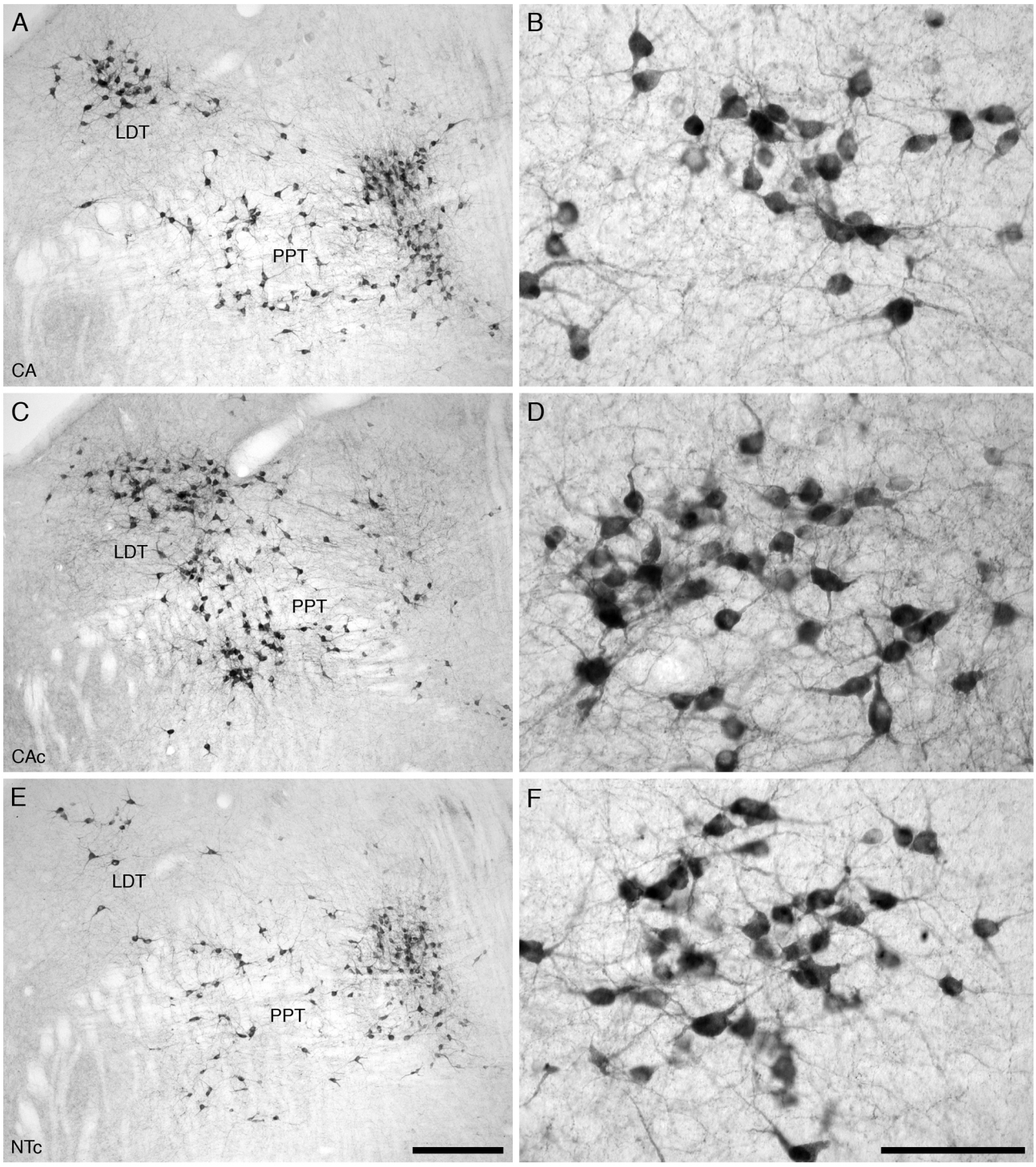
A
LDT
PPT
CA
B
C
LDT
PPT
CAc
D
E
LDT
PPT
NTc
F

Figure 5.2: Graphs showing the average numbers of cholinergic (ChAT) (**A**), catecholaminergic (TH) (**B**) and orexinergic (OxA) (**B**) immunoreactive cells in the brains of three different groups (n = 6 per group) analyzed in the present study, the group exposed to chronic prenatal alcohol (**CA**), the prenatal gavage control group (**CAc**) and the non-treated control group (**NTc**). (**A**) Note that while the numbers of ChAT immunoreactive neurons in the laterodorsal tegmental (**LDT**) and pedunculopontine (**PPT**) nuclei are lower in the **CA** group, this difference is not statistically significant. (**B**) Note that while the numbers of TH immunoreactive neurons in the locus coeruleus complex is higher in the **CA** group, this difference is not statistically significant. (**C**) Note that while the numbers of OxA immunoreactive neurons in the hypothalamus is higher in the **CA** group, this difference is not statistically significant.

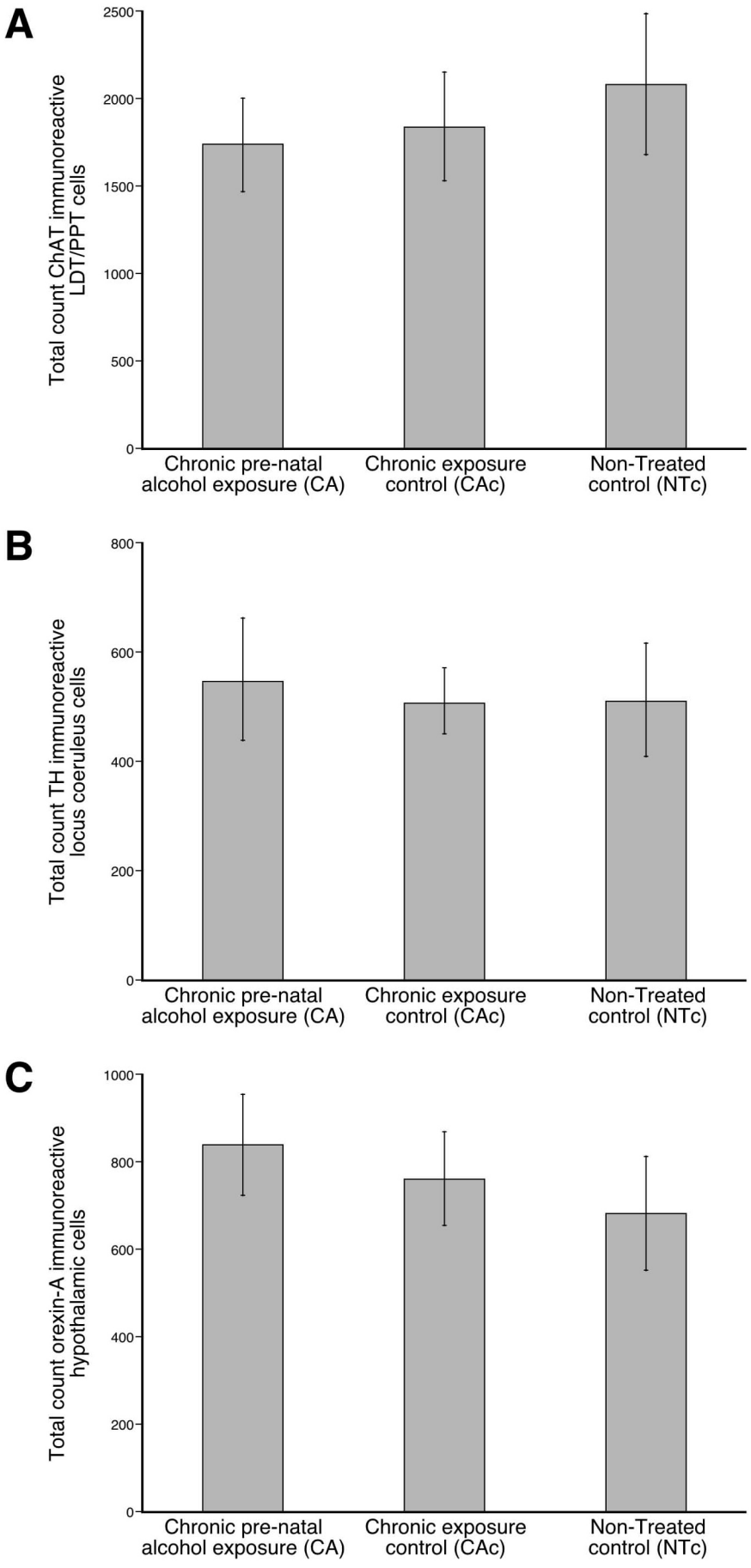
A
Total count ChAT immunoreactive LDT/PPT cells
2500
2000
1500
1000
500
0
Chronic pre-natal alcohol exposure (CA)
Chronic exposure control (CAc)
Non-Treated control (NTc)
B
Total count TH immunoreactive locus coeruleus cells
800
600
400
200
0
Chronic pre-natal alcohol exposure (CA)
Chronic exposure control (CAc)
Non-Treated control (NTc)
C
Total count orexin-A immunoreactive hypothalamic cells
1000
800
600
400
200
0
Chronic pre-natal alcohol exposure (CA)
Chronic exposure control (CAc)
Non-Treated control (NTc)

Figure 5.3: Graphs showing the average somal area (**A**, **C**, **E**) and average somal volume (**B**, **D**, **F**) of cholinergic (ChAT) (**A**, **B**), catecholaminergic (TH) (**C**, **D**) and orexinergic (OxA) (**E**, **F**) immunoreactive cells in the brains of three different groups (n = 6 per group) analyzed in the present study, the group exposed to chronic prenatal alcohol (**CA**), the prenatal gavage control group (**CAc**) and the non-treated control group (**NTc**). The average somal area and volume of the ChAT+ neurons of the laterodorsal tegmental (**LDT**) and pedunculopontine (**PPT**) nuclei (**A**, **B**) in the **CA** group are statistically significantly smaller than the control groups (**CAc** and **NTc**). The average somal area and volume of the TH+ neurons of the locus coeruleus complex (**C**, **D**) are not statistically significantly different between the three groups. The average somal area and volume of the OxA+ neurons of the hypothalamus (**E**, **F**) in the **CA** group are statistically significantly larger than the control groups (**CAc** and **NTc**).

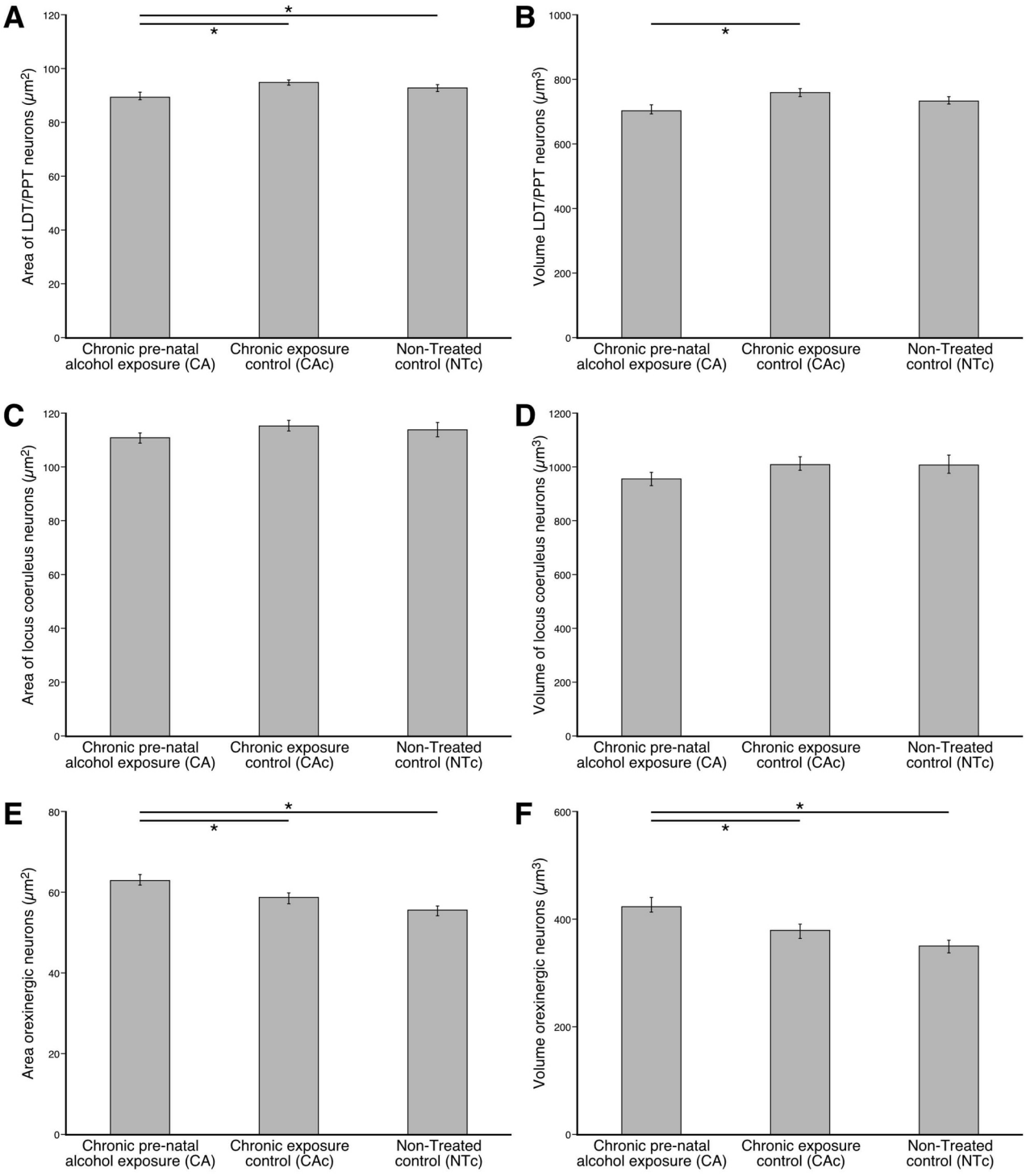
A
Area of LDT/PPT neurons (μm²)
120
100
80
60
40
20
0
*
*
Chronic pre-natal alcohol exposure (CA)
Chronic exposure control (CAc)
Non-Treated control (NTc)
B
Volume LDT/PPT neurons (μm³)
1000
800
600
400
200
0
*
Chronic pre-natal alcohol exposure (CA)
Chronic exposure control (CAc)
Non-Treated control (NTc)
C
Area of locus coeruleus neurons (μm²)
120
100
80
60
40
20
0
Chronic pre-natal alcohol exposure (CA)
Chronic exposure control (CAc)
Non-Treated control (NTc)
D
Volume of locus coeruleus neurons (μm³)
1200
1000
800
600
400
200
0
Chronic pre-natal alcohol exposure (CA)
Chronic exposure control (CAc)
Non-Treated control (NTc)
E
Area orexinergic neurons (μm²)
80
60
40
20
0
*
*
Chronic pre-natal alcohol exposure (CA)
Chronic exposure control (CAc)
Non-Treated control (NTc)
F
Volume orexinergic neurons (μm³)
600
400
200
0
*
*
Chronic pre-natal alcohol exposure (CA)
Chronic exposure control (CAc)
Non-Treated control (NTc)

Figure 5.4: Lower (**A**, **C**, **E**) and higher (**B**, **D**, **F**) magnification photomicrographs of the locus coeruleus (**A6**, **B**, **D**, **F**) and subcoeruleus (**A7**) nuclei of the mouse in the coronal plane immunostained for tyrosine hydroxylase (TH) in the three different groups analyzed in the present study, the group exposed to chronic prenatal alcohol (**CA**) (**A**, **B**), the prenatal gavage control group (**CAc**) (**C**, **D**) and the non-treated control group (**NTc**) (**E**, **F**). The nuclear organization, neuronal morphology, somal size and number of TH immunostained cells in the locus coeruleus complex is similar between groups. In all images dorsal is to the top and medial to the left. Scale bar in **E** = 250 µm and applies to **A**, **C** and **E**, scale bar in **F** = 100 µm and applies to **B**, **D** and **F**.

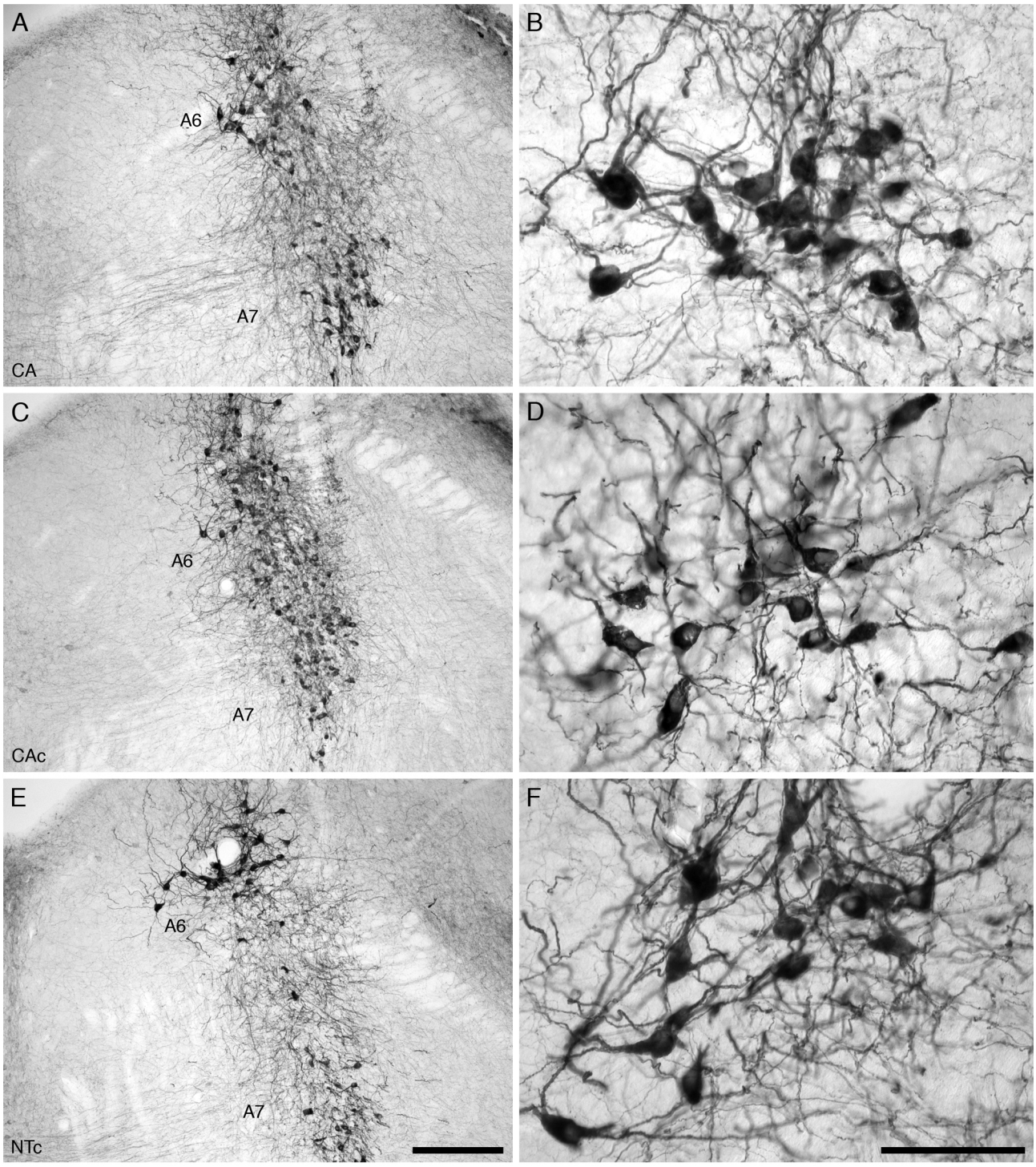
A
A6
A7
CA
B
C
A6
A7
CAc
D
E
A6
A7
NTc
F

Figure 5.5: Lower (**A**, **C**, **E**, several nuclei) and higher (**B**, **D**, **F**, dorsal raphe lateral nucleus, **DRl**) magnification photomicrographs of the dorsal raphe nuclear complex (**DR**) of the mouse in the coronal plane immunostained for serotonin (5-HT) in the three different groups analyzed in the present study, the group exposed to chronic prenatal alcohol (**CA**) (**A**, **B**), the prenatal gavage control group (**CAc**) (**C**, **D**) and the non-treated control group (**NTc**) (**E**, **F**). The nuclear organization and neuronal morphology of the 5-HT immunostained cells in the dorsal raphe complex is similar between groups. In images **A**, **C** and **E** dorsal is to the top with the midline in the middle of the image, while in images **B**, **D** and **F** dorsal is to the top and medial to the left. Scale bar in **E** = 250 µm and applies to **A**, **C** and **E**, scale bar in **F** = 100 µm and applies to **B**, **D** and **F**. **DRif** – dorsal raphe interfascicular nucleus, **DRv** – dorsal raphe ventral nucleus, **DRd** – dorsal raphe dorsal nucleus, **DRl** – dorsal raphe lateral nucleus, **DRp** – dorsal raphe peripheral nucleus.

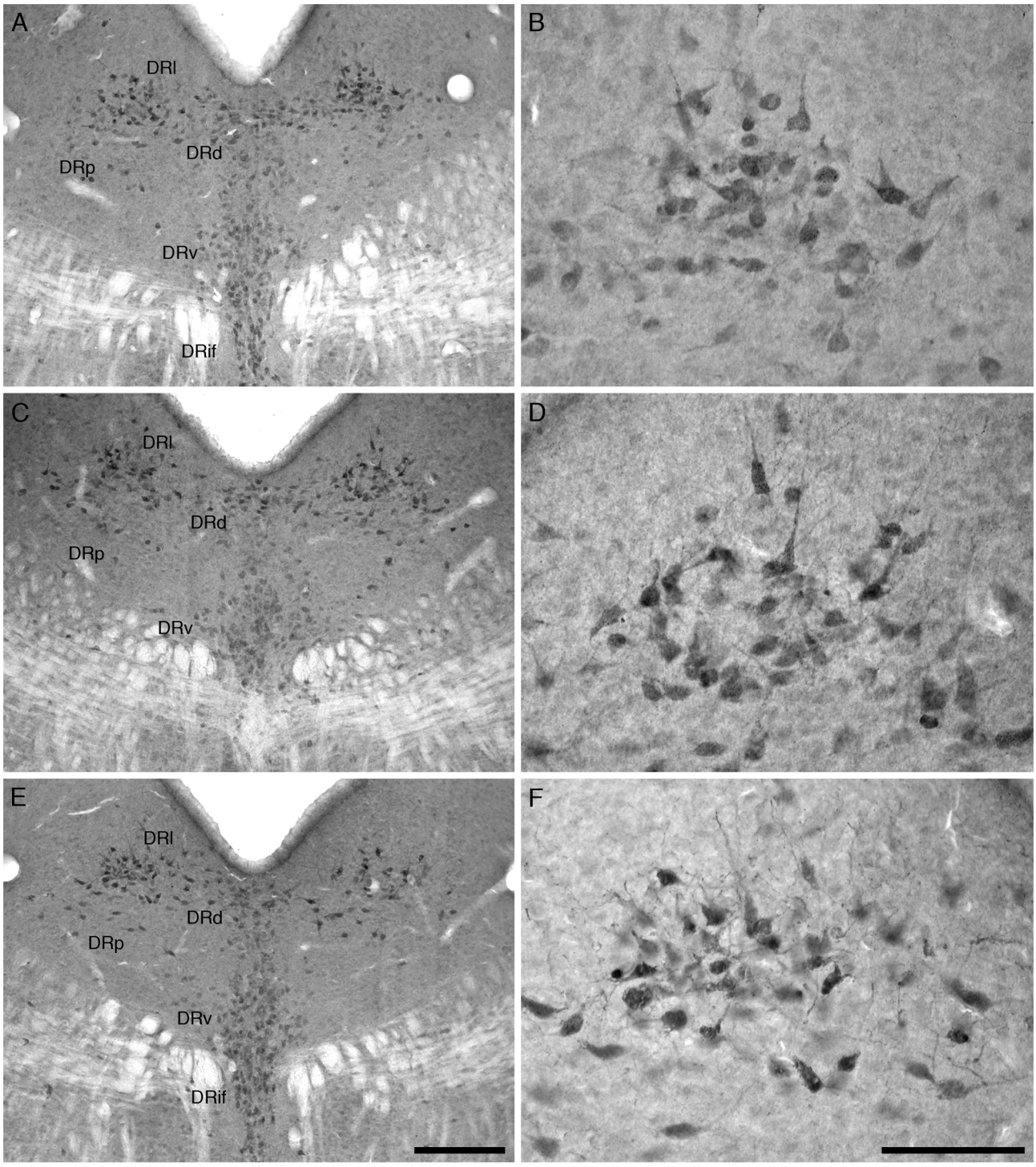
A
DRl
DRd
DRp
DRv
DRif
B
C
DRl
DRd
DRp
DRv
D
E
DRl
DRd
DRp
DRv
DRif
F

Figure 5.6: Lower (**A**, **C**, **E**) and higher (**B**, **D**, **F**) magnification photomicrographs of the hypothalamic orexinergic (OxA) neurons of the mouse in the coronal plane immunostained for cholineacetyltransferase (ChAT) in the three different groups analyzed in the present study, the group exposed to chronic prenatal alcohol (**CA**) (**A**, **B**), the prenatal gavage control group (**CAc**) (**C**, **D**) and the non-treated control group (**NTc**) (**E**, **F**). The nuclear organization and number of OxA immunostained cells was similar between groups, but the soma of the neurons in the **CA** group, exposed to chronic prenatal alcohol, were statistically significantly larger than the two control groups (**CAc** and **NTc**). In all images dorsal is to the top and medial to the left. Scale bar in **E** = 250 µm and applies to **A**, **C** and **E**, scale bar in **F** = 100 µm and applies to **B**, **D** and **F**. **Mc** – main orexinergic cluster, **OTc** – optic tract cluster, **Zic** – zona incerta cluster.

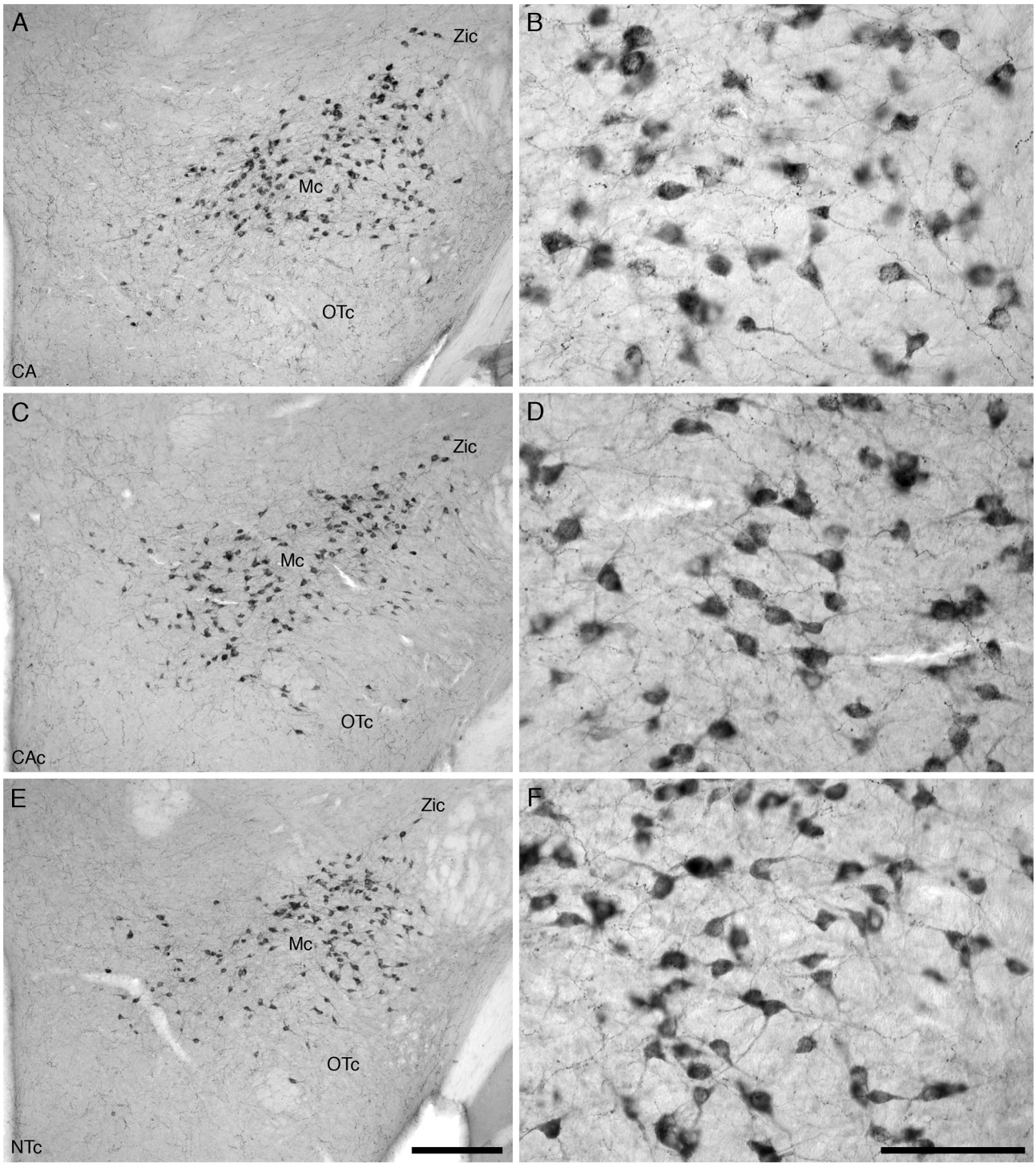
A
Zic
Mc
OTc
CA
B
C
Zic
Mc
OTc
CAc
D
E
Zic
Mc
OTc
NTc
F

5.4. Discussion:

In the present study we examined in detail the nuclear organization, neuronal morphology, total cell number and average cell size of four specific clusters of nuclei known to be involved in the control and regulation of the sleep-wake cycle. As outlined earlier, sleep in children suffering from fetal alcohol spectrum disorder (FASD) is perturbed in many ways, therefore a targeted analysis of some of the critical neuronal regulators of sleep was undertaken in mice exposed to a chronic prenatal alcohol regime to determine whether any clues to the basis for sleep disorders in FASD children could be found. For the most part, we did not record any specific differences between mice exposed to prenatal alcohol and those not. The organization of the nuclei that form the pontine cholinergic, pontine catecholaminergic, midbrain serotonergic and hypothalamic orexinergic was similar across all mice studied. Furthermore, the specific neuronal morphology within the various nuclei was also unaltered by prenatal exposure to alcohol. The somal volumes and areas of the pontine catecholaminergic neurons of the locus coeruleus complex were not affected by prenatal alcohol exposure; however, the somal volumes and areas of the pontine cholinergic and hypothalamic orexinergic did show significant variation in the group exposed to prenatal alcohol compared to both control groups. These two specific differences are discussed in terms of the effect they may have on the control and regulation of the sleep wake cycle and how this relates to the observed sleep disorders in children with FASD.

5.4.1. The soma of the pontine cholinergic neurons are smaller in mice exposed to prenatal alcohol:

The first specific difference observed in the mice that underwent a chronic prenatal alcohol regime compared to the control mice was the smaller size (around 95%) of the pontine cholinergic neuronal soma of the laterodorsal tegmental (LDT) and pedunculopontine tegmental (PPT) nuclei. The cholinergic neurons of the LDT and PPT are known to be involved in the generation of REM sleep, and the phasic events of REM sleep such as ponto-geniculo-occipital (PGO) spikes, through their projections to the thalamus and the basal forebrain (Webster and Jones, 1988; Semba et al., 1990). Additionally, these neurons are involved in the activation of thalamocortical systems by blocking synchronized oscillations such as seen in slow wave sleep (Pare et al., 1988). In the FASD mouse model generated in this study, these cholinergic neurons were reduced in size, which would hypothetically indicate that in the FASD model mice they would have a higher threshold potential, thus being less excitable, and being smaller, they would likely be able to support a smaller axon and axon terminal field (Shepherd, 1979), making their action upon the recipient neurons less intense. Indeed, in experimental models where these neurons have undergone chemical ablation it was found that the amount of time spent in wake was significantly increased (Webster and Jones, 1988). Thus, it appears that the difficulty experienced in going to sleep, short sleep durations, and increased sleep disruptions observed in FASD children (Meltzer and Mindell, 2004; Jan et al., 2010; Wengel et al., 2011) may in part be related to a reduction in size of the cholinergic neurons of the LDT and PPT.

5.4.2. The soma of the hypothalamic orexinergic neurons are larger in mice exposed to prenatal alcohol:

The second specific difference observed in the mice treated with a chronic prenatal alcohol regime when compared to the control groups was the significantly larger size of the soma of the hypothalamic orexinergic neurons. The hypothalamic orexinergic neurons are known to project throughout the entire central nervous system, but exhibit specifically intense projections to other regions of the brain involved in arousal (e.g. Peyron et al., 1998). Thus, orexin (or hypocretin) has been implicated in arousal as one of the main functions of this system (e.g. Saper et al., 2001; Siegel, 2004a,b). Many of the disorders associated with sleep in FASD children appear to be related to problems associated with arousal, and thus the arousal systems of the brain (Meltzer and Mindell, 2004; Haydon et al., 2009; Jan et al., 2010; Wengel et al., 2011). In this sense, the finding of larger orexinergic neurons in the currently used mouse model of FASD is of interest – perhaps the changes observed in this mouse model can help explain some of the sleep disturbances observed in FASD children.

The orexinergic neurons in the FASD mouse model were approximately 1.1 – 1.2 times larger than those measured in the control mice. One of the key cellular level phenomena associated with an increase in neuron size, and thus an increase in neuronal surface area, is a lower threshold potential (Shepherd, 1979). Thus, the larger orexinergic neurons found in the FASD mouse model would, theoretically, be more readily excitable when compared to the control groups. In this sense, the brain globally, and in particular the arousal systems receiving intense projections from the orexinergic neurons of the hypothalamus, would potentially be in receipt of a greater

number of excitatory action potentials from the hypothalamus in the FASD mouse model than the controls. This in turn would augment the arousal function of the orexinergic neurons. The second key feature associated with increased neuron size would be the theoretical ability of the larger cell to support a larger and more extensively branched axon and axonal bouton terminal field (Shepherd, 1979), as seen in previous studies of orexinergic projections (Dell et al., 2012, 2015). In this sense, the density of orexinergic boutons in the projections zones of the hypothalamic orexinergic axons may be increased, both throughout the brain and specifically in the regions of the arousal system intensely projected to by the orexinergic neurons. Thus, both possibilities indicate that the effect of orexin may be more influential in the FASD mouse model than the controls and that this may in part help to explain the disorders of arousal observed in FASD children.

5.4.3. Further studies:

In the current study we have observed two specific differences in two distinct neuronal systems involved in the regulation and control of the sleep-wake cycle. These two differences, when viewed in light of previous experimental studies of the sleep-wake cycle, appear to be directly related to the disorders of sleep experienced in children suffering from FASD. It would appear that prenatal alcohol exposure causes deficits within the arousal systems of both the hypothalamus (orexinergic) and pons (cholinergic), and that these deficits can cause the disorders observed in FASD children. It would be useful in future to undertake polysomnographic recording of sleep in the FASD mouse model and FASD children to determine to what degree the sleep disorders in the FASD children match any potential sleep disorders in the FASD

mouse model. Given the findings of the current study and the information to date for sleep in FASD children, REM sleep would appear to be an interesting target for study. Given the success in treatment of sleep disorders, such as narcolepsy (Didato and Nobili, 2009), further research into the precise mechanism causing sleep disorders in FASD models and children may open avenues for the use of neurotherapeutics to ameliorate and potentially alleviate sleep disorders associated with FASD. In future, such symptoms as night terrors (Durmer and Dinges, 2005), sleep walking (Randazzo et al., 1998), and daytime tiredness (Lancioni et al., 1999) may be treatable in FASD children and thus increase their quality of life significantly by keeping these symptoms under control.

CHAPTER SIX: Concluding discussion

In the current study four specific aspects of the brain morphology of an FAS/FASD mouse model and appropriate controls were explored both qualitatively and quantitatively. Central findings include: (1) the rate of proliferation of newly born cells in the dentate gyrus of the hippocampus do not appear affected, but the numbers of immature neurons in the dentate gyrus is significantly lower in the mice exposed to ethanol compared to the control groups; (2) The organization of the PMBSF barrel field is unaffected, but there was a non-significant trend toward the reduction in the mean sizes of barrels in the group exposed to prenatal alcohol; (3) there were no differences in the nuclear organization, neuronal morphology and numbers of cholinergic, catecholaminergic, orexinergic and serotonergic neurons involved in the sleep-wake cycle, but in the alcohol exposed group the orexinergic neurons had larger somas than the control groups and the cholinergic neurons had smaller somas than the control group, while no difference in soma size was observed in the catecholaminergic neurons; (4) no differences in the organization or neurochemistry of the vermal cerebellar cortex was detected either qualitatively or quantitatively.

Animal models of FAS or FASD are used to explore various aspects of this condition, with the hope that the model reflects what is happening in humans; however, these animal models do need to be verified as accurate reflectors of the condition in humans. This does not only involve the examination of specific aspects of the model, such as epigenetics (Haycock and Ramsay, 2009; Knezovich and Ramsay, 2012), but neuroanatomy, neurophysiology and behaviour. A holistic approach, from molecules to behaviour, for the validation of animal model of a human condition needs to be undertaken to ensure that the translation of findings in

the animal model to humans is appropriate (Perrin, 2014). The series of studies that form this thesis specifically targeted aspects of the neuroanatomy of a previously used FAS mouse model (Haycock and Ramsay, 2009; Knezovich and Ramsay, 2012) to determine whether alterations in the neuroanatomy in this model would predict behavioural outcomes consistent with those observed in humans suffering from FAS or FASD.

The overall results of this neuroanatomical investigation of an FAS/FASD mouse model are mixed in terms of the relationship of observed changes and lack of changes in the neuroanatomy to behaviours associated with humans suffering from FAS/FASD, and indeed to other animal models of FAS/FASD. This mixed bag of findings highlights the difficulties in the use of animal models in translational research – nothing is as clear as what it might seem from the scientific literature using animal models to mimic human conditions and infer potential therapeutic resolutions to these conditions. For the currently neuroanatomically assessed mouse model, the results of the studies targeting adult neurogenesis in the hippocampus, the sleep systems, and cortical sensory processing, do appear to be useful in understanding behavioural deficits associated with memory, sleep and sensory processing in humans suffering with FAS; however, the lack of changes in the cerebellum indicates that this FAS mouse model does not appear to account for the motor disorders associated with human FAS/FASD. Thus, for the most part, it would appear the FAS mouse model used in the current series of studies, and used previously (Haycock and Ramsay, 2009; Knezovich and Ramsay, 2012), does have neuroanatomical changes that appear to relate to specific behavioural disorders associated with human FAS, but there are both specific and more general shortfalls associated with this and other animal models of FAS/FASD.

The most striking shortfall that has been repeatedly mentioned in rodent model studies of FAS/FASD is the fact that the trimester periods in rodents do not directly match those in humans, making direct translations from rodent models to human subjects difficult and controversial. In rodents, the equivalent developmental stages of the third trimester of human pregnancy fall within the first week of rodent postnatal life. This indicates that the physiological states of the developing brain during this stage of development will be different between rodents and humans, complicating translations from the animal model to humans. To expand on this point, specific therapeutics developed in rodent models though to mimic human disorders show a failure rate of more than 80% when tested on humans in clinical trials (Perrin, 2014). This indicates that modelling diseases or specific conditions in animals is more often than not untranslatable to humans (Perrin, 2014). Interestingly, factors associated with the specific animal models are often blamed for the misalignment of findings with observations in humans (Perrin, 2014). Obviously, the best model animal for any clinical research relating to disorders in humans is to utilize human models; however, the use of humans in scientific experiments has huge limitations in the sense of ethical issues, it is extremely expensive, and there are logistical problems (Perrin, 2014). Thus, it is essential to attempt to understand the anatomy, physiology and behaviour of an animal model before utilizing these animal models in any experimental design – the basic biology of the animal model must coincide to a great enough degree to that of humans in order to be a useful animal model. In other words, basic biology is the building block for clinically related translational research, without understanding the true biology of the animal model and how it relates to humans, the success rates of translational research are likely to become even poorer than they are at present (Perrin, 2014). Despite this, the positive findings of changes in the FAS mouse model

used in the current studies, do indicate that with further development, this model may become a very efficient and useful model in the study of human FAS/FASD.

Further validation of this mouse model is clearly needed in order to progress our understanding of FAS/FASD in humans. An extensive series of behavioural studies examining sensory, motor, sleep/wake and cognitive aspects of the mouse model, and how any changes in the mouse model relate to human FAS behavioural disorders are needed. In addition, more detailed studies of the human behavioural disorders associated with FAS are sorely needed, such as polysomnographic recordings of sleep to determine what is truly disrupted in the sleep-wake cycle of human FAS sufferers. Studies of the neurophysiology involved with sensory, motor, sleep/wake and cognitive aspects of the FAS/FASD mouse model will bridge the gap between anatomical studies and behaviour, especially if these are run concurrently with imaging studies of FAS humans to determine how closely aligned the neurophysiology underpinning behavioural differences are in both humans and potential model animals. More anatomical studies of regions of the brain not targeted in the current study are also required. As FAS is not an inherited disorder, further studies of the epigenetics of this mouse model would also be instructive. Combined, these studies would bridge the gap between molecules and behaviour in this mouse model of FAS and allow for the proper determination of the usefulness of this model for understanding human FAS and the potential development of therapeutics.

Thus, while the FAS mouse model used in the current study clearly has potential for further use in understanding human FAS, it would be wise to undertake a concerted and multipronged approach to the validation of this model – something that appears to be missing for many models of human mental illness. There is a tendency for researchers, for reasons of economics and ease of use, to use rodents as model

animals for humans, but this almost reflexive recourse to rodent models clearly needs to be validated correctly before real progress will be made. It is hoped that the studies undertaken in this thesis provide at least some forward momentum in our developing understanding of the use of model animals for human disorders.

REFERENCES:

Abel, E.L. (1984). Prenatal effects of alcohol. *Drug and Alcohol Dependence, 14*, 1–10.

Abel, E.L. (1995). An update on incidence of FAS: FAS is not an equal opportunity birth defect. *Neurotoxicology and Teratology, 17*, 437–443.

Abel, E.L. (1998). Fetal alcohol syndrome: The 'American Paradox'. *Alcohol, 33,* 195–201.

Abel, E.L., & Sokol, R.J. (1987). Incidence of fetal alcohol syndrome and economic impact of FAS-related anomalies. *Drug Alcohol Dependence 19*, 51–70.

Abel, E.L., & Sokol, R.J. (1991). A revised estimate of the economic impact of fetal alcohol syndrome. *Recent Developments in Alcoholism, 9,* 117–125.

Åberg, E., Hofstetter, C.P., Olson, L., & Brené, S. (2005). Moderate ethanol consumption increases hippocampal cell proliferation and neurogenesis in the adult mouse. *The International Journal of Neuropsychopharmacology, 8,* 557–567.

Aimone, J.B., Deng, W., & Gage, F.H. (2011). Resolving new memories: a critical look at the dentate gyrus, adult neurogenesis, and pattern separation. *Neuron, 70,* 589–596.

Al-Rabiai, S., & Miller, M. (1989). Effect of prenatal exposure to ethanol on the ultrastructure of layer V of mature rat somatosensory cortex. *Journal of Neurocytology, 18,* 711–729.

Altman, J., & Sudarshan, K. (1975). Postnatal development of locomotion in the laboratory rat. *Animal Behavior, 23,* 896–920.

Anderson, W.J., & Sides, G.R. (1979). Alcohol induced defects in cerebellar development in the rat. *Currents in Alcoholism 5,* 135.

Archibald, S.L., Fennema-Notestine, C., Gamst, A., Riley, E.P., Mattson, S.N., & Jernigan, T.L. (2001). Brain dysmorphology in individuals with severe prenatal alcohol exposure. *Developmental Medicine & Child Neurology, 43,* 148–154.

Astley, S.J., Magnuson, S.I., Omnell, L.M., & Clarren, S.K. (1999). Fetal alcohol syndrome: changes in craniofacial form with age, cognition, and timing of ethanol exposure in the macaque. *Teratology, 59,* 163–172.

Autti-Rämö, I. (2002). Foetal alcohol syndrome–a multifaceted condition. *Developmental Medicine & Child Neurology, 44,* 141–144.

Autti-Rämö, I., Autti, T., Korkman, M., Kettunen, S., Salonen, O., & Valanne, L. (2002). MRI findings in children with school problems who had been exposed prenatally to alcohol. *Developmental Medicine & Child Neurology, 44,* 98–106.

Balaszczuk, V., Bender, C., Pereno, G., & Beltramino, C. (2011). Alcohol-induced neuronal death in central extended amygdala and pyriform cortex during the postnatal period of the rat. *International Journal of Developmental Neuroscience, 29,* 733–742.

Balthazart, J., & Ball, G.F. (2014). Endogenous versus exogenous markers of adult neurogenesis in canaries and other birds: advantages and disadvantages. *Journal of Comparative Neurology, 522,* 4100–4120.

Barlow, C., & Targum, S.D. (2007). Hippocampal neurogenesis: can it be a marker for new antidepressants? *Psychiatry, 4,* 18–20.

Bhagwandin, A., Gravett, N., Bennett, N.C., & Manger, P.R. (2013). Distribution of parvalbumin, calbindin and calretinin containing neurons and terminal networks in relation to sleep associated nuclei in the brain of the giant Zambian mole-rat (*Fukomys mechowii*). *Journal of Chemical Neuroanatomy, 52,* 69–79.

Bielawski, D.M., & Abel, E.L. (1997). Acute treatment of paternal alcohol exposure produces malformations in offspring. *Alcohol, 14,* 397–401.

Bjarkam, C.R., Sørensen, J.C., & Geneser, F.A. (1997). Distribution and morphology of serotonin-immunoreactive neurons in the brainstem of the New Zealand white rabbit. *Journal of Comparative Neurology 380,* 507–519.

Blader, P., & Strähle, U. (1998). Ethanol impairs migration of the prechordal plate in the zebrafish embryo. *Developmental Biology, 201,* 185–201.

Bonthius, D.J., Bonthius, N.E., Napper, R., Astley, S.J., Clarren, S.K., & West, J.R. (1996). Purkinje cell deficits in nonhuman primates following weekly exposure to ethanol during gestation. *Teratology, 53,* 230–236.

Braun, K. (1990). Calcium-binding proteins in avian and mammalian central nervous system: localization, development and possible functions. *Progress in Histochemistry and Cytochemistry, 21,* III1–V62.

Burd, L., Cotsonas-Hassler, T.M., Martsolf, J.T., & Kerbeshian, J. (2003). Recognition and management of fetal alcohol syndrome. *Neurotoxicology and teratology, 25*, 681–688.

Burden, M.J., Jacobson, S.W., Sokol, R.J., & Jacobson, J.L. (2005). Effects of prenatal alcohol exposure on attention and working memory at 7.5 year of age. *Alcoholism: Clinical and Experimental Research, 29,* 443–452.

Cameron, H.A., & Glover, L.R. (2015). Adult neurogenesis: beyond learning and memory. *Annual Review of Psychology 66,* 53–81.

Carr, J.L., Agnihotri, S., & Keightley, M. (2010). Sensory processign and adaptive behavior deficits of children across the fetal alcohol spectrum disorder continuum. *Alcoholism: Clinical and Experimental Research, 34,* 1022–1032.

Cartwright, M.M., & Smith, S.M. (1995). Increased cell death and reduced neural crest cell numbers in ethanol-exposed embryos: partial basis for the fetal alcohol syndrome phenotype. *Alcoholism: Clinical and Experimental Research, 19*, 378–386.

Celio, M.R. (1990). Calbindin D-28k and parvalbmin in the rat nervous system. *Neuroscience 35,* 375–475.

Chappell, T.D., Margret, C.P., Li, C.X., & Waters, R.S. (2007). Long-term effects of prenatal alcohol exposure on the size of the whisker representation in juvenile and adult rat barrel cortex. *Alcohol, 41,* 239–251.

Chen, M.L., Olson, H.C., Picciano, J.F., Starr, J.R., & Owens, J. (2012). Sleep problems in children with fetal alcohol spectrum disorders. *Journal of Clinical Sleep Medicine, 8,* 421–429.

Choi, I.Y., Allan, A.M., & Cunningham, L.A. (2005). Moderate fetal alcohol exposure impairs the neurogenic response to an enriched environment in adult mice. *Alcoholism: Clinical and Experimental Research, 29,* 2053–2062.

Clancy, B., Darlington, R.B., & Finlay, B.L. (2001). Translating developmental time across mammalian species. *Neuroscience, 105,* 7–17.

Clarren, S.K., & Smith, D.W. (1978). The fetal alcohol syndrome. *Lamp,* 35, 4–7.

Clarren, S.K., Astley, S.J., Gunderson, V.M., & Spellman, D. (1992). Cognitive and behavioral deficits in nonhuman primates associated with very early embryonic binge exposures to ethanol. *The Journal of Pediatrics*, *121*, 789–796.

Clelland, C.D., Choi, M., Romberg, C., Clemenson, G.D., Fragniere, A., Tyers, P., Jessberger, S., Saksida, L.M., Barker, R.A., Gage, F.H., & Bussey, T.J. (2009). A functional role for adult hippocampal neurogenesis in spatial pattern separation. *Science, 325,* 210–213.

Climent, E., Pascual, M., Renau-Piqueras, J., & Guerri, C. (2002). Ethanol exposure enhances cell death in the developing cerebral cortex: Role of brain-derived neurotrophic factor and its signaling pathways. *Journal of Neuroscience Research, 68,* 213–225.

Coggeshall, R.E., & Lekan, H.A. (1996). Methods for determining numbers of cells and synapses: a case for more uniform standards of review. *Journal of Comparative Neurology, 364,* 6–15.

Coles, C.D., Platzman, K.A., Lynch, M.E., & Freides, D. (2002). Auditory and visual sustained attention in adolescents prenatally exposed to alcohol. *Alcoholism: Clinical and Experimental Research, 26,* 263–271.

Collins, T., Chat, M., Lucas, M.G., Moreno, H., Racay, P., Schwaller, B., Marty, A., & Llano, I. (2005). Developmental changes in parvalbumin regulate presynaptic Ca2+ signaling. *The Journal of Neuroscience, 25,* 96–107.

Connor, P.D., Sampson, P.D., Bookstein, F.L., Barr, H.M., & Streissguth, A.P. (2000). Direct and indirect effects of prenatal alcohol damage on executive function. *Developmental Neuropsychology, 18,* 331–354.

Cortese, S., Faraone, S. V., Konofal, E., & Lecendreux, M. (2009). Sleep in children with attention-deficit/hyperactivity disorder: meta-analysis of subjective and objective studies. *Journal of the American Academy of Child and Adolescent Psychiatry, 48,* 894–908.

Crankshaw, T.L., Voce, A., King, R.L., Giddy, J., Sheon, N.M., & Butler, L.M. (2014) Double disclosure bind: Complexities of communicating an HIV diagnosis in the context of unintended pregnancy in Durban, South Africa. *AIDS and Behavior 18,* 53–59.

Crede, S., Sinanovic, E., Adnams, C., & London, L. (2011). The utilization of health care services by children with Foetal Alcohol Syndrome in the Western Cape, South Africa. *Drug and Alcohol Dependence, 115*, 175–182.

Cudd, T.A. (2005). Animal model systems for the study of alcohol teratology. *Experimental Biology and Medicine, 230*, 389–393.

D'Angelo, E., Mazzarello, P., Prestori, F., Mapelli, J., Solinas, S., Lombardo, P., Cesana, E., Gandolfi, D., & Congi, L. (2011). The cerebellar network: from structure to function and dynamics. *Brain Research Reviews, 66,* 5–15.

Dahlström, A., & Fuxe, K. (1964). A method for the demonstration of monoamine-containing nerve fibres in the central nervous system. *Acta Physiologica*, *60*, 293–294.

Datta, S., & MacLean, R.R. (2007). Neurobiological mechanisms for the regulation of mammalian sleep-wake behavior: reinterpretation of historical evidence and inclusion of contemporary cellular and molecular evidence. *Neuroscience and Biobehavioral Reviews, 31*, 775–824.

Dell, L.A., Patzke, N., Bhagwandin, A., Bux, F., Fuxe, K., Barber, G., Siegel, J.M., & Manger, P.R. (2012). Organization and number of orexinergic neurons in the hypothalamus of two species of Cetartiodactyla: a comparison of giraffe (Giraffa camelopardalis) and harbour porpoise (Phocoena phocoena). *Journal of Chemical Neuroanatomy, 44*, 98–109.

Dell, L.A., Patzke, N., Spocter, M.A., Siegel, J.M., & Manger, P.R. (2016). Organization of the sleep-related neural systems in the brain of the harbour porpoise (*Phocoena phocoena*). *Journal of Comparative Neurology, 524,* 1999–2007.

Dell, L.A., Spocter, M.A., Patzke, N., Karlson, K.Æ., Alagaili, A.N., Bennett, N.C., Muhammed, O.B., Bertelsen, M.F., Siegel, J.M., & Manger, P.R. (2015). Orexinergic bouton density is lower in the cerebral cortex of cetaceans compared to artiodactyls. *Journal of Chemical Neuroanatomy, 68,* 61–76.

Didato, G., & Nobili, L. (2009). Treatment of narcolepsy. *Expert Review of Neurotherapeutics, 9,* 897–910.

Dikranian, K., Qin, Y.Q., Labruyere, J., Nemmers, B., & Olney, J.W. (2005). Ethanol-induced neuroapoptosis in the developing rodent cerebellum and related brain stem structures. *Developmental Brain Research, 155,* 1–13.

Durmer, J.S., & Dinges, D.F. (2005). Neurocognitive consequences of sleep deprivation. *Seminars in Neurology, 25,* 117–129.

Erasso, D.M., Chaparro, R.E., del Rio, C.E.Q., Karlnoski, R., Camporesi, E.M., & Saporta, S. (2012). Quantitative assessment of new cell proliferation in the dentate gyrus and learning after isoflurane or propofol anesthesia in young and aged rats. *Brain Research, 1441,* 38–46.

Eriksson, P.S., Perfilieva, E., Björk-Eriksson, T., Alborn, A.M., Nordborg, C., Peterson, D.A., & Gage, F.H. (1998). Neurogenesis in the adult human hippocampus. *Nature Medicine, 4,* 1313–1317.

Ethen, M.K., Ramadhani, T.A., Scheuerle, A.E., Canfield, M.A., Wyszynski, D.F., Druschel, C.M., & Romitti, P.A. (2009). Alcohol consumption by women before and during pregnancy. *Maternal and Child Health Journal, 13,* 274–285.

Famy, C., Streissguth, A.P., & Unis, A.S. (1998). Mental illness in adults with fetal alcohol syndrome or fetal alcohol effects. *American Journal of Psychiatry, 155,* 552–554.

Franklin, L., Deitz, J., Jitikowic, T., & Astley, S. (2008). Children with fetal alcohol spectrum disorders: problem behaviors and sensory processing. *American Journal of Occupational Therapy, 62,* 265–273.

Fuglestad, A.J., Whitely, M.L., Carlson, S.M., Boys C.J., Eckerle, J.K., Fink, B.A., & Wozniak, J.R. (2015). Executive functioning deficits in preschool children with fetal alcohol spectrum disorders. *Child Neuropsychology, 21,* 716–731.

Fuss, J., Ben Abdullah, N.M.B., Vogt, M.A., Touma, C., Pacifici, P.G., Palme, R., Witzemann, V., Hellweg, R., & Gass, P. (2010). Voluntary exercise induces anxiety-like behavior in adult C57BL/6J mice correlating with hippocampal neurogenesis. *Hippocampus, 20,* 364–376.

Galofré, E., Ferrer, I., Fábregues, I., & López-Tejero, D. (1987). Effects of prenatal ethanol exposure on dendritic spines of layer V pyramidal neurons in the somatosensory cortex of the rat. *Journal of the Neurological Sciences, 81,* 185–195.

Gerashchenko, D., & Shiromani, P.J. (2004). Different neuronal phenotypes in the lateral hypothalamus and their role in sleep and wakefulness. *Molecular Neurobiology, 29,* 41–59.

Gil, O.D., Needleman, L., & Huntley, G.W. (2002). Developmental patterns of cadherin expression and localization in relation to compartmentalized thalamocortical terminations in rat barrel cortex. *Journal of Comparative Neurology, 453,* 372–388.

Gil-Mohapel, J., Boehme, F., Kainer, L., & Christie, B.R. (2010). Hippocampal cell loss and neurogenesis after fetal alcohol exposure: insights from different rodent models. *Brain Research Reviews, 64,* 283–303.

Gil-Mohapel, J., Boehme, F., Patten, A., Cox, A., Kainer, L., Giles, E., Brocardo, P.S., & Christie, B.R. (2011). Altered adult hippocampal neuronal maturation in a rat model of fetal alcohol syndrome. *Brain Research, 1384,* 29–41.

Gil-Mohapel, J., Titterness, A., Patten, A., Taylor, S., Ratzlaff, A., Ratzlaff, T., Helfer, J., & Christie, B. (2014). Prenatal ethanol exposure differentially affects hippocampal neurogenesis in the adolescent and aged brain. *Neuroscience, 273,* 174–188.

Gil-Perotin, S.G., Alvarez-Buylla, A., & García-Verdugo, J.M. (2009). Identification and Characterization of Neural Progenitor Cells in the Adult Mammalian Brain: 203 (Advances in Anatomty, Embryology and Cell Biology) (New York, NY: Springer).

Gleason, C.A., & Hotchkiss, K.J. (1992). Cerebral responses to acute maternal alcohol intoxication in immature fetal sheep. *Pediatric Research, 31,* 645–648.

Godin, E.A., Dehart, D.B., Parnell, S.E., O'Leary-Moore, S.K., & Sulik, K.K. (2011). Ventromedian forebrain dysgenesis follows early prenatal ethanol exposure in mice. *Neurotoxicology and Teratology 33,* 231–239.

Goodlett, C.R., & Horn, K.H. (2001). Mechanisms of alcohol-induced damage to the developing nervous system. *Alcohol research and Health, 25,* 175–184.

Gould, E., Tanapat, P., McEwen, B.S., Flügge, G., & Fuchs, E. (1998). Proliferation of granule cell precursors in the dentate gyrus of adult monkeys is diminished by stress. *Proceedings of the National Academy of Sciences USA, 95,* 3168–3171.

Granato, A., Santarelli, M., Sbriccoli, A., & Minciacchi, D. (1995). Multifaceted alterations of the thalamo-cortico-thalamic loop in adult rats prenatally exposed to ethanol. *Anatomy and Embryology, 191,* 11–23.

Green, C.A., Perrin, N.A., & Polen, M.R. (2004). Gender differences in the relationships between multiple measures of alcohol consumption and physical and mental health. *Alcoholism: Clinical and Experimental Research, 28,* 754–764.

Gundersen, H., Bagger, P., Bendtsen, T., Evans, S., Korbo, L., Marcussen, N., Møller, A., Nielsen, K., Nyengaard, J., & Pakkenberg, B. (1988). The new stereological tools: Disector, fractionator, nucleator and point sampled intercepts and their use in pathological research and diagnosis. *Apmis, 96,* 857–881.

Hamre, K.M., & West, J.R. (1993). The effects of the timing of ethanol exposure during the brain growth spurt on the number of cerebellar Purkinje and granule cell nuclear profiles. *Alcoholism: Clinical and Experimental Research, 17,* 610–622.

Haycock, P.C., & Ramsay, M. (2009). Exposure of mouse embryos to ethanol during preimplantation development: effect on DNA methylation in the h19 imprinting control region. *Biology of Reproduction, 81,* 618–627.

Haydon, P.G., Blendy, J., Moss, S.J., & Jackson, F.R. (2009). Astrocytic control of synaptic transmission and plasticity: a target for drugs of abuse? *Neuropharmacology*, *56,* 83–90.

Heaton, M.B., Paiva, M., Madorsky, I., & Shaw, G. (2003). Ethanol effects on neonatal rat cortex: comparative analyses of neurotrophic factors, apoptosis-related proteins, and oxidative processes during vulnerable and resistant periods. *Developmental Brain Research, 145,* 249–262.

Helfer, J.L., Goodlett, C.R., Greenough, W.T., & Klintsova, A.Y. (2009). The effects of exercise on adolescent hippocampal neurogenesis in a rat model of binge alcohol exposure during the brain growth spurt. *Brain Research, 1294,* 1–11.

Hellemans, K.G., Sliwowska, J.H., Verma, P., & Weinberg, J. (2010). Prenatal alcohol exposure: fetal programming and later life vulnerability to stress, depression and anxiety disorders. *Neuroscience and Biobehavioral Reviews, 34,* 791–807.

Ieraci, A., & Herrera, D.G. (2007). Single alcohol exposure in early life damages hippocampal stem/progenitor cells and reduces adult neurogenesis. *Neurobiology of Disease*, *26,* 597–605.

Ikonomidou, C., Bittigau, P., Ishimaru, M.J., Wozniak, D.F., Koch, C., Genz, K., Price, M.T., Stefovska, V., Horster, F., Tenkova, T., Dikranian, K., & Olney, J.W.

(2000). Ethanol-induced apoptotic neurodegeneration and fetal alcohol syndrome. *Science, 287,* 1056–1060.

Incerti, M., Vink, J., Roberson, R., Wood, L., Abebe, D., & Spong, C.Y. (2010). Reversal of alcohol-induced learning deficits in the young adult in a model of fetal alcohol syndrome. *Obstetrics and Gynecology, 115,* 350–356.

Ipsiroglu, O.S., McKellin, W.H., Carey, N., & Loock, C. (2013). …"They silently live in terror..." why sleep problems and night-time related quality-of-life are missed in children with a fetal alcohol spectrum disorder. *Social Science and Medicine, 79,* 76–83.

Jan, J.E., Asante, K.O., Conry, J.L., Fast, D.K., Bax, M.C., Ipsiroglu, O.S., Bredberg, E., Loock, C.A., & Wasdell, M.B. (2010a). Sleep Health Issues for Children with FASD: Clinical Considerations. *International journal of pediatrics, 2010.*

Jan, J.E., Reiter, R.J., Bax, M.C., Ribary, U., Freeman, R.D., & Wasdell, M.B. (2010b). Long-term sleep disturbances in children: a cause of neuronal loss. *European Journal of Paediatric Neurology, 14:* 380–390.

Jirikowic, T., Olson, H.C., & Kartin, D. (2009). Sensory processing, school performance, and adaptive behavior of young school-age children with fetal alcohol spectrum disorders. *Physical & Occupational Therapy in Pediatrics, 28,* 117–136.

Joshi, S., Guleria, R., Pan, J., Bayless, K., Davis, G., Dipette, D., & Singh, U. (2006). Ethanol impairs Rho GTPase signaling and differentiation of cerebellar granule

neurons in a rodent model of fetal alcohol syndrome. *Cellular and Molecular Life Sciences, 63,* 2859–2870.

Kaemingk, K.L., Mulvaney, S., & Halverson, P.T. (2003). Learning following prenatal alcohol exposure: performance on verbal and visual multitrial tasks. *Archives of Clinical Neuropsychology, 18,* 33–47.

Kane, C.J., Phelan, K.D., Han, L., Smith, R.R., Xie, J., Douglas, J.C., & Drew, P.D. (2011). Protection of neurons and microglia against ethanol in a mouse model of fetal alcohol spectrum disorders by peroxisome proliferator-activated receptor-γ agonists. *Brain, Behavior, and Immunity, 25,* S137–S145.

Kim, U., & Ebner, F.F. (1999). Barrels and septa: separate circuits in rat barrel field cortex. *The Journal of Comparative Neurology, 408,* 489–505.

Kiyashchenko, L.I., Mileykovskiy, B.Y., Maidment, N., Lam, H.A., Wu, M.F, John, J., Peever, J., & Siegel, J.M. (2002). Release of hypocretin (orexin) during waking and sleep states. *The Journal of Neuroscience, 22,* 5282–5286.

Kliegel, M.A., Jager, T., Altgassen, M., & Shum, D. (2008). Clinical neuropsychology of prospective memory. In Prospective Memory: Cognitive, Neuroscience, Developmental, and Applied Perspectives, M. Kliegel, M.A. McDaniel, and G.O. Einstein, eds. (New York: Lawrence Erlbaum Associates), pp. 283–303.

Klintsova, A.Y., Goodlett, C.R., & Greenough, W.T. (1999). Therapeutic motor training ameliorates cerebellar effects of postnatal binge alcohol. *Neurotoxicology and Teratology, 22,* 125–132.

Klintsova, A.Y., Helfer, J.L., Calizo, L.H., Dong, W.K., Goodlett, C.R., Greenough, W.T. (2007). Persistent impairment of hippocampal neurogenesis in young adult rats following early postnatal alcohol exposure. *Alcoholism: Clinical and Experimental Research, 31,* 2073–2082.

Knezovich, J.G., & Ramsay, M. (2012). The effect of preconception paternal alcohol expisure on epigenetic remodeling of the *H19* and *Rasgrf1* imprinting control regions in mouse offspring. *Frontiers in Genetics, 3,* 10.

Lai, Y., & Siegel, J. (1990). Muscle tone suppression and stepping produced by stimulation of midbrain and rostral pontine reticular formation. *The Journal of Neuroscience, 10,* 2727–2734.

Lancioni, G.E., O'Reilly, M.F., & Basili, G. (1999). Review of strategies for treating sleep problems in persons with severe or profound mental retardation or multiple handicaps. *American Journal on Mental Retardation, 104*, 170–186.

Landgraf, M.N., Nothacker, M., Kopp, I.B., & Heinen, F. (2013). The diagnosis of fetal alcohol syndrome. *Dtsch Arztebl Int, 110,* 703–710.

Landis, J.R., & Koch, G.G. (1977). The measurement of observer agreement for categorical data. B*iometrics*, 159–174.

Lazarov, O., & Hollands, C. (2016). Hippocampal neurogenesis: learning to remember. *Progress in Neurobiology, 138*, 1–18.

Lee, J., Duan, W., Long, J.M., Ingram, D.K., & Mattson, M.P. (2000). Dietary restriction increases the number of newly generated neural cells, and induces BDNF expression, in the dentate gyrus of rats. *Journal of Molecular Neuroscience, 15*, 99–108.

Lemaire, V., Lamarque, S., le Moal, M., Piazza, P.V., & Abrous, D.N. (2006). Postnatal stimulation of the pups counteracts prenatal stress-induced deficits in hippocampal neurogenesis. *Biological Psychiatry, 59*, 786–792.

Lewis, C.E., Thomas, K.G., Molteno, C.D., Kliegel, M., Meintjes, E.M., Jacobson, J.L., & Jacobson, S.W. (2016). Prospective memory impairment in children with prenatal alcohol exposure. *Alcoholism: Clinical and Experimental Research, 40*, 969–978.

Lewis, E.G., Dustman, R.E., & Beck, E.C. (1969). The effect of alcohol on sensory phenomenon and cognitive and motor tasks. *Quarterly Journal of Studies on Alcohol*.

Li, Z., Miller, M.W., & Luo, J. (2002). Effects of prenatal exposure to ethanol on the cyclin-dependent kinase system in the developing rat cerebellum. *Developmental brain research, 139*, 237–245.

Livy, D., Maier, S.E., & West, J.R. (2001). Fetal alcohol exposure and temporal vulnerability: effects of binge-like alcohol exposure on the ventrolateral nucleus of the thalamus. *Alcoholism: Clinical and Experimental Research, 25*, 774–780.

Livy, D., Miller, E.K., Maier, S.E., & West, J.R. (2003). Fetal alcohol exposure and temporal vulnerability: effects of binge-like alcohol exposure on the developing rat hippocampus. *Neurotoxicology and teratology, 25*, 447–458.

London, L. (1999). The 'dop' system, alcohol abuse and social control amongst farm workers in South Africa: A public health challenge. *Social Science and Medicine, 48,* 1407–1414.

London, L., Sanders, D., & te Water, N.J. (1998). Farm workers in South Africa-the challenge of eradicating alcohol abuse and the legacy of the 'dop' system. *South African Medical Journal, 88,* 1092–1095.

Luo, J. (2015). Effects of ethanol on the cerebellum: advances and prospects. *The Cerebellum, 14*, 383–385.

Lyamin, O.I., Manger, P.R., Ridgway, S.H., Mukhametov, L.M., & Siegel, J.M. (2008). Cetacean sleep: An unusual form of mammalian sleep. *Neuroscience & Biobehavioral Reviews, 32*, 1451–1484.

Maier, S.E., & West, J.R. (2003). Alcohol and nutritional control treatments during neurogenesis in rat brain reduce total neuron number in locus coeruleus, but not in cerebellum or inferior olive. *Alcohol, 30,* 67–74.

Maier, S.E., Miller, J.A., Blackwell, J.M., & West, J.R. (1999). Fetal Alcohol Exposure and temporal vulnerability: regional differences in cell loss as a function of the timing of binge-like alcohol exposure during brain development. *Alcoholism: Clinical and Experimental Research, 23*, 726–734.

Malberg, J.E., Eisch, A.J., Nestler, E.J., & Duman, R.S. (2000). Chronic antidepressant treatment increases neurogenesis in adult rat hippocampus. *The Journal of Neuroscience, 20,* 9104–9110.

Malow, B.A., Marzec, M.L., McGrew, S.G., Wang, L., Henderson, L.M., & Stone, W.L. (2006). Characterizing sleep in children with autism spectrum disorders: a multidimensional approach. *Sleep, 29,* 1563–1571.

Manger, P.R., Ridgway, S.H., & Siegel, J.M. (2003). The locus coeruleus complex of the bottlenose dolphin (Tursiops truncatus) as revealed by tyrosine hydroxylase immunohistochemistry. *Journal of Sleep Research, 12,* 149–155.

Margret, C.P., Li, C.X., Chappell, T.D., Elberger, A.J., Matta, S.G., & Waters, R.S. (2006). Prenatal alcohol exposure delays the development of the cortical barrel field in neonatal rats. *Experimental Brain Research, 172,* 1–13.

Margret, C.P., Li, C.X., Elberger, A.J., Matta, S.G., Chappell, T.D., & Waters, R.S. (2005) Prenatal alcohol exposure alters the size, but not the pattern, of the whisker representation in neonatal rat barrel cortex. *Experimental Brain Research, 165,* 167–178.

Markus, E.J., & Petit, T.L. (1987). Neocortical synaptogenesis, aging, and behavior: lifespan development in the motor-sensory system of the rat. *Experimental Neurology, 96,* 262–278.

Martinez, S. (2014). The cerebellum: from development to structural complexity and motor learning. *Frontier in Neuroanatomy, 8,* 118.

Maseko, B.C., Bourne, J.A., & Manger, P.R. (2007). Distribution and morphology of cholinergic, putative catecholaminergic and serotonergic neurons in the brain of the Egyptian Rousette flying fox, Rousettus aegyptiacus. *Journal of Chemical Neuroanatomy, 34,* 108–127.

Mattson, S.N., & Roebuck, T.M. (2002). Acquisition and retention of verbal and nonverbal information in children with heavy prenatal alcohol exposure. *Alcoholism: Clinical and Experimental Research, 26*, 875–882.

Mattson, S.N., Crocker, N., & Nguyen, T.T. (2011). Fetal alcohol spectrum disorders: neuropsychological and behavioral features. *Neuropsychology Review, 21,* 81–101.

Mattson, S.N., Riley, E.P., Sowell, E.R., Jernigan, T.L., Sobel, D.F., & Jones, K.L. (1996). A decrease in the size of the basal ganglia in children with fetal alcohol syndrome. *Alcoholism: Clinical and Experimental Research, 20*, 1088–1093

May, P.A., & Gossage, J.P. (2001). Estimating the prevalence of fetal alcohol syndrome. A summary. *Alcohol Research and Health, 25,* 159–167.

May, P.A., Brooke, L., Gossage, J.P., Croxford, J., Adnams, C., Jones, K.L., Robinson, L., & Viljoen, D. (2000). Epidemiology of fetal alcohol syndrome in a South African community in the Western Cape Province. *American Journal of Public Health, 90*, 1905–1912.

May, P.A., de Vries, M.M., Marais, A.S., Kalberg, W.O., Adnams, C.M., Hasken, J.M., Tabachnick, B., Robinson, L.K., Manning, M.A., Jones, K.L., Hoyme, D., Seedat, S., Parry, C.D., & Hoyme, H.E. (2016). The continuum of fetal alcohol

spectrum disorders in four rural communities in South Africa: Prevalence and characteristics. *Drug and Alcohol Dependence, 159,* 207–218.

May, P.A., Gossage, J.P., Kalberg, W.O., Robinson, L.K., Buckley, D., Manning, M., & Hoyme, H.E. (2009). Prevalence and epidemiologic characteristics of FASD from various research methods with an emphasis on recent in-school studies. *Developmental Disabilities Research Reviews, 15,* 176–192.

May, P.A., Gossage, J.P., Marais, A.S., Adnams, C.M., Hoyme, H.E., Jones, K.L., Robinson, L.K., Khaole, N.C., Snell, C., Kalberg, W.O., Hendricks, L., Brooke, L., Stellavato, C., & Viljoen, D.L. (2007). The epidemiology of fetal alcohol syndrome and partial FAS in a South African community. *Drug and Alcohol Dependence, 88,* 259–271.

May, P.A., Keaster, C., Bozeman, R., Goodover, J., Blankenship, J., Kalberg, W.O., Buckley D, Brooks M, Hasken J, Gossage JP, Robinson LK, Manning M, & Robinson, L.K. (2015). Prevalence and characteristics of fetal alcohol syndrome and partial fetal alcohol syndrome in a Rocky Mountain Region City. *Drug and Alcohol Dependence, 155,* 118–127.

McCandlish, C., Waters, R., & Cooper, N. (1989). Early development of the representation of the body surface in SI cortex barrel field in neonatal rats as demonstrated with peanut agglutinin binding: evidence for differential development within the rattunculus. *Experimental Brain Research, 77,* 425–431.

Medina, A.E., & Krahe, T.E. (2008). Neocortical plasticity deficits in fetal alcohol spectrum disorders: lessons from barrel and visual cortex. *Journal of Neuroscience Research, 86,* 256–263.

Meltzer, L.J., & Mindell, J.A. (2004). Nonpharmacologic treatments for pediatric sleeplessness. *Pediatric Clinics of North America, 51*, 135–151.

Miller, L.A., Shaikh, T., Stanton, C., Montgomery, A., Rickard, R., Keefer, S., & Hoffman, R. (1995). Surveillance for fetal alcohol syndrome in Colorado. *Public Health Reports*, *110*, 690–697.

Miller, M. (2006). Effect of prenatal exposure to ethanol on glutamate and GABA immunoreactivity in macaque somatosensory and motor cortices: critical timing of exposure. *Neuroscience, 138,* 97–107.

Miller, M.W. (1995). Generation of neurons in the rat dentate gyrus and hippocampus: effects of prenatal and postnatal treatment with ethanol. *Alcoholism: Clinical and Experimental Research, 19,* 1500–1509.

Miller, M.W. (1996). Effect of early exposure to ethanol on the protein and DNA contents of specific brain regions in the rat. *Brain Research, 734,* 286–294.

Miller, M.W., & Robertson, S. (1993). Prenatal exposure to ethanol alters the postnatal development and transformation of radial glia to astrocytes in the cortex. *Journal of Comparative Neurology, 337,* 253–266.

Mirescu, C., Peters, J.D., & Gould, E. (2004). Early life experience alters response of adult neurogenesis to stress. *Nature Neuroscience, 7,* 841–846.

Molnár, Z., Higashi, S., & López-Bendito, G. (2003). Choreography of early thalamocortical development. *Cerebral Cortex, 13,* 661–669.

Moore, D.B., Madorsky, I., Paiva, M., & Barrow-Heaton, M. (2004). Ethanol exposure alters neurotrophin receptor expression in the rat central nervous system: Effects of neonatal exposure. *Journal of Neurobiology, 60,* 114–126.

Moore, E.S., Ward, R.E., Jamison, P.L., Morris, C.A., Bader, P.I., & Hall, B.D. (2002). New perspectives on the face in fetal alcohol syndrome: what anthropometry tells us. *American Journal of Medical Genetics, 109,* 249–260.

Mouton, P.R., Kelley-Bell, B., Tweedie, D., Spangler, E.L., Perez, E., Carlson, O.D., Short, R.G., de Cabo, R., Chang, J., Ingram, D.K., Li, Y., & Greig, N.H. (2012). The effects of age and lipopolysaccharide (LPS)-mediated peripheral inflammation on numbers of central catecholaminergic neurons. *Neurobiology of Aging, 33,* 423.e27–423.e36.

Nada, M.B., Slomianka, L., Vyssotski, A.L., & Lipp, H.P. (2010). Early age-related changes in adult hippocampal neurogenesis in C57 mice. *Neurobiology of Aging, 31,* 151–161.

Niccols, A. (2007). Fetal alcohol syndrome and the developing socio-emotional brain. *Brain and Cognition, 65,* 135–142.

Nixon, K., & Crews, F.T. (2002). Binge ethanol exposure decreases neurogenesis in adult rat hippocampus. *Journal of Neurochemistry, 83,* 1087–1093.

Noori, H.R., & Fornal, C.A. (2011). The appropriateness of unbiased optical fractionators to assess cell proliferation in the adult hippocampus. *Frontiers in Neuroscience, 5*, 140.

Oladehin, A., Margret, C.P., Maier, S.E., Li, C.X., Jan, T.A., Chappell, T.D., & Waters, R.S. (2007). Early postnatal alcohol exposure reduced the size of vibrissal barrel field in rat somatosensory cortex (SI) but did not disrupt barrel field organization. *Alcohol*, *41*, 253–261.

Oliveira, S.A., Chuffa, L.G.A., Fioruci-Fontanelli, B. A., Neto, F.S.L., Novais, P.C., Tirapelli, L.F., Oishi, J.C., Takase, L.F., Stefanini, M.A., Martinez, M., & Martinez, F.E. (2014). Apoptosis of Purkinje and granular cells of the cerebellum following chronic ethanol intake. *The Cerebellum*, *13*, 728–738.

Olson, H.C., Oti, R., Gelo, J., & Beck, S. (2009). "Family matters:" Fetal alcohol spectrum disorders and the family. *Developmental Disabilities Research Reviews*, *15*, 235–249.

Olson, L., & Fuxe, K. (1972). Further mapping out of central noradrenaline neuron systems: Projections of the 'subcoeruleus' area. *Brain Research*, *43*, 289–295.

Opendak, M., Briones, B.A., & Gould, E. (2016). Social behavior, hormones and adult neurogenesis. *Frontiers in Neuroendocrinology*, *41*, 71–86.

Pantazis, N.J., Dohrman, D.P., Goodlett, C.R., Cook, R.T., & West, J.R. (1993). Vulnerability of cerebellar granule cells to alcohol-induced cell death diminishes with time in culture. *Alcoholism: Clinical and Experimental Research*, *17*, 1014–1021.

Pare, D., Smith, Y., Parent, A., & Steriade, M. (1988). Projections of brainstem core cholinergic and non-cholinergic neurons of cat to intralaminar and reticular thalamic nuclei. *Neuroscience, 25*, 69–86.

Parnell, S.E., O'Leary-Moore, S.K., Godin, E.A., Dehart, D.B., Johnson, B.W., Allan Johnson, G., Styner, M.A., & Sulik, K.K. (2009). Magnetic resonance microscopy defines ethanol-induced brain abnormalities in prenatal mice: effects of acute insult on gestational day 8. *Alcoholism: Clinical and Experimental Research, 33*, 1001–1011.

Patrick, J., Richardson, B., Hasen, G., Clarke, D., Wlodek, M., Bousquet, J., & Brien, J. (1985). Effects of maternal ethanol infusion on fetal cardiovascular and brain activity in lambs. *American Journal of Obstetrics and Gynecology*, *151*, 859–867.

Patten, A.R., Fontaine, C.J., & Christie, B.R. (2014). A comparison of the different animal models of fetal alcohol spectrum disorders and their use in studying complex behaviors. *Frontiers in Pediatrics, 2,* 1–19.

Patzke, N., Spocter, M.A., Karlsson, K.Æ., Bertelsen, M.F., Haagensen, M., Chawana, R., Streicher, S., Kaswera, C., Gilissen, E., Alagaili, A.N., Mohammed, O.B., Reep, R.L., Bennett, N.C., Siegel, J.M., Ihunwo, A.O., & Manger, P.R. (2015). In contrast to many other mammals, cetaceans have relatively small hippocampi that appear to lack adult neurogenesis. *Brain Structure and Function, 220,* 361–383.

Pawlak, R., Skrzypiec, A., Sulkowski, S., & Buczko, W. (2002). Ethanol-induced neurotoxicity is counterbalanced by increased cell proliferation in mouse dentate gyrus. *Neuroscience Letters, 327,* 83–86.

Perrin, S. (2014). Preclinical research: Make mouse studies work. *Nature, 507,* 423–425.

Petrovic, J., Ciric, J., Lazic, K., Kalauzi, A., & Saponjic, J. (2013). Lesion of the pedunculopontine tegmental nucleus in rat augments cortical activation and disturbs sleep-wake state transitions structure. *Experimental Neurology, 247,* 562–571.

Peyron, C., Tighe, D.K., Van Den Pol, A.N., De Lecea, L., Heller, H.C., Sutcliffe, J.G., & Kilduff, T.S. (1998). Neurons containing hypocretin (orexin) project to multiple neuronal systems. *Journal of Neuroscience, 18,* 9996–10015.

Powrozek, T.A., & Zhou, F.C. (2005). Effects of prenatal alcohol exposure on the development of the vibrissal somatosensory cortical barrel network. *Developmental Brain Research, 155,* 135–146.

Randazzo, A.C., Muehlbach, M.J., Schweitzer, P.K., & Walsh, J.K. (1998). Cognitive function following acute sleep restriction in children ages 10-14. *Sleep: Journal of Sleep Research & Sleep Medicine. 21,* 861–868.

Redila, V.A., Olson, A.K., Swann, S E., Mohades, G., Webber, A.J., Weinberg, J., & Christie, B.R. (2006). Hippocampal cell proliferation is reduced following prenatal ethanol exposure but can be rescued with voluntary exercise. *Hippocampus, 16,* 305–311.

Resibois, A., & Rogers, J.H. (1992). Calretinin in rat brain: an immunohistochemical study. *Neuroscience, 46,* 101–134.

Rhodes, J.S., Best, K., Belknap, J.K., Finn, D.A., & Crabbe, J.C. (2005). Evaluation of a simple model of ethanol drinking to intoxication in C57BL/6J mice. *Physiology and Behavior, 84*, 53–63.

Rice, F.L. (1995). Comparative aspects of barrel structure and development. In: The Barrel Cortex of Rodents, pp 1–75: *Springer*.

Rice, F.L., & van der Loos, H. (1977). Development of the barrels and barrel field in the somatosensory cortex of the mouse. *The Journal of Comparative Neurology, 171*, 545–560.

Richardson, B.S., Patrick, J.E., Bousquet, J.A.M.E.S., Homan, J.A.C.O.B.U.S., & Brien, J.F. (1985). Cerebral metabolism in fetal lamb after maternal infusion of ethanol. *American Journal of Physiology-Regulatory, Integrative and Comparative Physiology*, *249*, R505–R509.

Richmond, G., & Sachs, B.D. (1980). Grooming in Norway rats: The development and adult expression of a complex motor pattern. *Behavior, 75*, 82-95.

Riley, E.P., Infante, M.A., & Warren, K.R. (2011). Fetal alcohol spectrum disorders: An overview. *Neuropsychology Review, 21*, 73–80.

Riley, E.P., Mattson, S.N., Sowell, E.R., Jernigan, T.L., Sobel, D.F., & Jones, K.L. (1995). Abnormalities of the corpus callosum in children prenatally exposed to alcohol. *Alcoholism: Clinical and Experimental Research*, *19*(5), 1198–1202.

Roebuck, T.M., Simmons, R.W., Mattson, S.N., & Riley, E.P. (1998a). Prenatal exposure to alcohol affects the ability to maintain postural balance. *Alcoholism: Clinical and Experimental Research, 22,* 252–258.

Roebuck, T.M., Simmons, R.W., Richardson, C., Mattson, S.N., & Riley, E.P. (1998b). Neuromuscular responses to disturbance of balance in children with prenatal exposure to alcohol. *Alcoholism: Clinical and Experimental Research, 22,* 1992–1997.

Rogers, J.H. (1989). Immunoreactivity for calretinin and other calcium-binding proteins in cerebellum. *Neuroscience, 31,* 711–721.

Sahay, A., Scobie, K.N., Hill, A.S., O'Carroll, C.M., Kheirbek, M.A., Burghardt, N.S., Fenton, A.A., Dranovsky, A., & Hen, R. (2011). Increasing adult hippocampal neurogenesis is sufficient to improve pattern separation. *Nature, 472,* 466–470.

Saper, C.B., Chou, T.C., & Scammell, T.E. (2001). The sleep switch: hypothalamic control of sleep and wakefulness. *Trends in Neuroscience 24,* 726–731.

Seelke, A.M., Dooley, J.C., & Krubitzer, L.A. (2012). The emergence of somatotopic maps of the body in S1 in rats: the correspondence between functional and anatomical organization. *PLoS One, 7,* e32322.

Segi-Nishida, E., Warner-Schmidt, J.L., & Duman, R.S. (2008). Electroconvulsive seizure and VEGF increase the proliferation of neural stem-like cells in rat hippocampus. *Proceedings of the National Academy of Sciences USA, 105,* 11352–11357.

Semba, K., Reiner, P.B., & Fibiger, H.C. (1990). Single cholinergic mesopontine tegmental neurons project to both the pontine reticular formation and the thalamus in the rat. *Neuroscience, 38,* 643–654.

Senft, S.L., & Woolsey, T.A. (1991). Growth of thalamic afferents into mouse barrel cortex. *Cerebral Cortex, 1,* 308–335.

Servais, L., Hourez, R., Bearzatto, B., Gall, D., Schiffmann, S.N., & Cheron, G. (2007). Purkinje cell dysfunction and alteration of long-term synaptic plasticity in fetal alcohol syndrome. *Proceedings of the National Academy of Sciences, 104,* 9858–9863.

Shepherd, G.M. (Ed.). (1998). *The synaptic organization of the brain*. Oxford University Press, USA.

Shors, T., Anderson, M., Curlik, D., & Nokia, M. (2012). Use it or lose it: how neurogenesis keeps the brain fit for learning. *Behavioural Brain Research, 227,* 450–458.

Siegel, J. M. (2004a). The neurotransmitters of sleep. *Journal of Clinical Psychiatry*, *65*, 4–7.

Siegel, J.M. (2004b). Hypocretin (orexin): Role in normal behavior and neuropathology. *Annual Review of Psychology*, *55,* 125–148.

Simons, D.J., & Woolsey, T.A. (1979). Functional organization in mouse barrel cortex. *Brain Research, 165*, 327–332.

Sloviter, R.S., Sollas, A.L., Barbaro, N.M., & Laxer, K.D. (1991). Calcium-binding protein (calbindin-D28K) and parvalbumin immunocytochemistry in the normal and epileptic human hippocampus. *Journal of Comparative Neurology*, *308*, 381–396.

Song, J., Zhong, C., Bonaguidi, M.A., Sun, G.J., Hsu, D., Gu, Y., Meletis, K., Huang, Z.J., Ge, S., Enikolopov, G., Deisseroth, K., Luscher, B., Christian, K.M., Ming, G.I., & Song, H. (2012). Neuronal circuitry mechanism regulating adult quiescent neural stem-cell fate decision. *Nature, 489*, 150–154.

Sowell, E.R., Jernigan, T.L., Mattson, S.N., Riley, E.P., Sobel, D.F., & Jones, K.L. (1996). Abnormal development of the cerebellar vermis in children prenatally exposed to alcohol: Size reduction in lobules I–V. *Alcoholism: Clinical and Experimental Research*, *20*, 31–34.

Spottiswoode, B.S., Meintjes, E.M., Anderson, A.W., Molteno, C.D., Stanton, M.E., Dodge, N.C., Gore, J.C., Peterson, B.S., Jacobson, J.L., & Jacobson, S.W. (2011). Diffusion tensor imaging of the cerebellum and eyeblink conditioning in fetal alcohol spectrum disorder. *Alcoholism: Clinical and Experimental Research*, *35*, 2174–2183.

Stockard, C.R. (1910). The influence of alcohol and other anaesthetics on embryonic development. *American Journal of Anatomy*, *10*, 369–392.

Stratton, K., Howe, C., & Battaglia, F. C. (Eds.). (1996). Fetal alcohol syndrome: Diagnosis, epidemiology, prevention, and treatment. *National Academies Press.*

Streissguth, A.P., Barr, H.M., & Martin, D.C. (1984). Alcohol Exposure in vitro and Functional Deficits in Children During the First Four Years of Life. In *Ciba*

Foundation Symposium 105-Mechanisms of Alcohol Damage In Utero (pp. 176-196). John Wiley & Sons, Ltd..

Streissguth, A.P., Bookstein, F.L., Barr, H.M., Sampson, P.D., O'Malley, K.I.E.R.A.N., & Young, J.K. (2004). Risk factors for adverse life outcomes in fetal alcohol syndrome and fetal alcohol effects. *Journal of Developmental & Behavioral Pediatrics*, *25*, 228–238.

Sulik, K.K. (2005). Genesis of alcohol-induced craniofacial dysmorphism. *Experimental Biology and Medicine*, *230*, 366–375.

Sulik, K.K., Johnston, M.C., & Webb, M.A. (1981). Fetal alcohol syndrome: Embryogenesis in a mouse model. *Science*, *214*, 936–938.

Sullivan, E.V., Desmond, J.E., Lim, K.O., & Pfefferbaum, A. (2002). Speed and efficiency but not accuracy or timing deficits of limb movements in alcoholic men and women. *Alcoholism: Clinical and Experimental Research*, *26*, 705–713.

Swenson, R.S. (2006). Review of clinical and functional neuroscience. *Educational Review Manual in Neurology*.

Takahashi, K., Kayama, Y., Lin, J.S., & Sakai, K. (2010). Locus coeruleus neuronal activity during the sleep-waking cycle in mice. *Neuroscience, 169,* 1115–1126.

Tootell, R.B., & Silverman, M.S. (1985). Two methods for flat-mounting cortical tissue. *Journal of Neuroscience Methods, 15*, 177–190.

Tran, T.D., & Kelly, S.J. (2003). Critical periods for ethanol-induced cell loss in the hippocampal formation. *Neurotoxicology and Teratology, 25,* 519–528.

Treves, A., Tashiro, A., Witter, M.P., & Moser, E.I. (2008). What is the mammalian dentate gyrus good for? *Neuroscience, 154,* 1155–1172.

Tronel, S., Fabre, A., Charrier, V., Oliet, S.H., Gage, F.H., & Abrous, D.N. (2010). Spatial learning sculpts the dendritic arbor of adult-born hippocampal neurons. *Proceedings of the National Academy of Sciences USA, 107,* 7963–7969.

Turner, P.V., Brabb, T., Pekow, C., & Vasbinder, M.A. (2011). Administration of substances to laboratory animals: routes of administration and factors to consider. *Journal of the American Association for Laboratory Animal Science, 50,* 600–613.

Uecker, A., & Nadel, L. (1996). Spatial locations gone awry: object and spatial memory deficits in children with fetal alcohol syndrome. *Neuropsychologia, 34,* 209–223.

Ulleland, C. N. (1972). The offspring of alcoholic mothers. *Annals of the New York Academy of Sciences, 197,* 173.

Viljoen, D.L., Gossage, J.P., Brooke, L., Adnams, C.M., Jones, K.L., Robinson, L.K., Hoyme, H.E., Snell, C., Khaole, N.C., Kodituwakku, P., Asante, K.O., Findlay, R., Quinton, B., Marais, A.S., Kalberg, W.O., & May, P.A. (2005). Fetal alcohol syndrome epidemiology in a South African community: a second study of a very high prevalence area. *Journal of Studies on Alcohol, 66,* 593–604.

Watt, M.H., Eaton, L.A., Choi, K.W., Velloza, J., Kalichman, S.C., Skinner, D., & Sikkema, K.J. (2014). "It's better for me to drink, at least the stress is going away": Perspectives on alcohol use during pregnancy among South African women attending drinking establishments. *Social Science and Medicine, 116,* 119–125.

Webster, H.H., & Jones, B.E. (1988). Neurotoxic lesions of the dorsolateral pontomesencephalic tegmentum-cholinergic cell area in the cat. II. Effect upon sleep-waking states. *Brain Research, 458,* 285–302.

Webster, W.S., Walsh, D.A., Lipson, A.H., & McEwen, S.E. (1980). Teratogenesis after acute alcohol exposure in inbred and outbred mice. *Neurobehavioral Toxicology, 2,* 227–234.

Webster, W.S., Walsh, D.A., McEwen, S.E., & Lipson, A.H. (1983). Some teratogenic properties of ethanol and acetaldehyde in C57BL/6J mice: Implications for the study of the fetal alcohol syndrome. *Teratology, 27,* 231–243.

Welker, C., & Woolsey, T.A. (1974). Structure of layer IV in the somatosensory neocortex of the rat: Description and comparison with the mouse. *The Journal of Comparative Neurology, 158,* 437–453.

Wengel, T., Hanlon-Dearman, A.C., & Fjeldsted, B. (2011). Sleep and sensory characteristics in young children with fetal alcohol spectrum disorder. *Journal of Developmental & Behavioral Pediatrics, 32,* 384–392.

West, M.J. (1993). New stereological methods for counting neurons. *Neurobiology of Aging, 14,* 275–285.

West, M.J., Slomianka, L., & Gundersen, H.J. (1991). Unbiased stereological estimation of the total number of neurons in the subdivisions of the rat hippocampus using the optical fractionator. *Anatomical Record, 231,* 482–497.

Whishaw, I.Q., Pellis, S.M., & Gorny, B.P. (1992). Skilled reaching in rats and humans: evidence for parallel development or homology. *Behavioral Brain Research, 47,* 59–70.

Wierzba-Bobrowicz, T., Lewandowska, E., Stepien, T., & Szpak, G.M. (2011). Differential expression of calbindin D28k, calretinin and parvalbumin in the cerebellum of pups of ethanol-treated female rats. *Folia Neuropathologica*, *49,* 47–55.

Willoughby, K.A., Sheard, E.D., Nash, K., & Rovet, J. (2008). Effects of prenatal alcohol exposure on hippocampal volume, verbal learning, and verbal and spatial recall in late childhood. *Journal of the International Neuropsychological Society*, *14*, 1022–1033.

Wisniewski, K., Dambska, M., Sher, J.H., & Qazi, Q. (1983). A clinical neuropathological study of the fetal alcohol syndrome. *Neuropediatrics*, *14*, 197–201.

Wong-Riley, M. (1979). Changes in the visual system of monocularly sutured or enucleated cats demonstrable with cytochrome oxidase histochemistry. *Brain Research, 171,* 11–28.

Woods, K.J., Meintjes, E.M., Molteno, C.D., Jacobson, S.W., & Jacobson, J.L. (2015). Parietal dysfunction during number processing in children with fetal alcohol spectrum disorders. *NeuroImage: Clinical, 8*, 594–605.

Woosley, T.A., & van der Loos H. (1970). The structural organization of layer IV in the somatosensory region (S1) of mouse cerebral cortex. *Brain Research, 17*, 205–242.

Wozniak, D.F., Hartman, R.E., Boyle, M.P., Vogt, S.K., Brooks, A.R., Tenkova, T., Young, C., Olney, J.W., & Muglia, L.J. (2004). Apoptotic neurodegeneration induced by ethanol in neonatal mice is associated with profound learning/memory deficits in juveniles followed by progressive functional recovery in adults. *Neurobiology of Disease, 17*, 403–414.

Yew, D.T., Luo, C.B., Heizmann, C.W., & Chan, W.Y. (1997). Differential expression of calretinin, calbindin D28K and parvalbumin in the developing human cerebellum. *Developmental Brain Research, 103*, 37–45.

Zafar, H., Shelat, S.G., Redei, E., & Tejani-Butt, S. (2000). Fetal alcohol exposure alters serotonin transporter sites in rat brain. *Brain Research, 856*, 184–192.

Zagron, G., & Weinstock, M. (2006). Maternal adrenal hormone secretion mediates behavioural alterations induced by prenatal stress in male and female rats. *Behavioural Brain Research, 175*, 323–328.

Zharkovsky, T., Kaasik, A., Jaako, K., & Zharkovsky, A. (2003). Neurodegeneration and production of the new cells in the dentate gyrus of juvenile rat hippocampus after a single administration of ethanol. *Brain Research, 978*, 115–123.

Zharkovsky, T., Kaasik, A., Jaako, K., & Zharkovsky, A. (2003). Neurodegeneration and production of the new cells in the dentate gyrus of juvenile rat hippocampus after a single administration of ethanol. *Brain Research, 978*, 115–123.

Zimmerberg, B., Sukel, H.L., & Stekler, J.D. (1991). Spatial learning of adult rats with fetal alcohol exposure: deficits are sex-dependent. *Behavioural Brain Research, 42*, 49–56.